ANCR-NUREG-1285
DATE PUBLISHED - JUNE 1976

IDAHO NATIONAL ENGINEERING LABORATORY

CORE THERMAL RESPONSE DURING SEMISCALE MOD-1 BLOWDOWN HEAT TRANSFER TESTS

PREPARED BY AEROJET NUCLEAR COMPANY FOR
U. S. NUCLEAR REGULATORY COMMISSION
AND
ENERGY RESEARCH AND DEVELOPMENT ADMINISTRATION
IDAHO OPERATIONS OFFICE UNDER CONTRACT E(10-1) -1375

DISCLAIMER

Printed in the United States of America
Available from
National Technical Information Service
U. S. Department of Commerce
5285 Port Royal Road
Springfield, Virginia 22161
Price: Printed Copy $6.00; Microfiche $2.25

"The NRC will make available data tapes and operational computer codes on research programs dealing with postulated loss-of-coolant accidents in light water reactors. Persons requesting this information must reimburse the NRC contractors for their expenses in preparing copies of the data tapes and the operational computer codes. Requests should be submitted to the Research Applications Branch, Office of Nuclear Regulatory Research, Nuclear Regulatory Commission, Washington, D.C. 20555."

Approved:

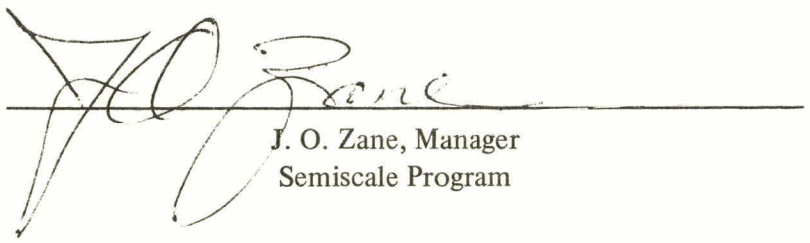

J. O. Zane, Manager
Semiscale Program

E. P. Eales, Manager
Systems Research Division

NOTICE

ANCR-NUREG-1285

Distributed Under Category:
NRC-2
Water Reactor Safety
Research Systems
Engineering

CORE THERMAL RESPONSE DURING SEMISCALE MOD-1 BLOWDOWN HEAT TRANSFER TESTS

by

Thomas K. Larson

AEROJET NUCLEAR COMPANY

Date Published – June 1976

PREPARED FOR THE
U.S. NUCLEAR REGULATORY COMMISSION
AND
ENERGY RESEARCH AND DEVELOPMENT ADMINISTRATION
IDAHO OPERATIONS OFFICE
UNDER CONTRACT E(10-1)-1375

ACKNOWLEDGMENTS

The author wishes to express his thanks to the personnel of the Fluids Laboratory Division for their efforts in conducting the tests and gathering the data, to the personnel of the Test Integration and Coordination Section for verification and documentation of the data, to R. F. Farman and R. W. Shumway for technical support, to D. M. Snider for supplying core heat transfer calculations, to G. W. Johnsen and J. K. Meier for supplying RELAP4 calculations, to K. A. Dietz for editing and improving the quality of the overall report, and to L. A. Nelson and L. K. Keller for typing the various drafts.

ABSTRACT

Selected experimental data and results calculated from experimental data obtained from the Semiscale Mod-1 blowdown heat transfer test series are analyzed. These tests were designed primarily to provide information on the core thermal response to a loss-of-coolant accident. The data are analyzed to determine the effect of core flow on the heater rod thermal response. The data are also analyzed to determine the effects of initial operating conditions on the rod cladding temperature behavior during the transient. The departure from nucleate boiling and rewetting characteristics of the rod sufaces are examined for radial and axial patterns in the response. Repeatability of core thermal response data is also investigated. The test data and the core thermal response calculated with the RELAP4 code are compared.

SUMMARY

Core heater rod thermal response data from the Semiscale Mod-1 blowdown heat transfer test series have been analyzed to determine the effects of blowdown on the heater rod thermal behavior. In addition, the measured data have been compared with calculations obtained from RELAP4 computer program models to evaluate the differences between the measured and calculated core response.

The same procedure was followed in the approach to every Semiscale blowdown heat transfer test: (a) the system was brought up to pressure (2,250 psig), desired flow rate, and an isothermal temperature of 540°F; (b) core power was increased in successive steps to the desired value; (c) core power and core flow rate were adjusted to achieve the desired core differential temperature, and the system was allowed to equilibrate; and (d) after the desired initial steady state conditions had been achieved, the system was subjected to decompression by introducting a leak in the broken loop piping. Results from the data analysis include the following.

The heater rod cladding temperature response is strongly influenced by the core fluid flow direction during the blowdown transient. Sustained positive flow (the normal upward direction) through the core, which occurred in the simulated hot leg piping break test, provides excellent cooling to the heater rods. Under these circumstances, the rod cladding temperatures continually decline from the initial steady state values until core dryout occurs. Immediate core flow reversal, which occurs in all of the simulated cold leg piping break tests, results in severe degradation in heat transfer between the rods and the coolant shortly after initiation of the piping break. During the cold leg break tests in which a radially peaked power profile was imposed on the core, departure from nucleate boiling (DNB) occurred at the high power rod peak power locations between about 0.4 and 0.6 second after rupture. The low power rods usually experienced DNB between 1 and 5 seconds after rupture. Rod surface rewetting (an increase in heat transfer subsequent to DNB) did not occur on the high power rods but did occur in many instances on the low power rods. In the cold leg break tests in which a radially flat power profile was imposed on the core, DNB occurred at rod peak power locations between 0.5 and 0.8 second after rupture. Rod surface rewetting occurred on many of the heater rod peak power zones during the flat radial profile tests.

Data comparisons between the radially peaked core power tests indicate that variations in the magnitude and duration of the core flow reversal affect both the time to DNB and the post-DNB heat transfer on the low power rods. The high power rods were relatively unaffected by these core flow variations.

The different core fluid temperature distributions imposed on the system during the blowdown heat transfer tests indirectly affect the heater rod cladding temperature response. The initial fluid temperature distribution affects the magnitude of the transient core flow which in turn alters the time to DNB and post-DNB heat transfer on some of the rods.

The different power densities and radial power distributions imposed on the rods seemed to affect only the maximum cladding temperature attained during the transient.

No correlation could be found between the rod rewetting phenomena and heater rod local power density variations. More rewets occurred in the upper left and lower right quadrants of the core for some of the tests, but no definite radial pattern in the rewet phenomena could be established.

A definite axial pattern in the rewet phenomena existed for all of the 100% initial core power tests. Rewetting occurred only between certain axial elevations. The implication of this axial pattern is that the close interaction between rod power density and fluid conditions, and also perhaps the location of the grid spacers, controls rewetting.

The penetration of rod surface rewetting into the heater rod high power zones appeared to be a linear function of the rod initial peak power density. For peak power densities of 14.25 kW/ft, rewets did not occur in the high power zone. For power densities of about 8 kW/ft, rewets occurred throughout the high power zone. Between power densities of 8 and 14.25 kW/ft, the elevation within the rod peak power zone below which rewetting did not occur was a function of the power density.

The core thermal response data are repeatable both in terms of the occurrence of DNB and rewet at the rod surfaces and also in terms of the post-DNB cladding temperature response.

Given the correct core hydraulic conditions, the heat transfer models used in the RELAP4 MOD5 computer code appear to adequately predict the Semiscale Mod-1 heater rod high power zone cladding temperature response during a 200% cold leg break. The occurrence of rewetting at some of the high power zone thermocouple locations (such as occurred during Tests S-02-7 and S-02-9) was not predicted by the analytical models. This may be a result of the nodalization used in the models (one fluid volume was used to simulate the fluid adjacent to the rod high power zones) and the inability to simulate the effects of the grid spacers on the core flow patterns.

CONTENTS

FIGURES

TABLES

CORE THERMAL RESPONSE DURING SEMISCALE MOD-1 BLOWDOWN HEAT TRANSFER TESTS

I. INTRODUCTION

The Semiscale Mod-1 experimental program conducted by Aerojet Nuclear Company is part of the overall United States Nuclear Regulatory Commission and Energy Research and Development Administration-sponsored research and development program to investigate the behavior of a pressurized water reactor (PWR) system during a hypothesized loss-of-coolant accident (LOCA). The Semiscale Mod-1 program is intended to provide transient thermal hydraulic data from a simulated LOCA using a small-scale experimental system. This program is a major contributor of experimental data that will aid in understanding the response of the system, the response of the individual components, and the interactions that occur between the major components and subsystems. These data provide a means of evaluating the adequacy of the overall system analytical models as well as the models of the individual system components. The objectives of the Semiscale Mod-1 experimental program are to: (a) produce integral and separate effects experimental thermal hydraulic data that are needed to provide an experimental basis for analytical model assessment, (b) provide data for assessing the requirements and reliability of selected Loss-of-Fluid Test (LOFT) program instrumentation, and (c) produce experimental data to aid in optimizing the selection of test parameters and the evaluation of test results from the LOFT program.

The blowdown heat transfer tests were the second group of tests conducted in the Semiscale Mod-1 program and were the first tests with power applied to the electrically heated core. The primary objectives of the blowdown heat transfer test series were to obtain information required to evaluate the heat transfer characteristics of the Semiscale Mod-1 core and to obtain the information necessary for evaluating the analytical models currently used to calculate core flow and heat transfer coefficients. Components of the heat transfer behavior of primary interest are:

(1) Nucleate boiling heat transfer during blowdown

(2) Time to departure from nucleate boiling (DNB)

(3) Post-DNB heat transfer.

The Semiscale Mod-1 blowdown heat transfer test series, conducted in a system simulating a PWR, consisted of one test initiated by a double-ended offset shear hot leg break, eight tests initiated by a double-ended offset shear cold leg break, and one test initiated by a single-ended "small" break. Two of these tests were conducted as "standard

problems"[a] for the United States Nuclear Regulatory Commission; therefore, results from these tests are not discussed in this report. Uninterpreted data for the blowdown heat transfer tests are available in References 1 through 7. Each of the tests was conducted by establishing system core inlet fluid conditions at about 544°F and 2,262 psia, adjusting the core power and core flow to achieve the desired core differential temperature, and then rupturing the piping in the broken loop to cause the system fluid to flow out through two rupture nozzles and into a pressure suppression tank. The depressurization (blowdown) lasted about 30 seconds.

This report documents the observed core thermal response for the blowdown heat transfer series tests. General discussions concerning the departure from nucleate boiling and rewetting characteristics of the heater rods are presented as well as are discussions concerning the radial and axial symmetry of the thermal response of the heater rods. Rod surface heat transfer coefficients as calculated from measured test data using an inversion technique described by Beck[8] are also presented. Since wide variations in responses during similar tests would tend to limit the usefulness of the test results, repeatability of the data from heater rod cladding thermocouples is also examined for the tests that had similar initial conditions. Core thermal response calculations that were obtained through use of RELAP4[9] computer code models are also compared with experimental core thermal response data. These comparisons were made to evaluate the agreements and differences between the measured and calculated response of the Semiscale core.

Section II of this report contains a description of the Semiscale Mod-1 system and the test plan followed for the blowdown heat transfer test series. The results of the analysis of the core thermal response data are presented in Section III. Section IV contains discussions concerning comparisons between the calculated and measured core thermal response and the RELAP4 models most influential on the calculated core thermal response. The significant conclusions concerning the core thermal response are presented in Section V. Appendixes are devoted to discussions of the post-DNB power control method, the analysis of special tests conducted in support of this test series, the axial rewet phenomena in the core during one test, the repeatability of core thermal response data, and the RELAP4 core model used in the core thermal response calculations.

[a] A Nuclear Regulatory Commission standard problem test is a test conducted to establish an experimental data base for the purpose of comparison with unbiased analytical calculations supplied by the standard problem program participants.

II. EXPERIMENT DESCRIPTION

The Semiscale Mod-1 experimental system and test plan for the blowdown heat transfer test series are described. The topics discussed briefly include the overall system configuration and core power simulator, core measurements and power control, and test plan.

1. SYSTEM HARDWARE DESCRIPTION

The Semiscale Mod-1 experimental apparatus shown in Figure 1 is a small-scale model of the LOFT[a] which is in turn a model of a four-loop pressurized water reactor. This apparatus is used to obtain transient thermal hydraulic data under simulated loss-of-coolant accident conditions. The Semiscale system, which has a liquid volume of approximately 7.8 ft^3, consists of a pressure vessel and internals; an intact loop consisting of a pressurizer, active steam generator, and coolant pump; and a broken loop with hydraulic resistances that simulate an inactive steam generator and and a locked rotor pump. The intact loop of the Semiscale system models three loops of a typical four-loop PWR. The broken loop simulates the fourth PWR loop. A detailed description of the system configuration, peripheral equipment, instrumentation, and data acquisition system can be found in Reference 10.

The core simulator in the Semiscale system consists of 40 electrically heated rods of typical PWR fuel rod diameter (0.422 inch) and axial power peaking factor (1.58). Figure 2 illustrates the general construction of a Semiscale heater rod. The overall length of the rod is about 207 inches, and the bottom of the 5.5-foot heated section is about 143 inches below the vessel cold leg centerline as shown in Figure 3. The rods extend from the bottom of the heated section to the upper plenum and pass out through the vessel upper head.

The rod heating element is constructed of constantan wire (55% copper, 45% nickel), coiled with a varying pitch, and sized to develop a specified power. Compacted boron nitride surrounds the element and insulates it from a composite sheath. The composite sheath (Figure 2) was manufactured from 316L stainless steel. The inner sheath was creased along the total rod length (concavely) at four locations spaced azimuthly around the rod circumference so as to accept four 0.025-inch-diameter thermocouple assemblies. The outer sheath was positioned over the inner sheath after installation of the thermocouples, and the composite assembly was redrawn. The thermocouples provide rod cladding temperature measurements at four different axial locations along the 5.5-foot heated length of the heater rods.

---

[a] Loss-of-Fluid Test Facility – a 55-MW test reactor located at the Idaho National Engineering Laboratory.

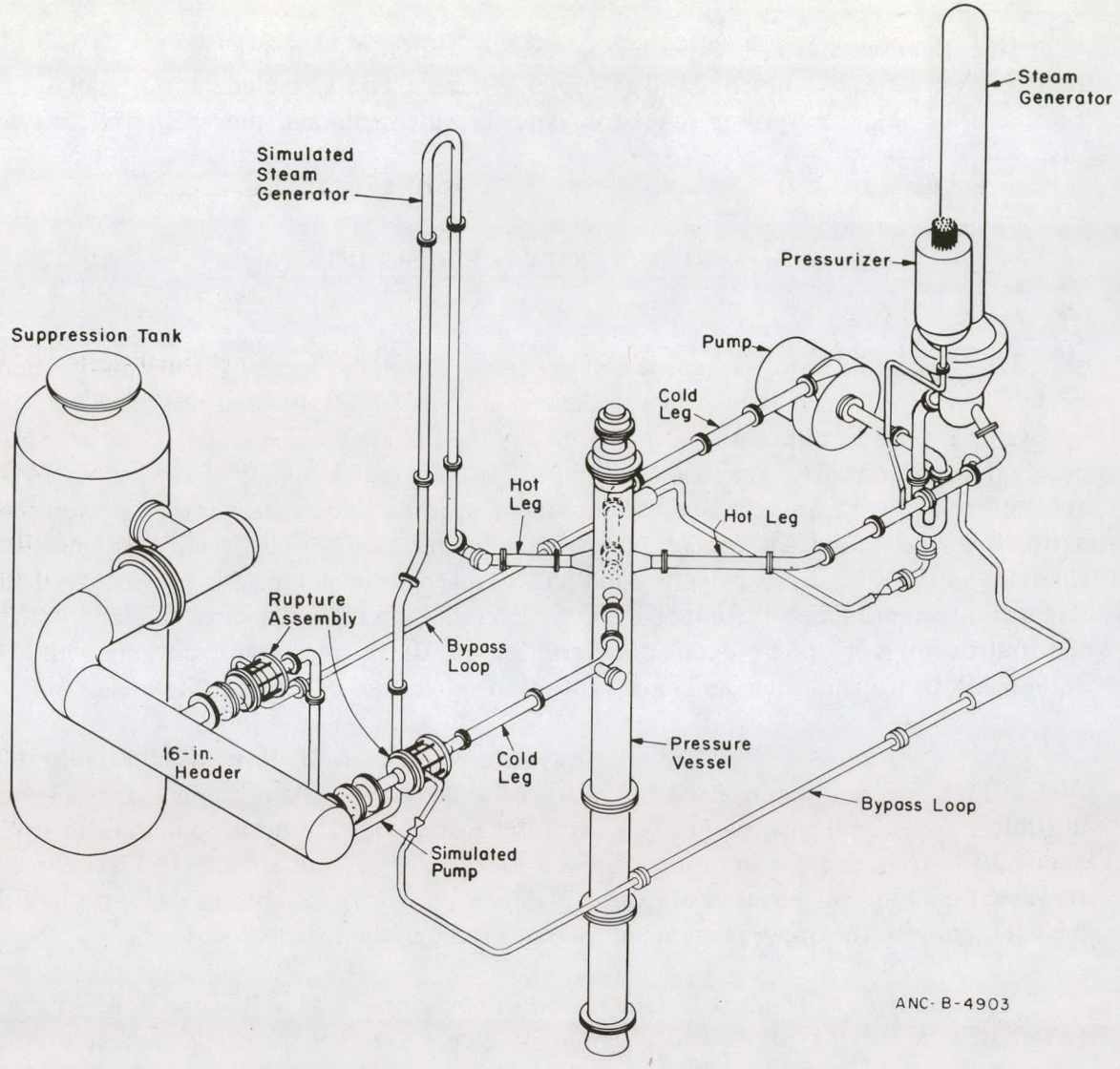

Fig. 1 Semiscale Mod-1 system cold leg break configuration – isometric.

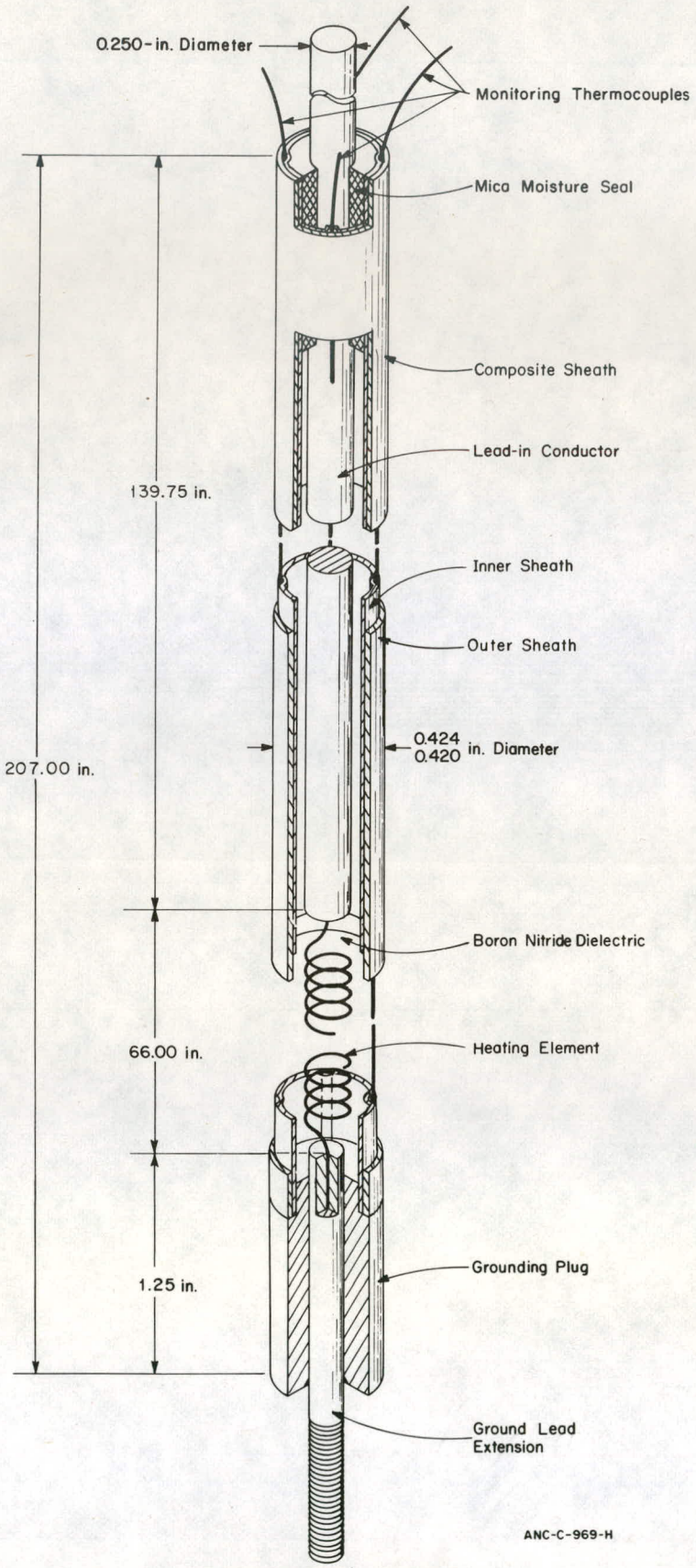

Fig. 2 Semiscale Mod-1 electric heater rod.

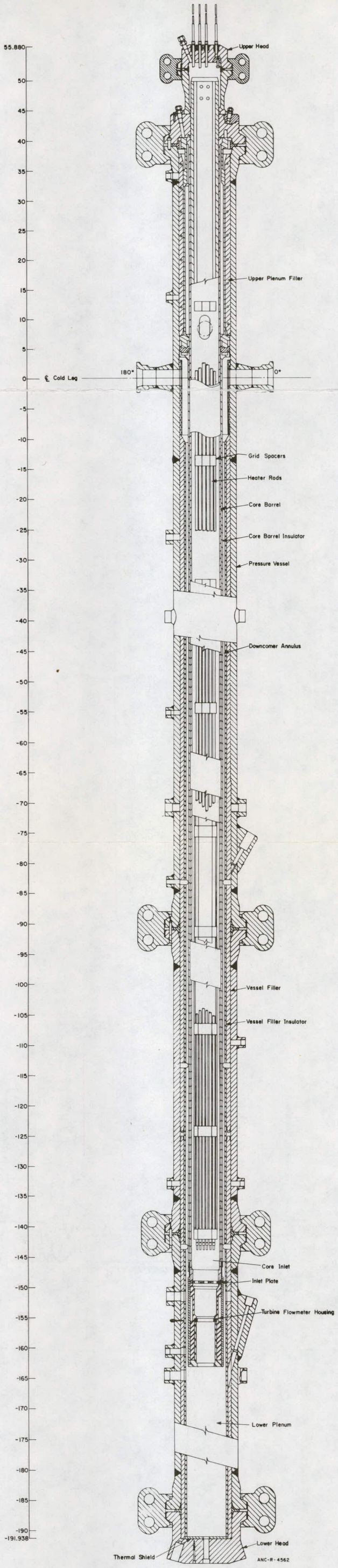

Fig. 3 Cross section of vessel with core.

The 40 rods are positioned and held in the core with 10 grid spacers which maintain the heaters on a typical PWR pitch (0.563 inch). Figure 4 shows a plan view of the Semiscale vessel and core simulator assembly, and Figure 5 illustrates the heater rod matrix and cladding thermocouple locations. The heater rods are located within the matrix by reference to the row of letters across the top and the column of numbers down the side of the matrix. Similarily, the thermocouples are located by the rod that they are on and by their elevation above the bottom of the heated length of the core. The thermocouple on Rod D5 at the 29-inch elevation is thus referred to as TH-D5-29 where TH means a core heater cladding temperature, D5 refers to the rod upon which the thermocouple is located, and 29 gives the thermocouple elevation in inches above the core bottom. (The arrows in Figure 5 indicate thermocouple azimuthal locations.) A heat shield assembly composed of 0.018-inch-thick stainless steel surrounds the rod matrix and reduces the core flow area to 7.39 $in.^2$. The four centrally located rods (the high power rods) individually produce 66.23 kW at 173 Vdc and the remaining 36 rods (the low power rods) each produce 36.9 kW at 173 Vdc. The as-constructed axial power profile for the rods is illustrated in Figure 6. These profiles allow the simulation of radial peaking that exists in nuclear cores. A sufficient factor of safety was built into the rods, however, to allow for the implementation of a flat radial power profile on the core simulator if desired. When assembled in the core simulator, the 40 rods produce a total core power of 1.6 MW.

2. CORE MEASUREMENTS

Core measurements taken in addition to the heater rod cladding temperatures included core voltage, power, current, fluid temperature, inlet flow, and inlet density. Electrical current was measured using a shunt circuit technique, and voltage was obtained from a digital voltmeter. The voltage and current measurements were processed through a Hall-effect multiplier to obtain the total core power. Core inlet flow rate and density measurements were provided by instrumentation consisting of a turbine flowmeter, drag disc, and gamma densitometer located below the bottom of the heater rods. Core fluid temperatures were measured with thermocouples attached to the grid spacers located along the heated length of the rods.

3. CORE POWER CONTROL

Figure 7 shows the transient electrical core power control used during the first five blowdown heat transfer tests. This electrical power was determined by analytically matching the surface heat flux calculated for an electrical rod to the surface heat flux calculated for a nuclear rod, assuming that both rods were subjected to the same transient boundary conditions as described in Reference 10. After more appropriate boundary conditions became available (from the measured test data), the electrical core power control was redefined to allow better simulation of a nuclear rod with the electrical rods. A more detailed description of the technique used to determine the core power control is contained in Appendix A.

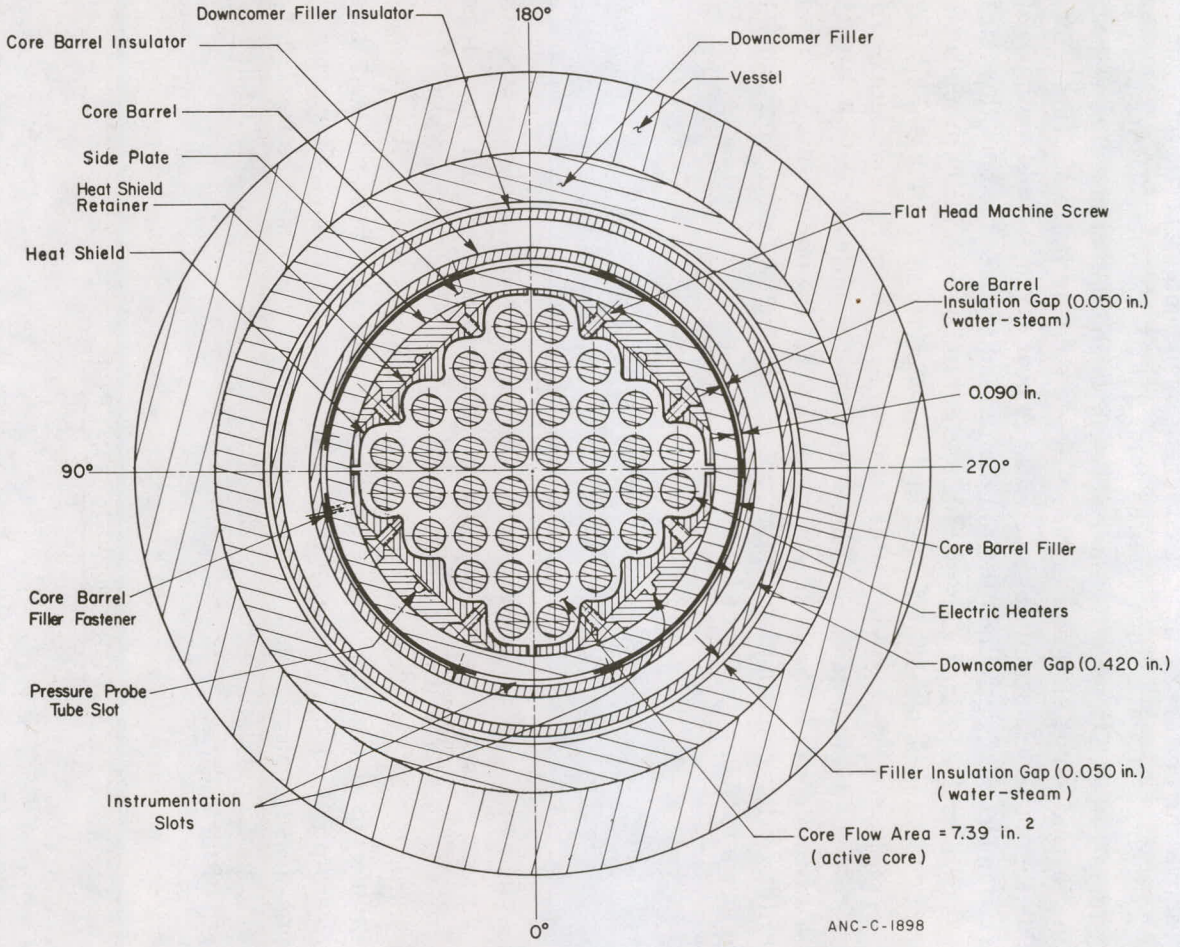

Fig. 4 Vessel cross section and core layout.

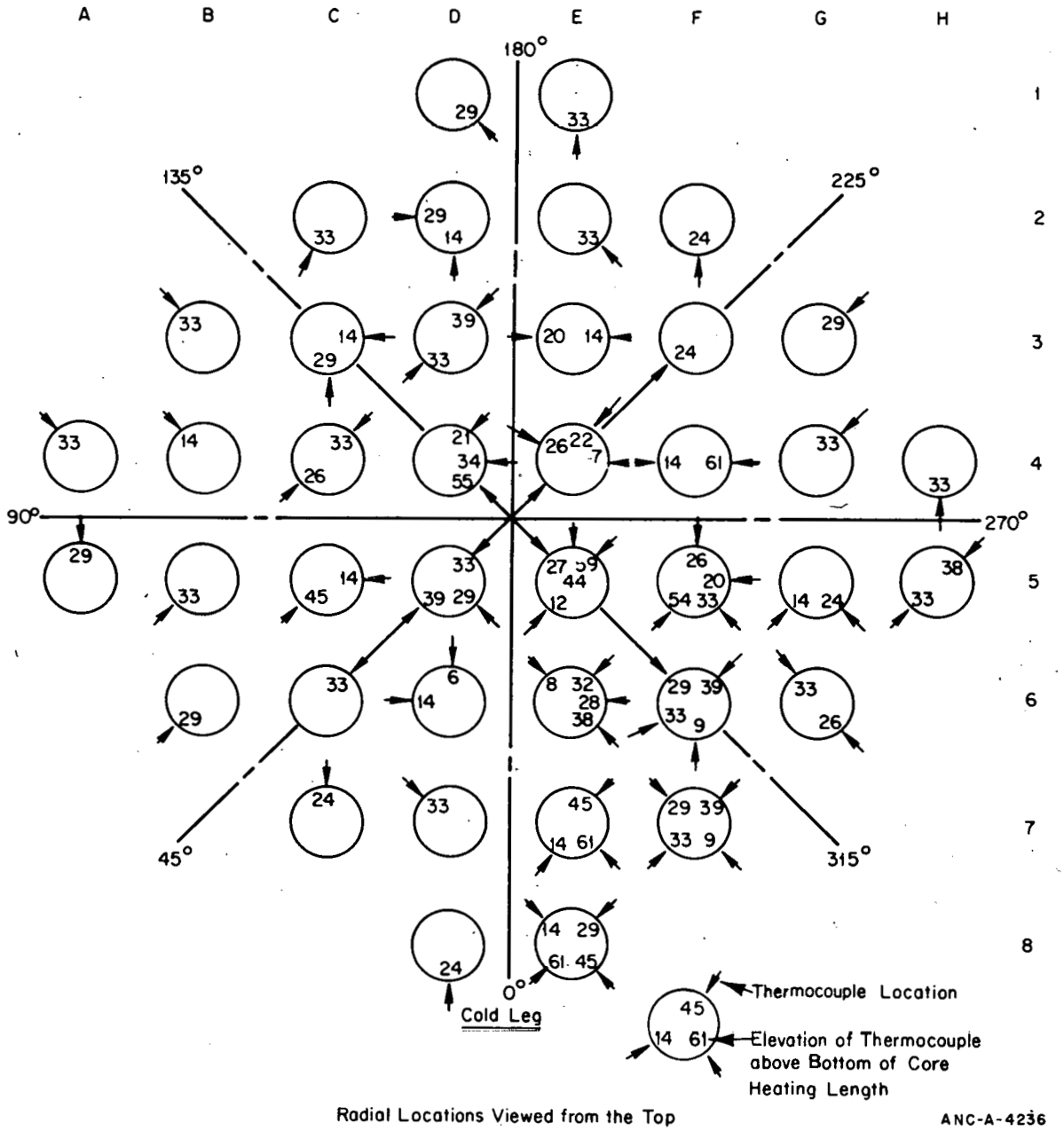

Fig. 5 Semiscale Mod-1 heated core – plan view showing instrumentation.

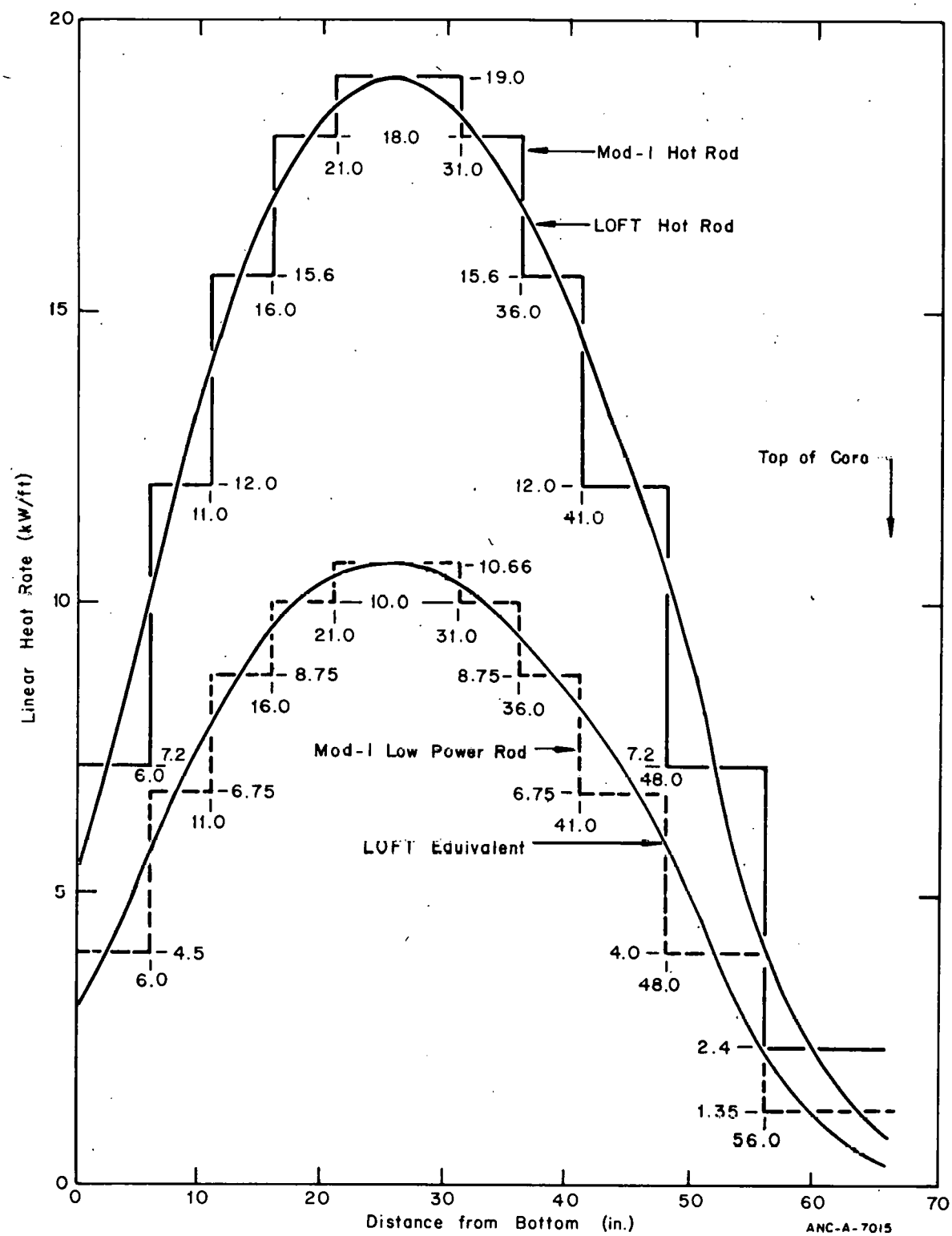

Fig. 6 Semiscale Mod-1 heater rod axial power distribution.

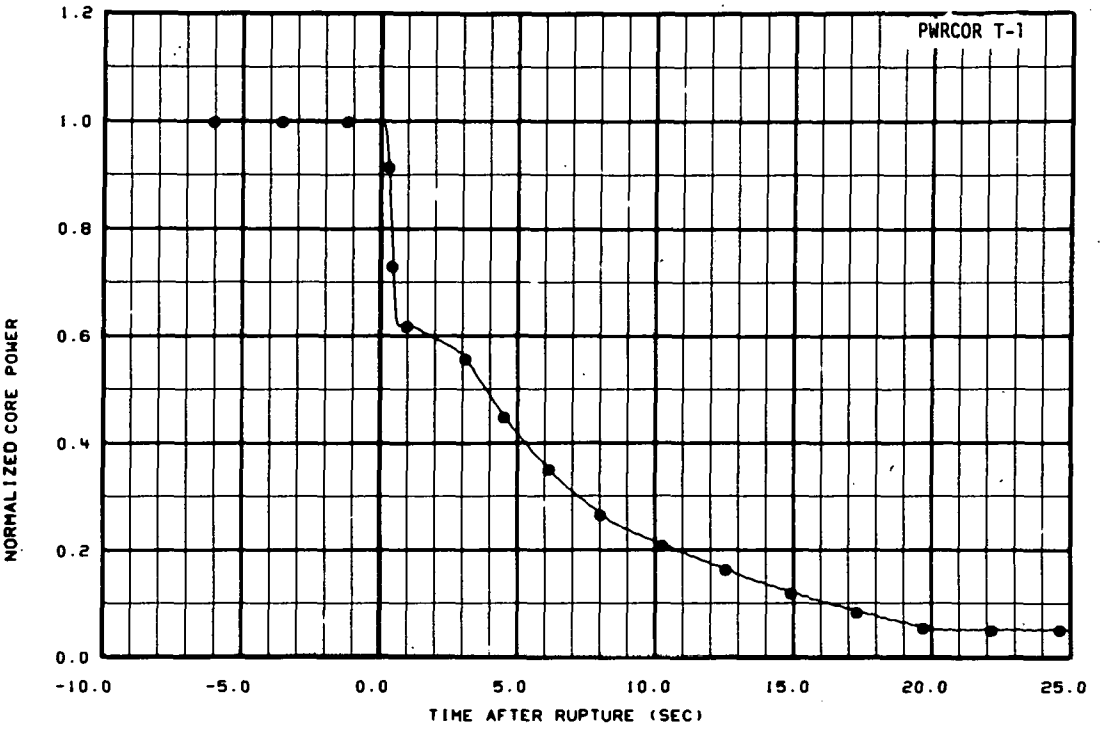

Fig. 7 Normalized transient core power.

4. TEST PLAN

Table I presents an overview of the test conditions and other pertinent information relating to the blowdown heat transfer test series. The test plan was structured to proceed to the most thermally severe test conditions (full power double-ended cold leg break) from more modest test conditions. Test S-02-1 was the only hot leg break test conducted during the series. Test S-02-6 was the only "small" break test. All other tests were 200% double-ended offset shear cold leg break tests. Tests S-02-1 through S-02-3 were 75% power tests that were conducted mainly to provide operating experience with the Mod-1 core so the system characteristics would be understood by the time the first full power test with radially peaked core power was run. Tests S-02-4 and S-02-5 were full power tests conducted with peaked radial core power profiles in which the four center rods had a peak power density of 14.25 kW/ft, and the remaining rods had a peak power density of 11.54 kW/ft. Test S-02-5 was a repeat of Test S-02-4 with the exception of the post-DNB transient core power control.

Four blowdown heat transfer tests (Tests S-02-7, S-02-8, S-02-9A, and S-02-9) in which a radially flat power profile was imposed on all of the active heater rods were conducted with the Semiscale Mod-1 system. These tests were conducted to investigate the effect of radial power distribution on core response during blowdown. The core power

TABLE I

DESCRIPTION OF BLOWDOWN HEAT TRANSFER TESTS

Variable	Test S-02-1	S-02-2	S-02-3	S-02-4	S-02-5	S-02-6[a]	S-02-7	S-02-8[a]	S-02-9	S-02-9A
Break Size (%)	200[b]	200	200	200	200	6%	200	200	200	200
Break Location	Hot Leg	Cold Leg	Cold Leg	Cold Leg	Cold Leg	Cold Leg	Cold Leg	Cold Leg	Cold Leg	Cold Leg
System Pressure (psia)	2,265	2,272	2,263	2,263	2,253	2,265	2,263	2,273	2,253	2,263
Core Flow (gpm)[c]	166	162	119	156	155	148	154	155	146	148
Core Power (MW)[c]	1.18	1.2	1.19	1.6	1.6	1.56	1.61	1.57	1.56	1.56
Core Inlet Temperature (°F)	545	542	543	542	543	542	541	543	542	542
Core ΔT (°F)[c]	49	48	68	67	66	67	63	67	68	65
Peak Power Density on High Power Rods (kW/ft)	14.25	14.25	14.25	14.25	14.25	14.25	11.84	11.84	11.84	11.84
Peak Power Density on Low Power Rods (kW/ft)	8.0	8.0	8.0	11.54	11.54	11.54	11.84	11.84	11.84	11.84
ECC Injection	None	None	None	None	Yes	Yes	None	None	Yes	Yes
Intact Loop										
Accumulator										
Location					Cold Leg	Cold Leg			Cold Leg	Cold Leg
Injection Pressure (psig)					600	600			600	600
Low Pressure Injection System										
Location					Cold Leg	Cold Leg			Cold Leg	Cold Leg
Injection Pressure (psig)					150	150			150	150
Broken Loop										
Accumulator										
Location					Cold Leg	Cold Leg			Cold Leg	Cold Leg
Injection Pressure (psig)					600	600			600	600
Low Pressure Injection System										
Location					Cold Leg	Cold Leg			Cold Leg	Cold Leg
Injection Pressure (psig)					150	150			150	150
Heated Rods in Core	40	40	40	39[d]	38[d,e]	37[d,e]	39[d]	39[d]	37[d,e]	37[d,e]

[a] U.S. Nuclear Regulatory Commission Standard Problem.
[b] A 200% break is a full sized double-ended offset shear.
[c] Rated conditions for Semiscale are: core flow - 165 gpm; core power - 1.6 MW; core ΔT - 66°F.
[d] Liquid level probe replaced one rod.
[e] Rod(s) failed.

control shown in Figure 7 was used during Test S-02-7, whereas a different post-DNB power control was used during Tests S-02-9A and S-02-9. The only other test specification difference in these three tests was that emergency core coolant (ECC) was injected during Tests S-02-9A and S-02-9 but not during Test S-02-7. Test S-02-9 was essentially a rerun of Test S-02-9A to correct hardware problems associated with the the ECC injection systems.

Tests S-02-6 and S-02-8 were conducted as data bases for U.S. Nuclear Regulatory Commission standard problems; consequently, results from these two test are not discussed in this report.

The same basic procedure was followed in the approach to every blowdown heat transfer test: (a) the system was brought up to pressure (2,250 psig), desired flow rate, and an isothermal temperature of 540°F; (b) core power was increased to the desired value in successive steps; (c) core power and flow rate were adjusted to achieve the desired core differential temperature, and the system was allowed to equilibrate; and (d) after the desired initial steady state conditions had been achieved, blowdown was initiated by introducing a leak in the system piping.

III. TEST RESULTS

The following sections describe the observed Semiscale Mod-1 core thermal response for the blowdown heat transfer test series. The first section discusses the general response of the heater rods to core flow during the transient. Heater rod temperatures are discussed in relation to both core flow direction and variations in the magnitudes of the transient core flow. The second section discusses the effect of the specified core operating conditions on the heater rods and the method of electrical core power control. The third section is concerned with the rod rewetting phenomena observed during the cold leg break tests in the blowdown heat transfer test series. Both radial and axial rewet patterns are discussed. Data repeatability is addressed in the fourth section. Repeatability of both the rod rewetting characteristics and rod cladding temperature profiles is the topic of discussion.

1. GENERAL HEATER ROD RESPONSE TO CORE FLOW

The tests conducted with the Semiscale system caused the core simulator to be subjected to various flow rates during the course of the blowdown transient. The following sections are concerned with the general response of the heater rods in relation to the core flow. A thorough discussion of the causes of the core flow variations is contained in Reference 11.

1.1 Heater Rod Response to Core Flow Direction

The heater rod cladding temperature response was strongly influenced by the transient core flow direction. The flow direction at the core inlet during the blowdown was basically controlled by the break location in the Semiscale system. Figure 8 shows the general trends of the core inlet flow behavior for both a hot leg break test (Test S-02-1)[1] and a cold leg break test (Test S-02-3)[3]. Test S-02-1 is distinct from all of the other blowdown heat transfer tests because of the location of the break in the hot leg. Several tests were conducted with the break in the cold leg; however, the data from Test S-02-3 are considered sufficiently illustrative of the general trends of behavior during a cold leg break test that they can be used as a typical example for comparison with Test S-02-1.

The location of the break for Test S-02-1 (between the vessel nozzle and the high resistance components in the broken loop) caused the path of lowest flow resistance to be through the core in the normal flow direction. Consequently, flow through the core remained in the normal upward (positive) direction throughout the transient as shown in Figure 8, and excellent cooling was provided to the heater rods. Figures 9 and 10, which show the axial temperature variation on a high power rod (Rod E5) and a heat transfer coefficient from a high power rod (Rod E4) hot spot (axial position of maximum power generation), respectively, illustrate the good cooling characteristics during the hot leg break transient. The rod cladding temperatures shown in Figure 9 decrease from their initial values until about 23.5 seconds when core dryout occurs; that is, when the fluid quality in the core

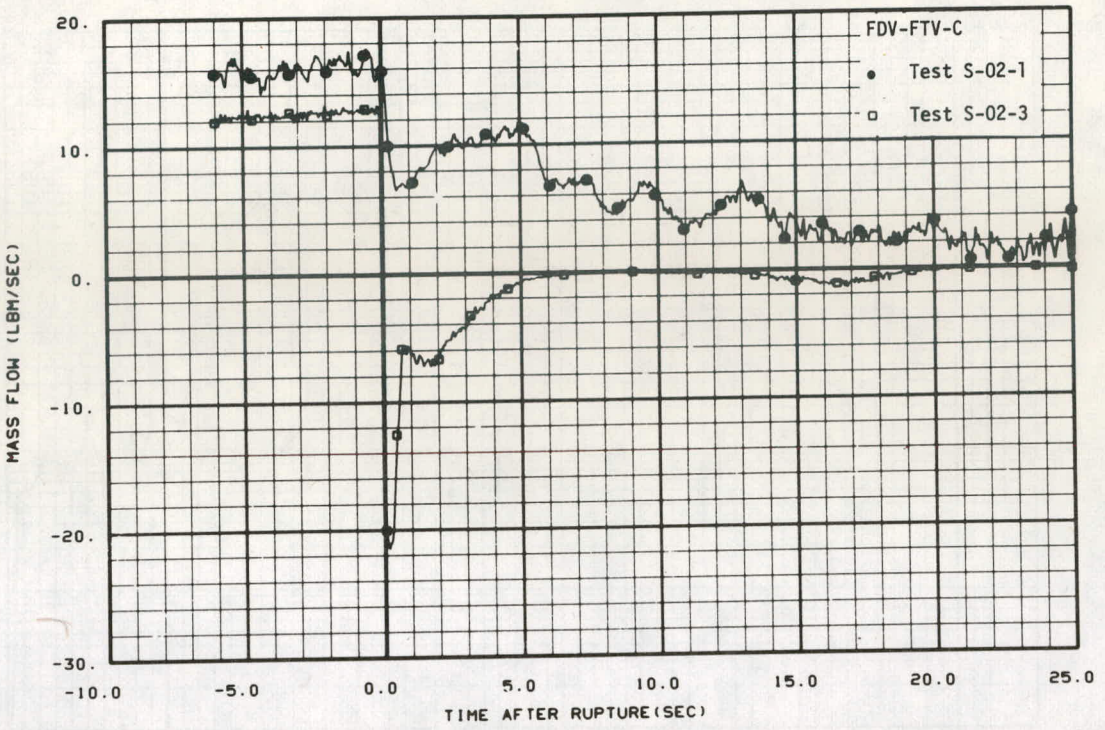

Fig. 8 Comparison of core mass flow rates from a hot leg break test (Test S-02-1) and a cold leg break test (Test S-02-3).

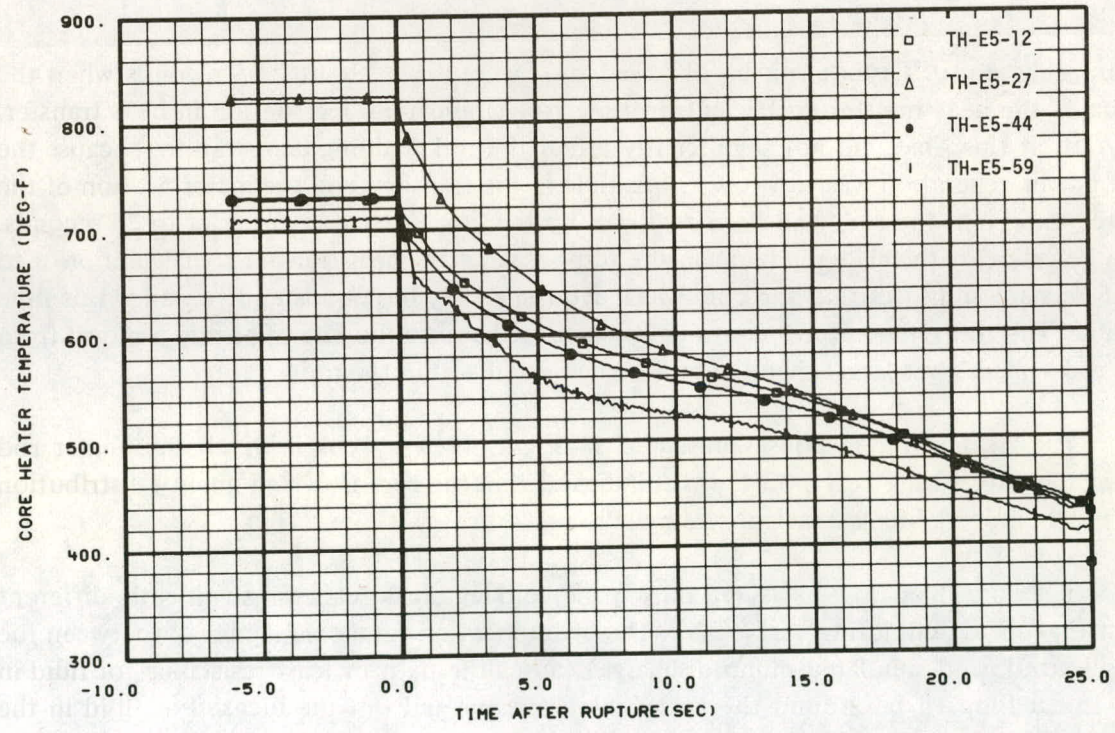

Fig. 9 Axial cladding temperatures on Rod E5 – Test S-02-1.

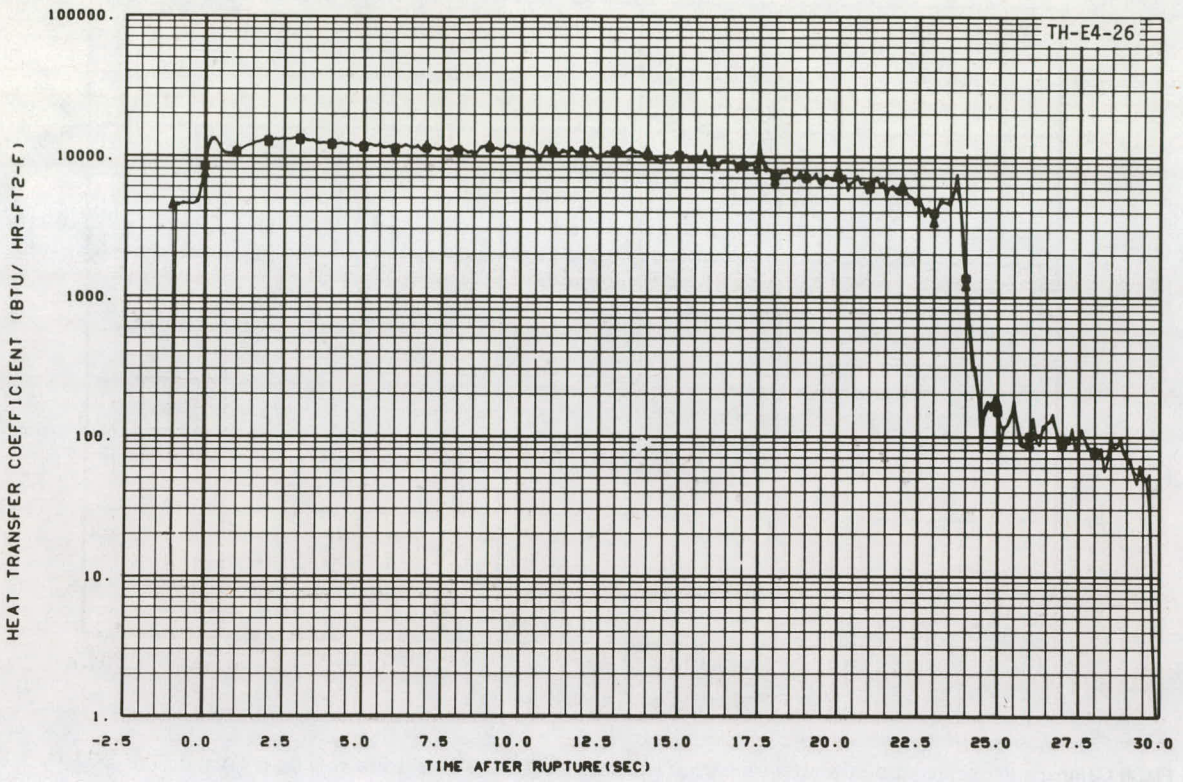

Fig. 10 Heat transfer coefficient at 26-inch elevation on Rod E4 – Test S-02-1.

approaches unity. Dryout can be observed on Figure 10 at about 23.5 seconds when the value of the heat transfer coefficient drops sharply indicating degradation in heat transfer. Dryout, at this time, did not significantly affect the rod cladding temperatures because the rod power generation was very low at this time in the transient and the major portion of the stored energy in the rods had been removed by the large heat transfer prior to 23 seconds. The behavior of the cladding temperature response and the heat transfer coefficient prior to 23.5 seconds indicates that the core was in a quasi-steady heat transfer process for this time period. The rod temperatures continually declined because the rate of energy removal from the rod surfaces was larger than the power generation within the rods.

The heater rod response presented in Figure 9 was typical of all the heater rod measurements during Test S-02-1, which indicates that the core flow and quality distribution during the hot leg break transient was radially uniform.

The core inlet flow measured during the cold leg break tests was significatly different from that measured during Test S-02-1. The break location for a cold leg break (between the vessel nozzle and simulated pump discharge) causes the path of least resistance for fluid in the intact loop to be around the vessel inlet annulus and out the break. For fluid in the vessel, the path of least flow resistance is down the core, up the downcomer, and out the break. The potential thus exists of voiding the core after break initiation and severely reducing the capability of cooling the heater rods. As shown in Figure 8, the core flow

reversed almost immediately at break initiation during the cold leg break test (Test S-02-3), whereas during the hot leg break test, the core flow remained in the positive direction.

Figure 11 shows the core inlet mass flow rate and measured hot spot temperature (on high power Rod E4) versus time after break initiation for Test S-02-3. In response to rupture, the core flow reversed almost immediately to about 22 lbm/sec. The magnitude of the core flow then started to decrease (become less negative) at about 0.4 second. The measured temperature profile shows that DNB also occurred at about 0.4 second. The measured temperature profile represents the cladding temperature at a radial location approximately 32.5 mils beneath the rod surface which indicates that DNB occurred at the rod surface sometime between 0 and 0.4 second after rupture. Figure 12 presents the calculated heat transfer coefficient for the 26-inch elevation on Rod E4 and illustrates the severe degradation in heat transfer that occurs following DNB. The heat transfer coefficient for the same location calculated from Test S-02-1 data is also shown in Figure 12 for comparison. The differences between the heat transfer coefficients subsequent to 0.5 second after rupture clearly indicate superior heat transfer from the heater rods to the coolant during the hot leg break test. Comparison of the maximum high power rod, hot spot cladding temperatures reached during Tests S-02-1 and S-02-3 also indicates the differences in core heat transfer between the two tests. Figure 9, for example, showed that the peak cladding temperatures reached were the steady state values in Test S-02-1. In Test S-02-3, however, the early DNB caused most of the power input to the rods to be retained within the rods, resulting in an increase in the cladding temperatures. Figure 11 showed that the peak cladding temperature reached at the hot spot location on Rod E4 during Test S-02-3 was about 1,746^{o}F.

Figures 13 and 14 show the cladding temperature response at different axial locations on Rod E5 (high power) and E7 (low power) as measured during Test S-02-3. These two figures suggest that the post-DNB heat transfer is somewhat better (the heat transfer coefficient is larger) in the upper end of the core than in the lower end. This observation indicates that the initial reversal of flow in the core causes the quality at the bottom of the core to be higher than the quality near the top of the core. This quality gradient is believed to be the result of energy being received by the fluid from the heater rods as the fluid traveled downward in the core. Figure 15 shows the quality gradient in the core as calculated with the COBRA[12] computer code. Test results measured during Test S-02-3 were used as boundary conditions for the computer calculation. This calculation substantiates the indication that the fluid quality is larger in the lower portions of the core than in the upper portion for the early part (0 to 4 seconds) of blowdown. As a consequence of this quality gradient, maximum cladding temperatures reached during the transient would be expected to be skewed towards the bottom of the core. Figure 16 shows the peak rod cladding temperatures as a function of core elevation for Test S-02-3. This figure shows that the maximum cladding temperatures are skewed towards the bottom of the core and also illustrates that thermocouples on the same power zones but on different sides of the hot spot indicate temperatures below the hot spot that are higher than those above the hot spot. This phenomenon is consistent with the postulated (and calculated) quality distribution within the core.

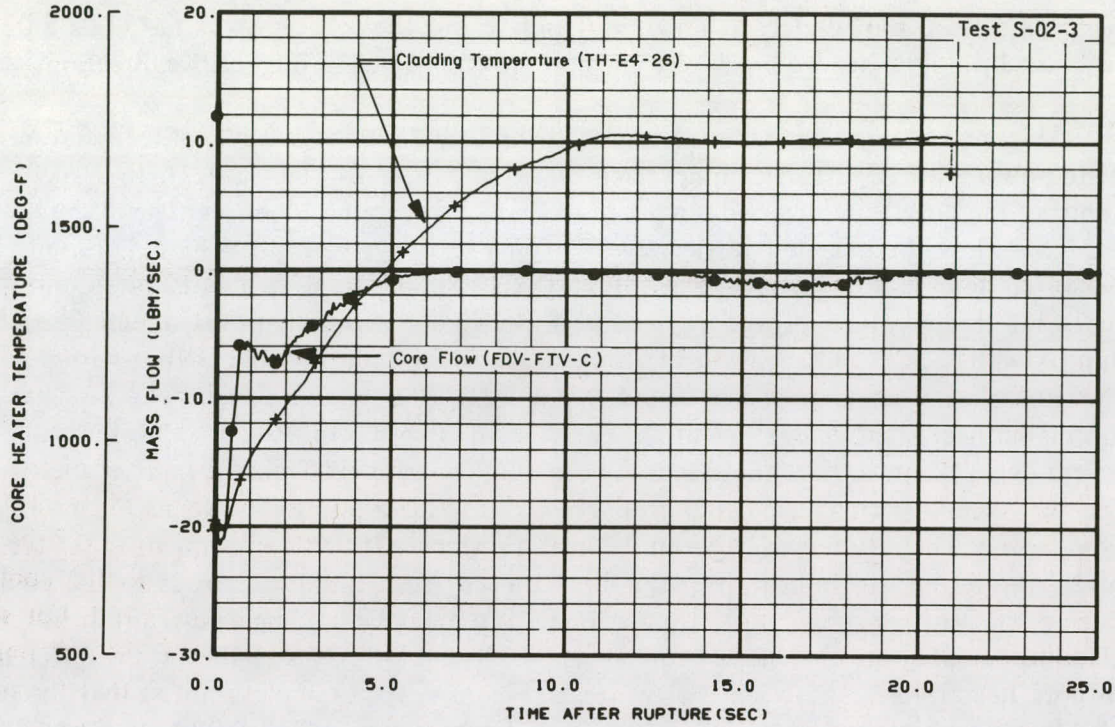

Fig. 11 Core inlet flow rate and high power hot spot response – Test S-02-3.

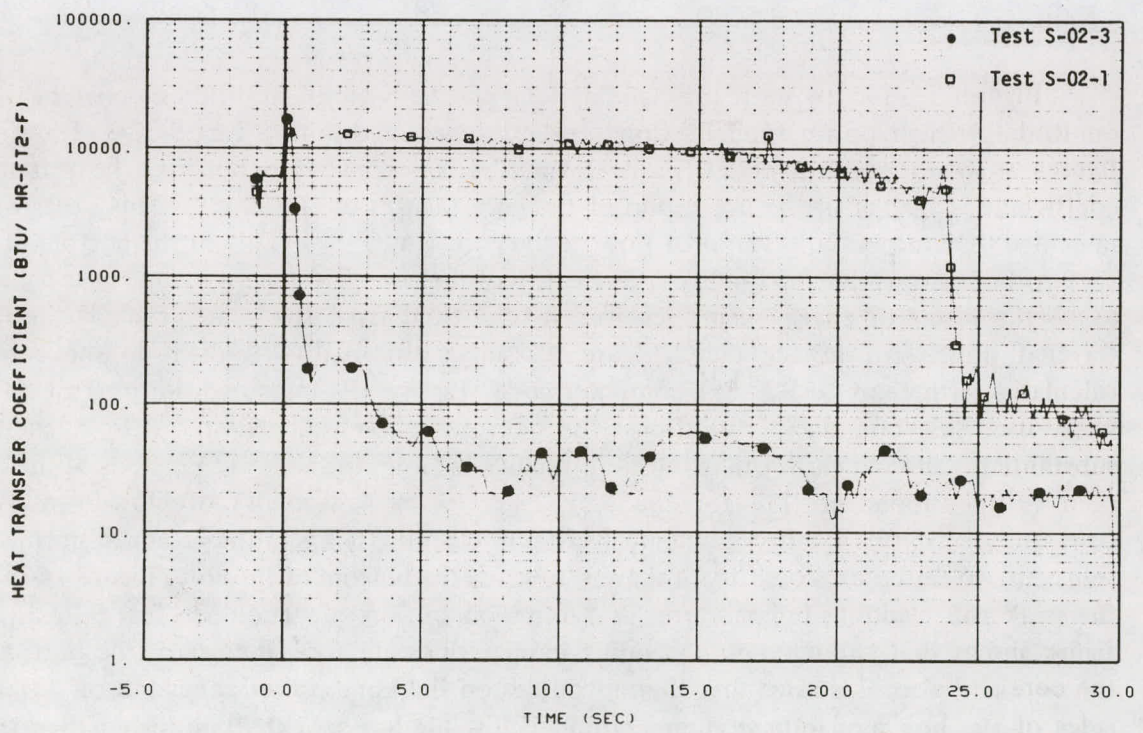

Fig. 12 Heat transfer coefficient at 26-inch elevation on Rod E4 – Tests S-02-3 and S-02-1.

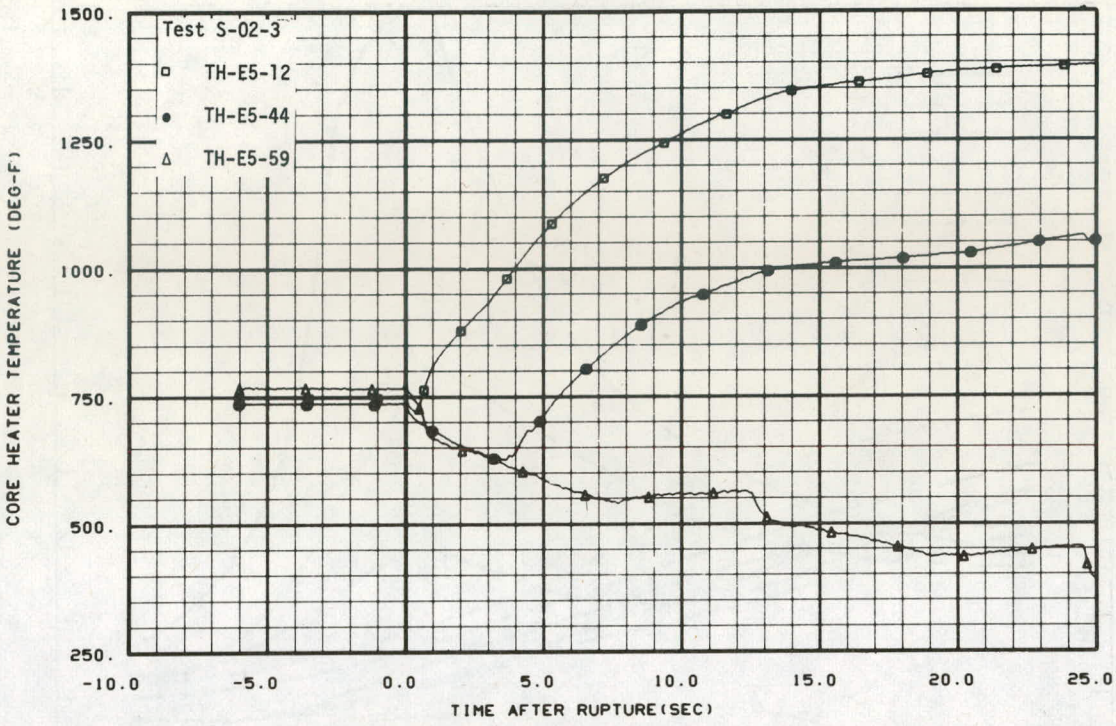

Fig. 13 Axial cladding temperatures on Rod E5 – Test S-02-3.

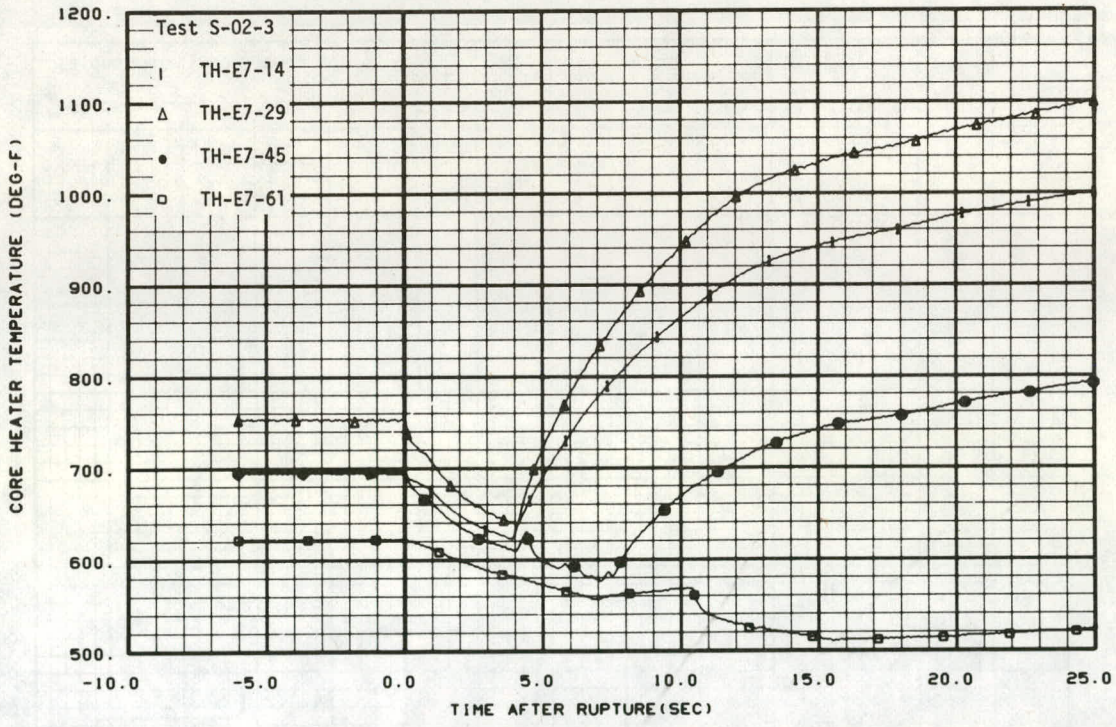

Fig. 14 Axial cladding temperature on E7 – Test S-02-3.

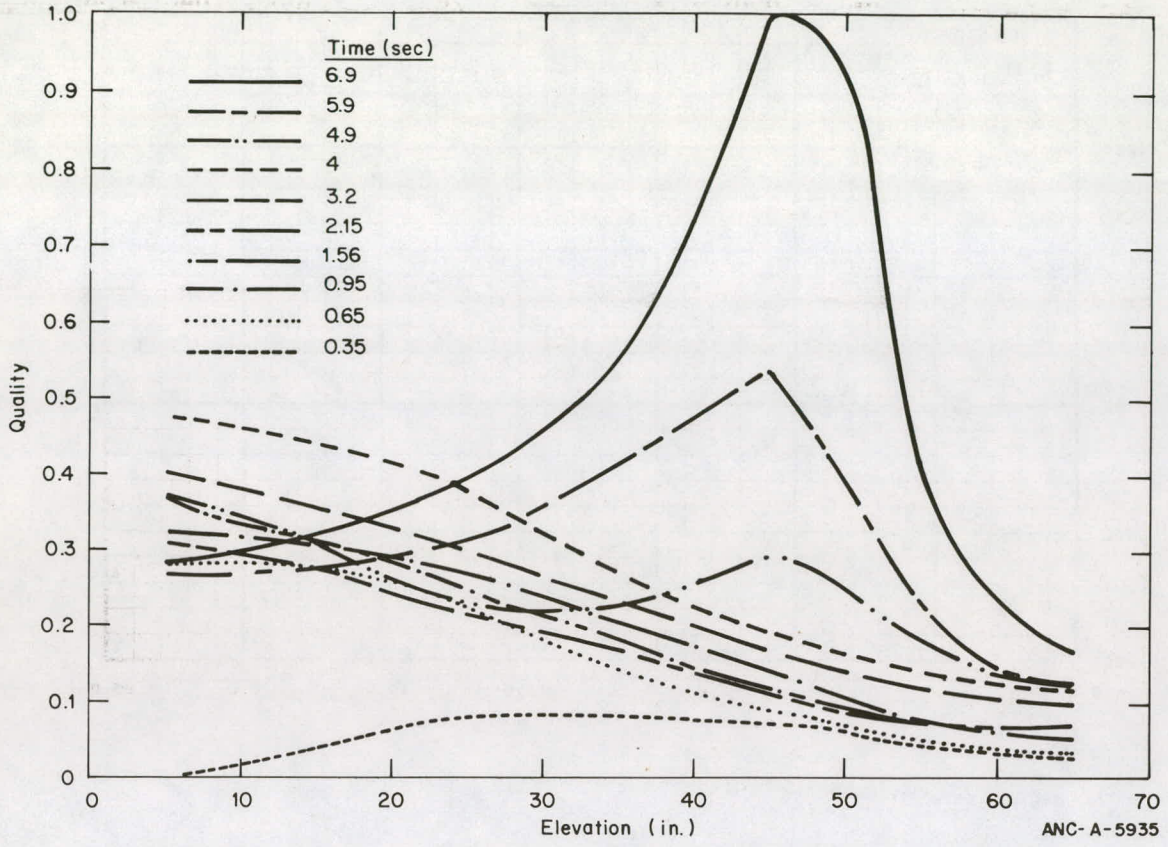

Fig. 15 Calculated quality gradient in core – Test S-02-3.

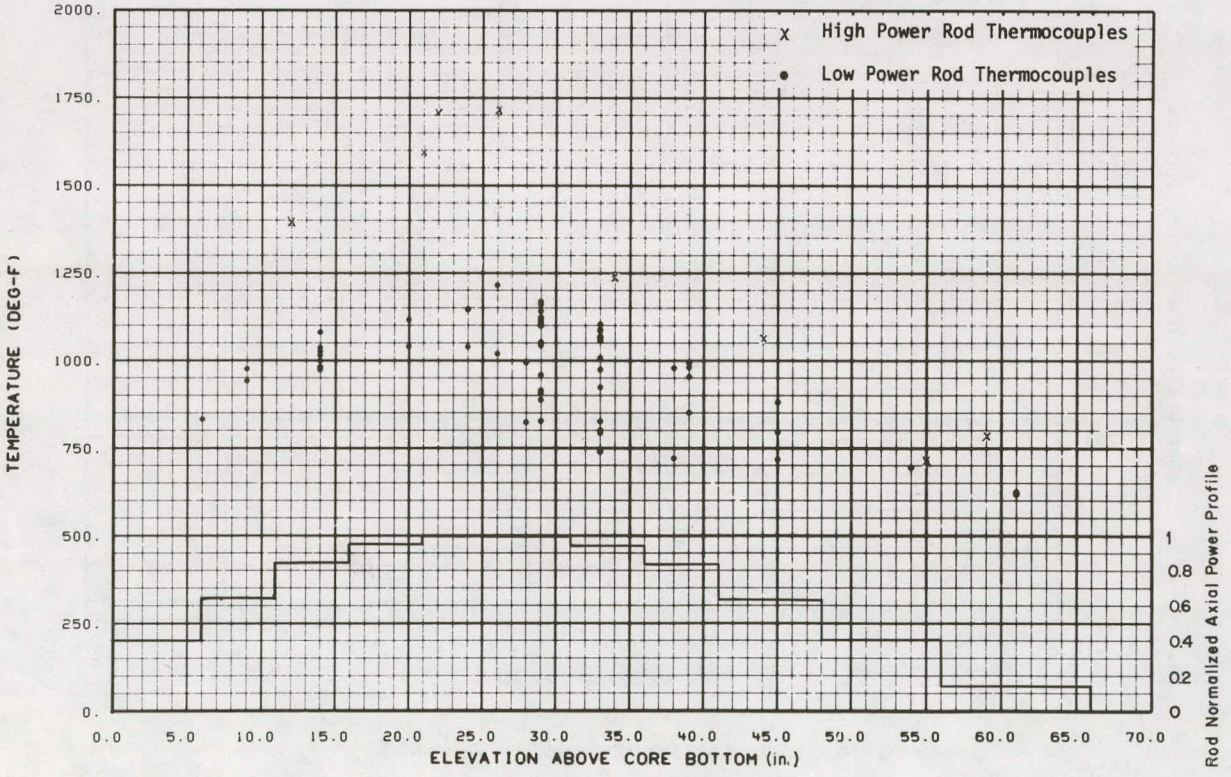

Fig. 16 Maximum cladding temperatures versus elevation – Test S-02-3.

The high power rod cladding temperature behavior presented in Figure 13 was typical of the response of the high power rods in Test S-02-3. Axial locations at and below the hot spot experienced early DNB, whereas locations above the hot spot generally indicated delayed DNB (about four seconds) or no DNB. The cladding temperature response presented in Figure 14 was also fairly typical of the low power rods. DNB usually occurred at and below the hot spots of the rods about four seconds after rupture. Upper elevations on the lower power rods usually experienced delayed DNB and some rewetting or no DNB. Details of the DNB-rewet characteristics are discussed in a later section of this report (Section III-3).

1.2 Heater Rod Response to Core Flow Magnitude

The immediate core flow reversal shown in Figure 8 for Test S-02-3 occurred in all the Semiscale cold leg break tests. Small variations in the magnitude or duration of the reversal were noted, however, in the data from Test S-02-2, S-02-3, and S-02-4. The effects of these core flow variations on the heater rod cladding temperature behavior are discussed in the following paragraphs. The reasons for the core flow variations, discussed in detail in Reference 11, are primarily due to the effects of break flow and intact loop pump behavior.

The behavior of high power rods during all three tests should be directly comparable because these rods were operating at the same initial peak power density of 14.25 kW/ft. The low power rods, however, were operated at 11.54 kW/ft peak power for Test S-02-4 and 8 kW/ft for Tests S-02-2 and S-02-3 (both 75% power tests). Therefore, differences between Test S-02-4 and Tests S-02-2 and S-02-3 in the behavior of the low power rods cannot be attributed to core flow differences only.

Figures 17 and 18 show the core inlet flow and high power rod, hot spot cladding temperature (26-inch elevation on Rod E4) from Tests S-02-2 and S-02-3. As shown in Figure 17, the core flow reversal was larger in magnitude and somewhat longer in duration during Test S-02-3 than it was during Test S-02-2. This difference in core flow is not reflected significantly in the high power cladding temperatures presented in Figure 18. The time to DNB was about the same (0.4 to 0.5 second) and the post-DNB cladding temperature response was nearly identical until 15 seconds after rupture. Figure 19 shows the heat transfer coefficient at the 26-inch elevation on Rod E4. The heat transfer coefficient for Test S-02-3 is larger than the coefficient for Test S-02-2 for the period between one and seven seconds. Since the cladding temperatures were nearly identical for this period, the difference in the heat transfer coefficients apparently were mainly due to differences in the fluid temperature. The fluid temperature differences were in turn a result of the initial test specifications. The deviation of the two temperatures shown in Figure 18 subsequent to 15 seconds appears to be due to the core flow differences between Tests S-02-2 and S-02-3. Comparison of the Test S-02-2 and Test S-02-3 core mass flow rates indicates that core stagnation occurred in Test S-02-2 from seven seconds on, whereas, for

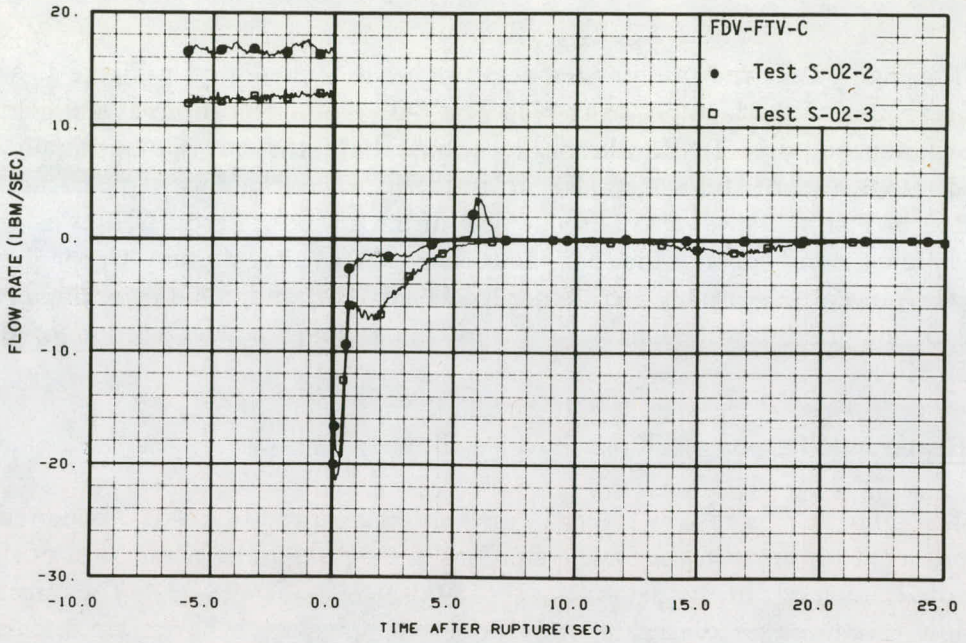

Fig. 17 Core inlet mass flow rate – Tests S-02-2 and S-02-3.

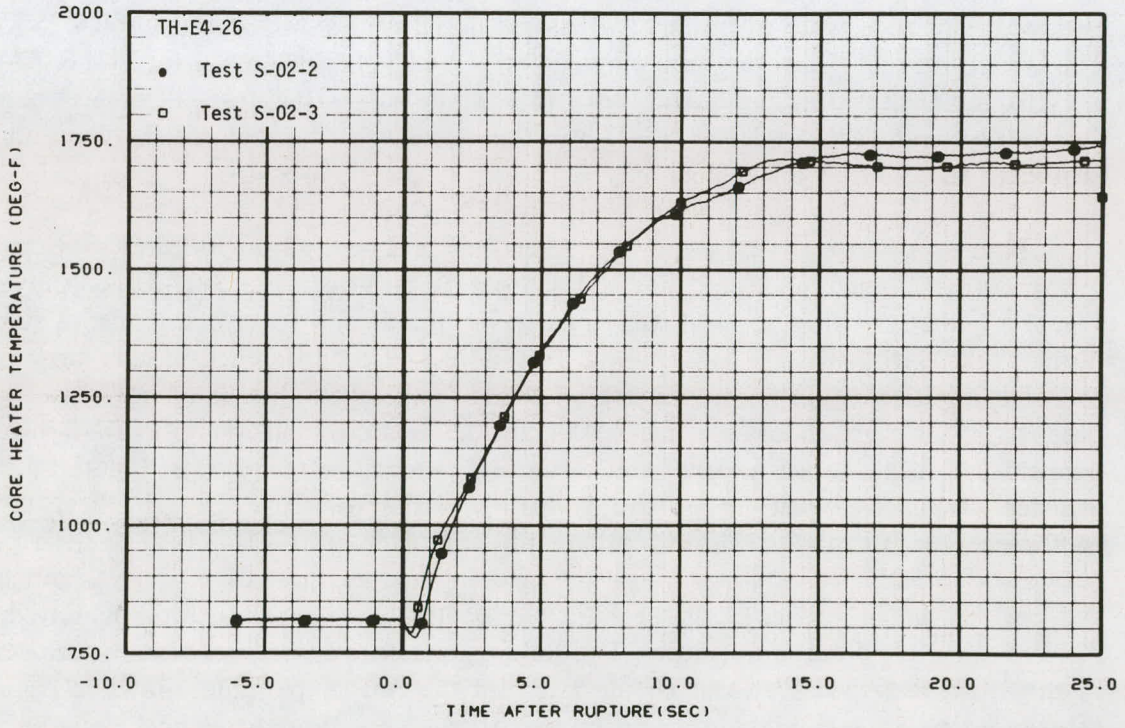

Fig. 18 Cladding temperature at 26-inch elevation on Rod E4 – Tests S-02-2 and S-02-3.

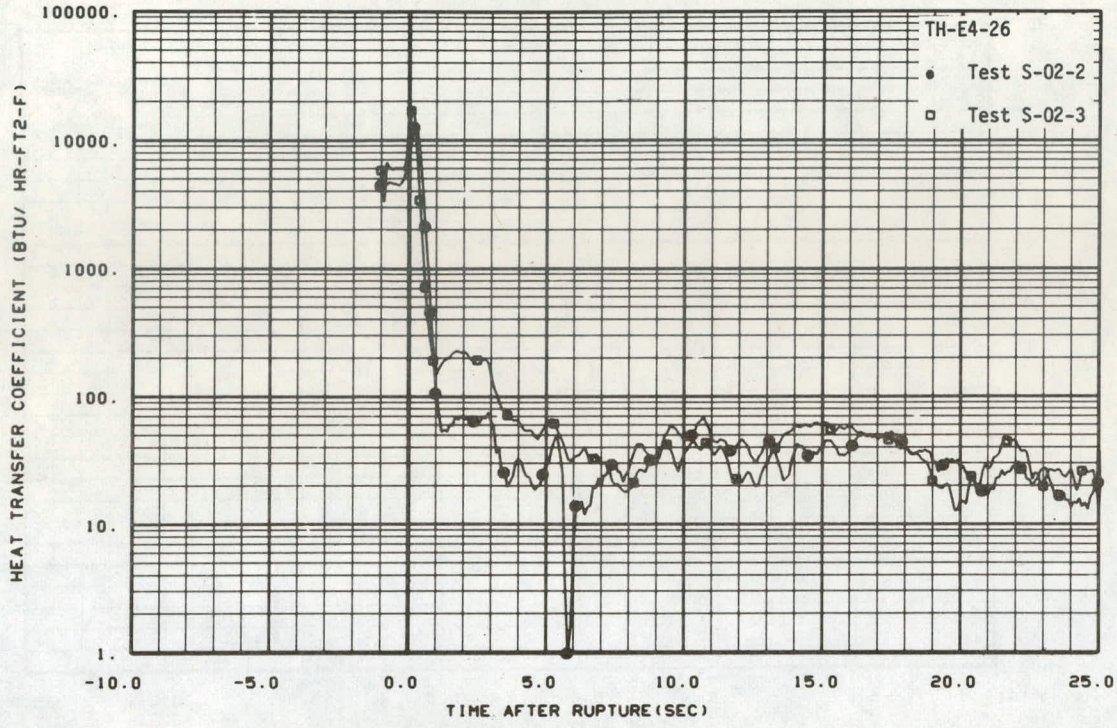

Fig. 19 Heat transfer coefficient at 26-inch elevation on Rod E4 – Tests S-02-2 and S-02-3.

Test S-02-3, a small reverse flow is indicated between 14 and 19 seconds. This reverse flow results in a slight cooling effect as evidenced by the turnover in the Test S-02-3 temperature profile on Figure 18. The core flow measurement during Test S-02-2 indicated a small positive spike in flow between 5.5 and 6.5 seconds, but this flow surge did not affect the core cooling. Apparently, the flow surge penetrated only to the core inlet and did not progress into the heated core. The volumetric core inlet flows from Tests S-02-2 and S-02-3 are compared in Figure 20. Differences in the flows between the two tests are amplified in the figure because the data are presented in gallons per minute.

The larger core flow reversal during Test S-02-3 relative to that of Test S-02-2 had an effect on the behavior of the low power rods. DNB occurred at and below the high power zone usually about four seconds after rupture although a few of the lower elevations experienced earlier DNB. Rewetting also occurred at some of the high power zone locations. In Test S-02-2, several of the high power zone locations experienced DNB at one second after rupture and subsequent rewets, whereas others experienced DNB at about four seconds. Comparison of results for elevations above the hot spot on the low power rods indicates generally similar response during the two tests. Times to DNB were usually about the same although, in some instances, the thermocouples indicated DNB earlier during Test S-02-2. Rewetting was more frequent in the upper core during Test S-02-3 than it was during Test S-02-2. During Tests S-02-2 and S-02-3, the thermocouples at elevations below the high power zone exhibited significant differences in thermal behavior. In Test S-02-2, these thermocouples usually indicated DNB at one second after rupture, whereas in Test S-02-3,

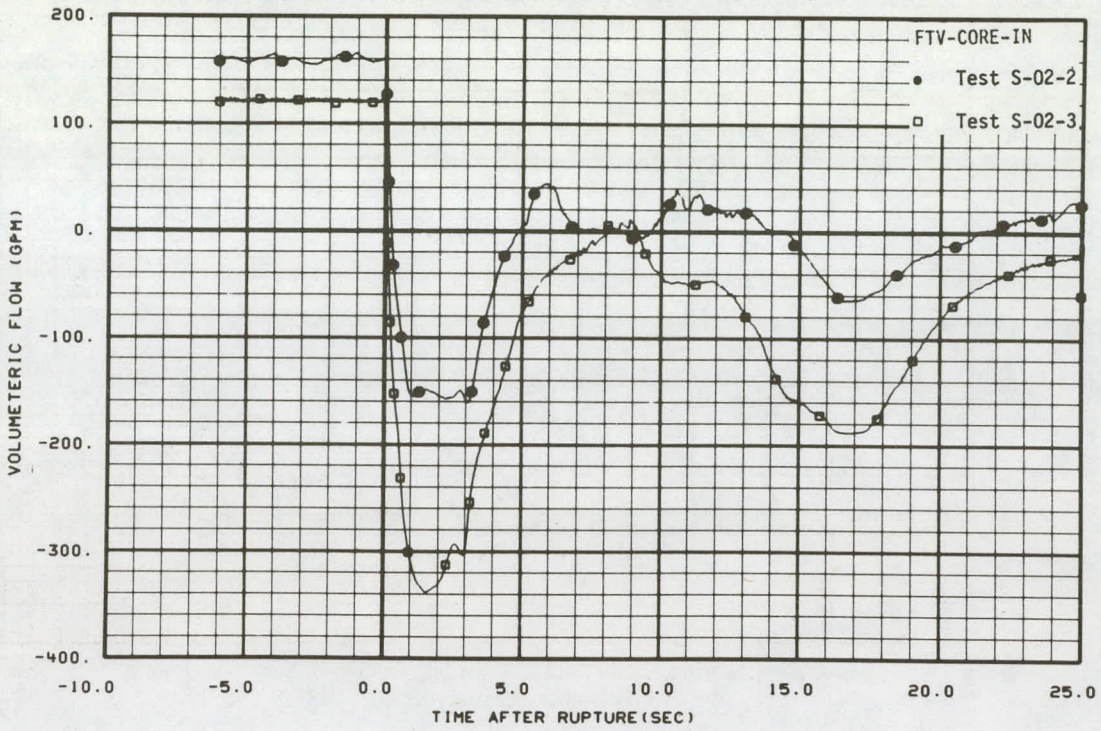

Fig. 20 Volumetric flow at core inlet – Tests S-02-2 and S-02-3.

DNB occurred at about four seconds after rupture. Figures 21 and 22 show the response at the 14-inch elevation on Rod F4 and at the 26-inch elevation on Rod F5 (Thermocouples TH-F4-14 and TH-F5-26) during the two tests and illustrate some of the differences discussed.

In general, the post-DNB heat transfer on the low power rods appears to have been better during Test S-02-3 than during Test S-02-2. Comparison of the cladding temperature data obtained from thermocouples common to both tests indicates for the most part that the peak temperatures attained in Test S-02-3 were lower than those reached in Test S-02-2. This difference in maximum temperatures was caused by the differences between the two tests in times to DNB and rewetting characteristics of the low power rods, which in turn were due mainly to core flow differences.

The cladding temperature responses of the high power Rod E4 during Tests S-02-3 and S-02-4, compared in Figure 23, indicate that the cladding temperature was slightly higher throughout the transient in Test S-02-3 and the time to DNB was shorter[a]. The core inlet flow and heat transfer coefficients (at the 26-inch elevation on Rod E4) during

[a] The two temperatures compared in this figure are not from the same rod because all the high power rods were replaced between Tests S-02-3 and S-02-4.

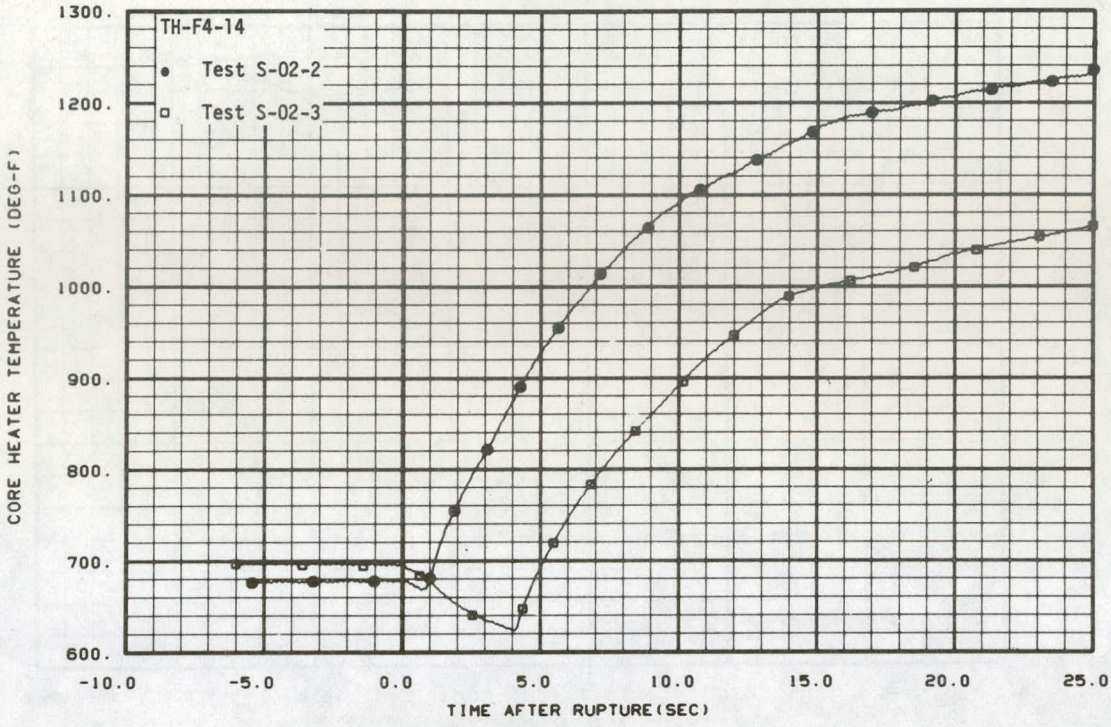

Fig. 21 Heater rod response at Thermocouple TH-F4-14 – Tests S-02-2 and S-02-3.

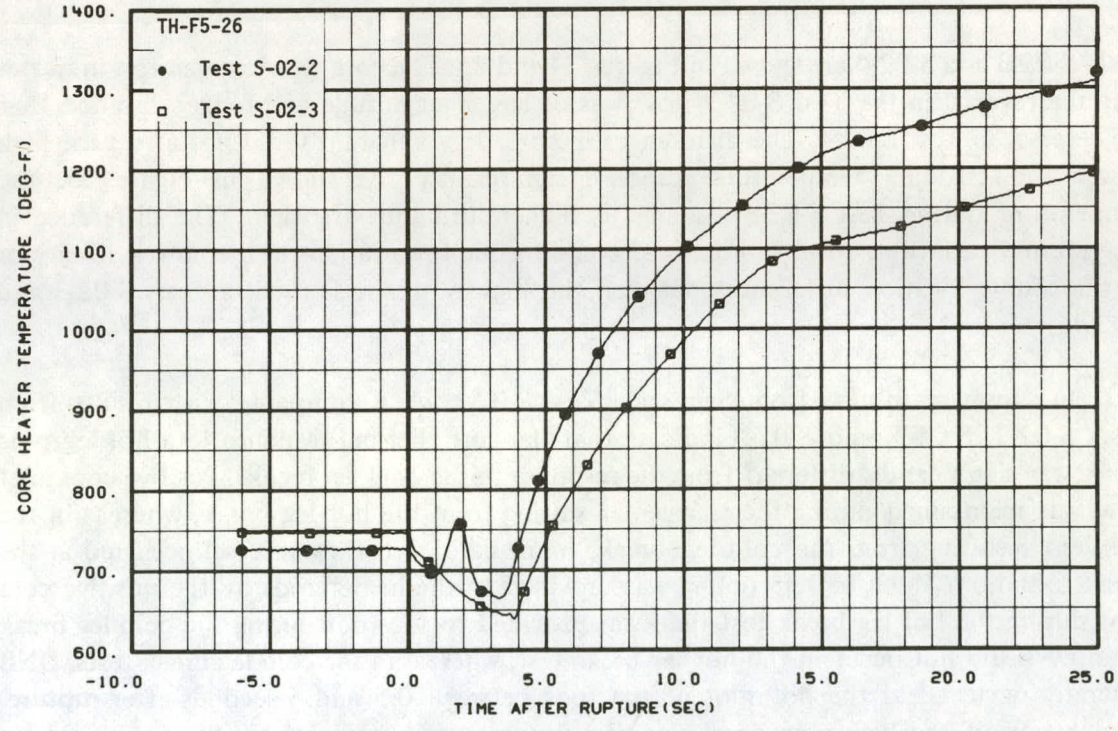

Fig. 22 Heater rod response at Thermocouple TH-F5-26 – Tests S-02-2 and S-02-3.

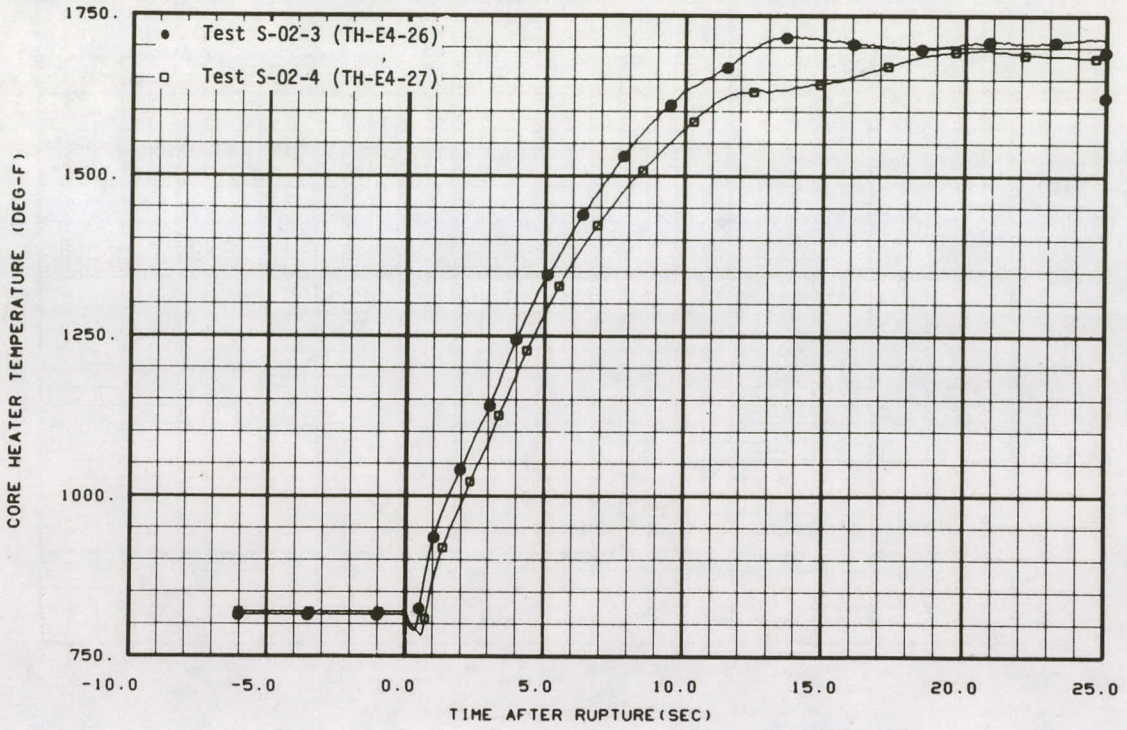

Fig. 23 Cladding temperature at hot spot on Rod E4 – Tests S-02-3 and S-02-4.

Tests S-02-3 and S-02-4 are shown in Figures 24 and 25. The core flow comparison indicates that the reversal in the Test S-02-3 flow was of larger magnitude and longer duration than the reversal in Test S-02-4. The differences in core flow apparently did not affect the high power rod cladding temperature response significantly. As shown in Figure 23, the temperature during Test S-02-3 was slightly higher during the transient. The difference in temperature behavior shown in Figure 23 could be due to variations in the power density or thermocouple location differences between the high power rods used in Tests S-02-3 and S-02-4.

In summary, results from Semiscale Test S-02-1 when compared with results from Tests S-02-2, S-02-3, and S-02-4 indicate that the core thermal response to a hot leg pipe break was significantly different from the response to the cold leg breaks. Positive core inlet flow was maintained during the transient resulting from the hot leg break, whereas in the transient resulting from the cold leg break, immediate core flow reversal occurred at the break initiation. Much better cooling was provided to the heater rods by the positive core flow during the hot leg break test than was provided to the rods during the cold leg break tests. DNB did not occur in the hot leg break test, whereas in the cold leg break tests, DNB generally occurred at the hot spot of the rods between 0.5 and 5 seconds after rupture. Comparison of the high power rod cladding temperature behavior from the three cold leg break tests indicated minimal differences. Therefore, the conclusion reached was that the small variation in core inlet flow noted among these tests had relatively little effect on the

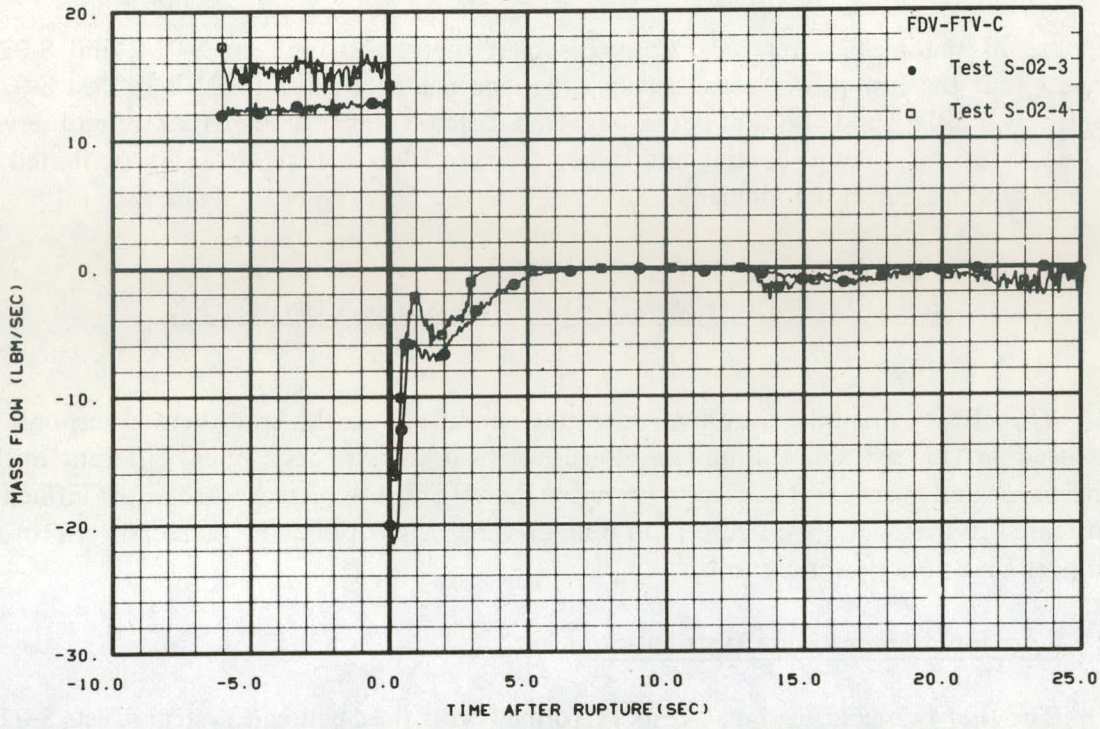

Fig. 24 Core inlet flow rate – Tests S-02-3 and S-02-4.

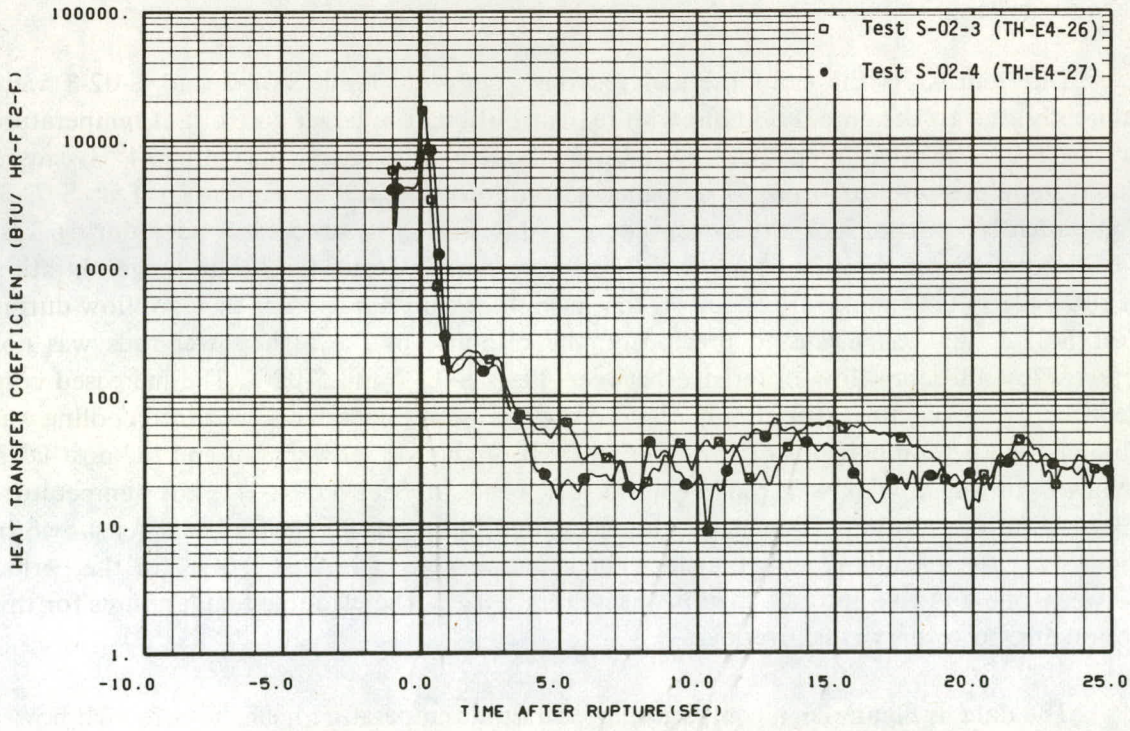

Fig. 25 Heat transfer coefficient at Rod E4 hot spot – Tests S-02-3 and S-02-4.

response of the high power rods. Comparison of the results of Tests S-02-2 and S-02-3 showed that the low power rods usually experienced longer times to DNB in Test S-02-3 than in Test S-02-2 and also that better post-DNB core cooling characteristics were observed in Test S-02-3. The better cooling and longer times to DNB in Test S-02-3 are attributed to the increased magnitude and longer duration of the core flow reversal for that test.

2. INFLUENCE OF SPECIFIED OPERATING CONDITIONS

The effect of specified system operating conditions on the core thermal response is discussed in this section. During the blowdown heat transfer test series, different initial conditions and post-DNB controls were imposed on the system. Areas of influence considered in this section are core fluid temperature distribution, core radial power profile, and post-DNB core power control.

2.1 Core Fluid Temperature Distribution

The first two cold leg break tests performed with the Semiscale system (Tests S-02-2 and S-02-3) were conducted at 75% (1.2 MW) of rated initial core power. These tests were designed primarily so that experience relative to the heat transfer characteristics of the electrical core could be gained with minimal risk of core damage. Different initial core fluid conditions were obtained in these two tests by controlling the initial core flow rate to achieve the desired core outlet temperature while maintaining the same inlet temperature between tests.

Differences in the core thermal response between Tests S-02-2 and S-02-3 were indirectly due to the core fluid temperature distribution. The larger core outlet temperature in Test S-02-3 relative to that of Test S-02-2 (about 610°F compared with 594°F) caused the system pressure to drop to a higher saturation pressure at rupture in Test S-02-3. Consequently, portions of the system were maintained in a subcooled state during Test S-02-3 for a longer period of time than they were during Test S-02-2. This longer duration of subcooling had significant effect on the magnitude and duration of the core flow during Test S-02-3. As was discussed previously, the response of the high power rods was not affected by the core flow difference between Tests S-02-2 and S-02-3. The increased core flow did, however, provide better cooling to the low power rods. This enhanced cooling was observed in the comparisons of the time to DNB of the low power rods and the post-DNB behavior of the low power rods. As was discussed in Section III-1.2, the temperature distribution does affect the value of the calculated heat transfer coefficients. As shown in Figure 21, the calculated heat transfer coefficient was larger in Test S-02-3 for the period between one and five seconds than it was in Test S-02-2. The cladding temperatures for this period are, however, virtual overlays.

The data in Figure 26, a comparison of the fluid temperature near the core high power zone during Tests S-02-2 and S-02-3, show that the fluid temperature in Test S-02-3 was higher than the fluid temperature in Test S-02-2 for the first five seconds after rupture. The

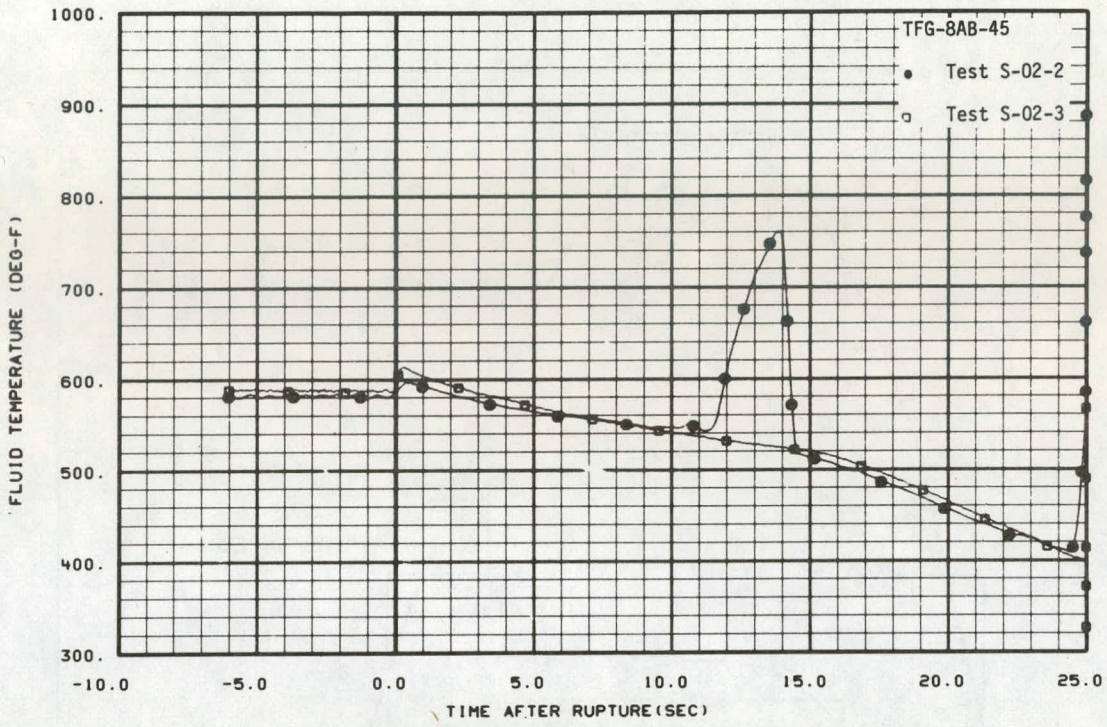

Fig. 26 Core fluid temperature near rod high power zone – Tests S-02-2 and S-02-3.

differences in heat transfer coefficients and core fluid temperatures between Tests S-02-2 and S-02-3 are then consistent with the cladding temperature comparison. Any difference in fluid temperature tends to disappear between 6 and 11 seconds as the core flow stagnates.

2.2 Peaked Versus Radially Flat Power Distribution

As indicated in Table I, some of the blowdown heat transfer tests were conducted with a radially peaked core power distribution in which the four center rods were operated at a higher power density than the remaining rods, and some of the tests were conducted with a radially flat core power distribution in which all the rods were operated at the same power density. The purpose of this section is to identify the different heater rod axial power profiles used in the tests and to discuss their effect on the cladding temperature behavior.

Figures 27 and 28 show the heater rod axial power distributions imposed on the heater rods for the peaked and flat radial full power tests, respectively. Implementation of the flat radial power profile removed the distinction of "high" and "low" power rods and, consequently, eliminated the hot fluid channel previously formed by the center four high power rods. As shown in Table II, which presents a summary of the peak cladding temperatures attained in each test, larger maximum temperatures were attained in the tests conducted with peaked radial core power distributions (Tests S-02-2, S-02-3, S-02-4, and S-02-5) because of the larger power density of the high power rods. All of the peaked power

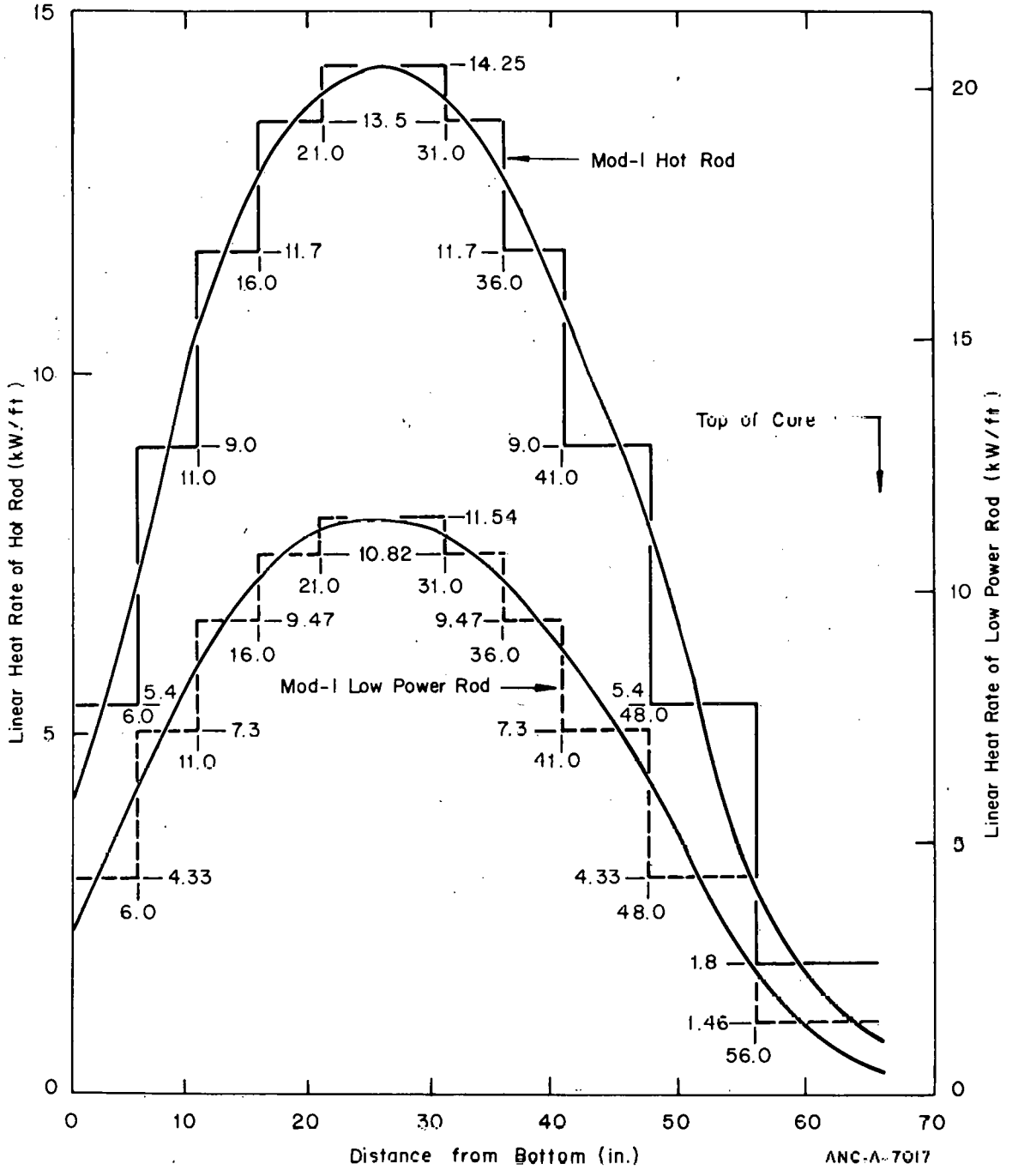

Fig. 27 Heater rod axial power distributions for the peaked radial power profile – Tests S-02-4 and S-02-5.

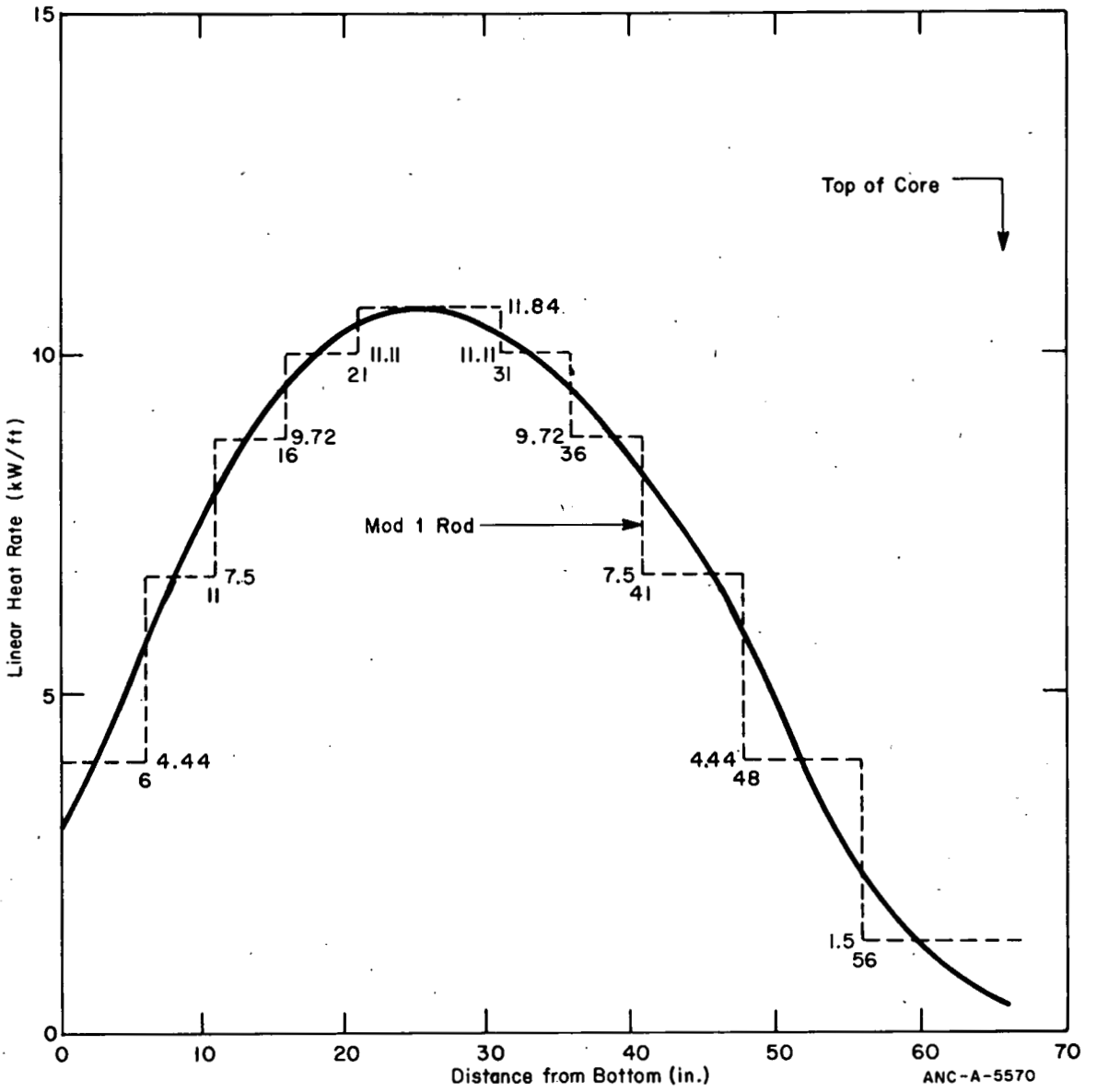

Fig. 28 Heater rod axial power distribution for the flat radial power profile – Tests S-02-7, S-02-9, and S-02-9A.

distribution tests were conducted with the high power rods operated at a peak power density of 14.25 kW/ft. The low power rods in Tests S-02-2 and S-02-3 were operated with a peak power density of 8 kW/ft, whereas in Tests S-02-4 and S-02-5, these rods were operated at 11.5 kW/ft. These power density differences account for the similarities in the peak temperature of the high power rods and the dissimilarity in the maximum temperature on the low power rods among the four peaked power distribution tests.

The flat radial power distribution tests (Tests S-02-7, S-02-9, and S-02-9A) were conducted with a maximum peak power of 11.8 kW/ft on all of the rods. The peak cladding temperatures attained were not the same in these three tests because a different core power

TABLE II

MAXIMUM CLADDING TEMPERATURES MEASURED DURING BLOWDOWN HEAT TRANSFER TEST SERIES

	Radially Peaked Core Power Profile				Radially Flat Core Power Profile	
	High Power Rod[a]		Low Power Rod			
Test	Thermocouple	Temperature (°F)	Thermocouple	Temperature (°F)	Thermocouple	Temperature (°F)
S-02-2	TH-E5-27	1,779	TH-F5-26	1,362		
S-02-3	TH-E4-26	1,717	TH-F3-24	1,147		
S-02-4	TH-E5-25	1,729	TH-D6-25	1,590		
S-02-5	TH-E4-27	1,798	TH-F3-24	1,665		
S-02-7					TH-D8-25	1,584
S-02-9A					TH-F3-25	1,493
S-02-9					TH-A5-29	1,476

[a] Only the maximum measured cladding temperature is presented.

control was used in Test S-02-7 than was used in Tests S-02-9A and S-02-9. The peak cladding temperature reached in Test S-02-7 was, however, about the same as the peak attained on the low power rods during the peaked radial power distribution Test S-02-4. Transient cladding temperature comparisons between Tests S-02-4 and Test S-02-7 indicate very similar behavior of the rods that had essentially the same power density in the two tests. A comparison of the response of Thermocouple TH-F2-25 during the two tests is shown in Figure 29. This figure illustrates the general trends of the majority of the cladding temperature comparisons from rods in these two tests that were operated at essentially the same power density. The results from Test S-02-7 generally indicate a slightly higher heatup rate for the period between 2 and 20 seconds which is due to the slightly larger power density employed on the rods during Test S-02-7 (11.8 versus 11.5 kW/ft). Other comparisons of Test S-02-4 and Test S-02-7 data have revealed that a larger number of the low power rod hot spots experienced rewetting during Test S-02-4 than during Test S-02-7. This trend in the data could also be related to the slight differences in rod power density employed during the two tests. A comparison of the hot spot cladding temperature response of Rod E4 during the same two tests is shown in Figure 30. This figure illustrates the difference in the cladding temperature behavior due to the radially peaked core power distribution versus the flat power distribution in the core (14.25 kW/ft compared with 11.8 kW/ft). The two profiles shown in Figure 30 indicate almost exactly the same time to DNB even though substantial difference existed in the initial power density.

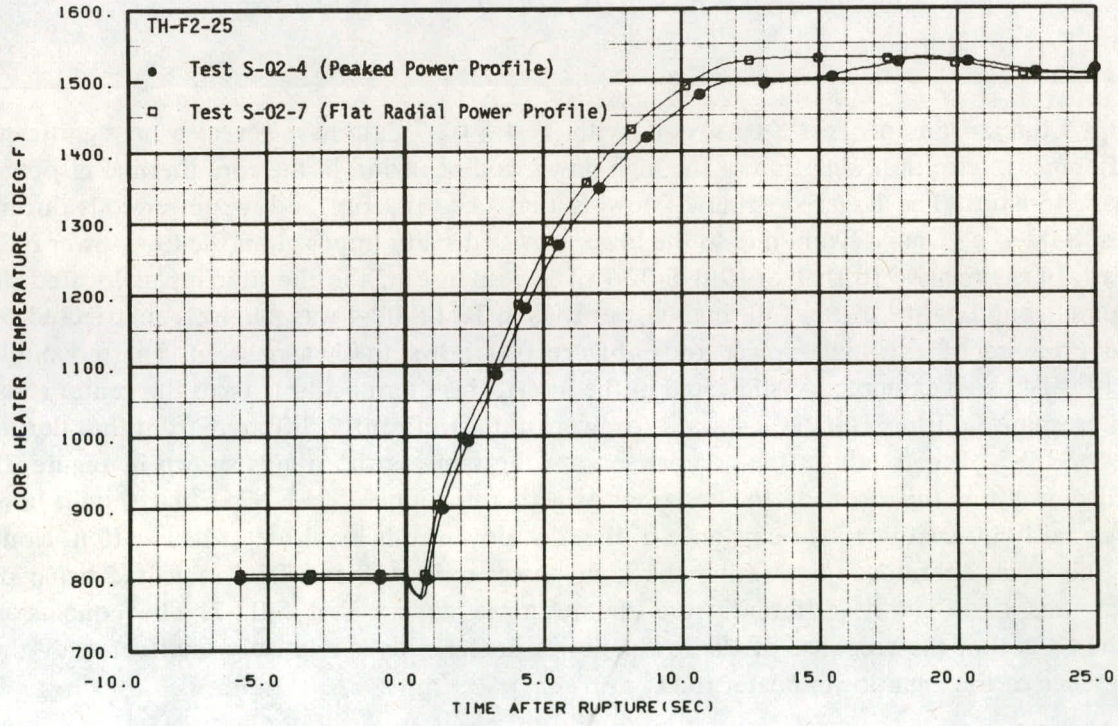

Fig. 29 Response of Thermocouple TH-F2-25 – Tests S-02-4 and S-02-7.

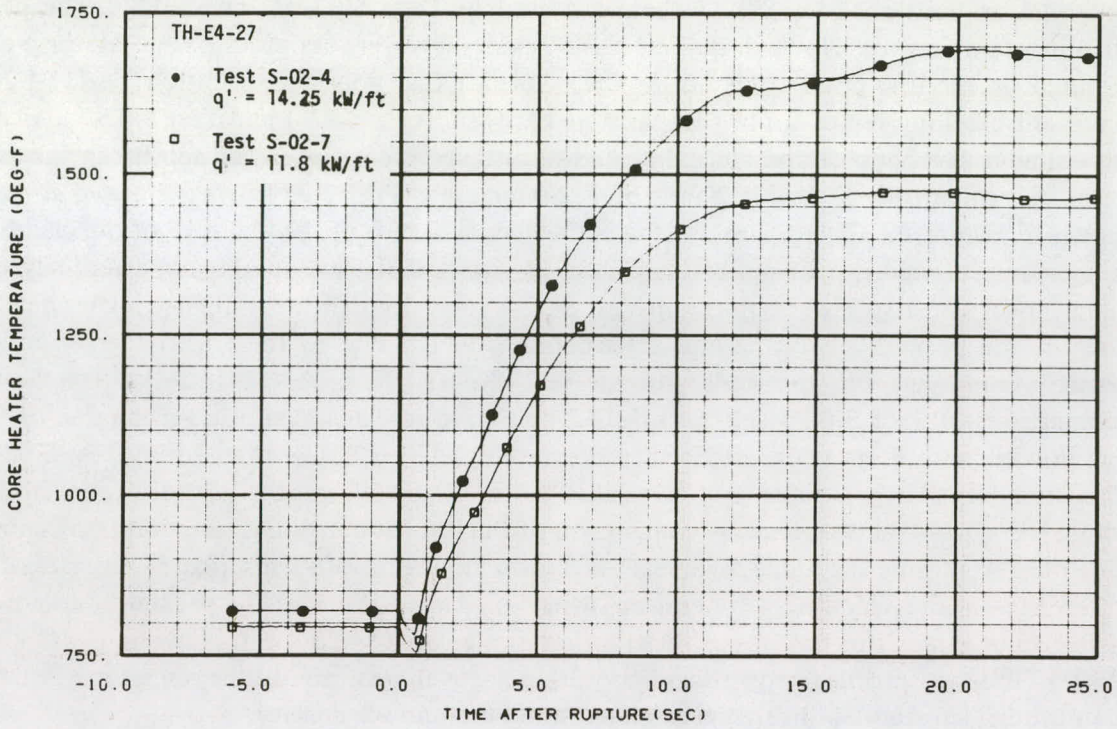

Fig. 30 Response of Thermocouple TH-E4-27 – Tests S-02-4 and S-02-7.

Comparisons of Test S-02-4 data with Test S-02-7 data have revealed no significant differences, with the exception of the high power rod behavior, in the core thermal response characteristics. The larger number of rewets that occurred on the low power rods during Test S-02-4 was most likely due to the lower power density imposed on the low power rods in that test, relative to that of Test S-02-7. The response of the thermocouples located on rods surrounding the center four high power rods in Test S-02-4 was relatively unaffected by the presense of the high power rods. Figure 31 shows the response of Thermocouple TH-F4-14 as an example. As indicated in the insert, this thermocouple faces the center rods. The response during Test S-02-4 was, however, not significantly different from that during Test S-02-7. The trends in the comparison are the same as the trends shown in Figure 29 which was a comparison of the response of a thermocouple (TH-F2-25) that should have been fairly insensitive to the existence of the high power rods by virtue of its location. None of the other thermocouples facing the high power rods in Test S-02-4 indicated behavior that was significantly different from the response during Test S-02-7. The conclusion reached is that the response of the lower power heater rods is relatively unaffected by the presence of the high power heater rods.

2.3 Post-DNB Core Power Control

Five of the tests (Tests S-02-1, S-02-2, S-02-3, S-02-4; and S-02-7) conducted with the Semiscale system utilized the core power control shown in Figure 7. The other tests, however, utilized improved versions of power control designed so that the Semiscale

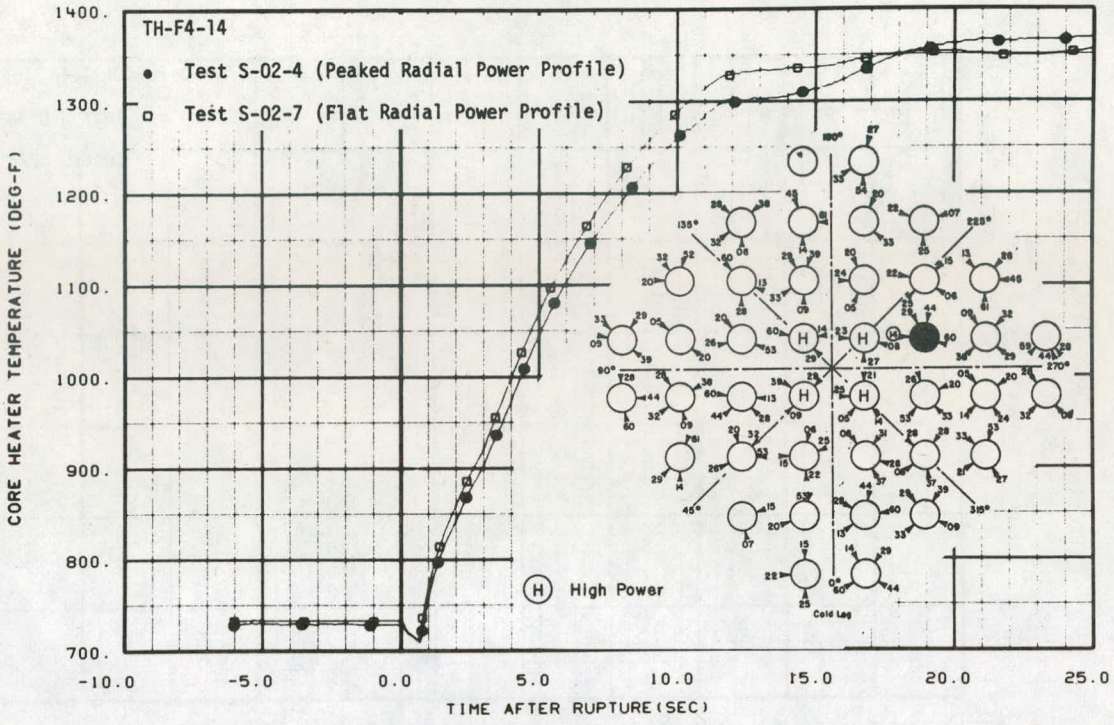

Fig. 31 Response of Thermocouple TH-F4-14 – Tests S-02-4 and S-02-7.

electrical rod response would more closely simulate the response expected of a nuclear rod. An explanation of the method used to determine the improved power control is contained in Appendix A.

The electrical core powers used for Tests S-02-4 and S-02-5 are shown in Figure 32. The significant feature of the electrical power for Test S-02-5 is that the power was maintained at 100% for about four seconds after rupture. This full power period helped compensate for differences in the thermal diffusivity between the nuclear and electrical rod material properties. The difference in core power control used during Tests S-02-4 and S-02-5 did not affect the time to DNB at the rod hot spots. The behavior exhibited by Thermocouple TH-D5-29, as shown in Figure 33 for example, indicates the same time to DNB for both tests. The effects of the new power control used in Test S-02-5 are evident at about one second on the Test S-02-5 behavior. In comparison with the Test S-02-4 behavior, the Test S-02-5 temperature trace was much steeper for the period between one and six seconds mainly because of the differences between the two tests in the total amount of power (integrated power) applied to the core over the first eight seconds. The data of Figure 33 indicate that the two temperature profiles tend to converge at about 18 seconds which is coincidental with convergence of the core power profiles. The cladding temperature response shown in Figure 33 was typical of the response of the hot spot of every high power rod during Tests S-02-4 and S-02-5. The different trends in this response are also typical of the behavior of the hot spot on the low power rods.

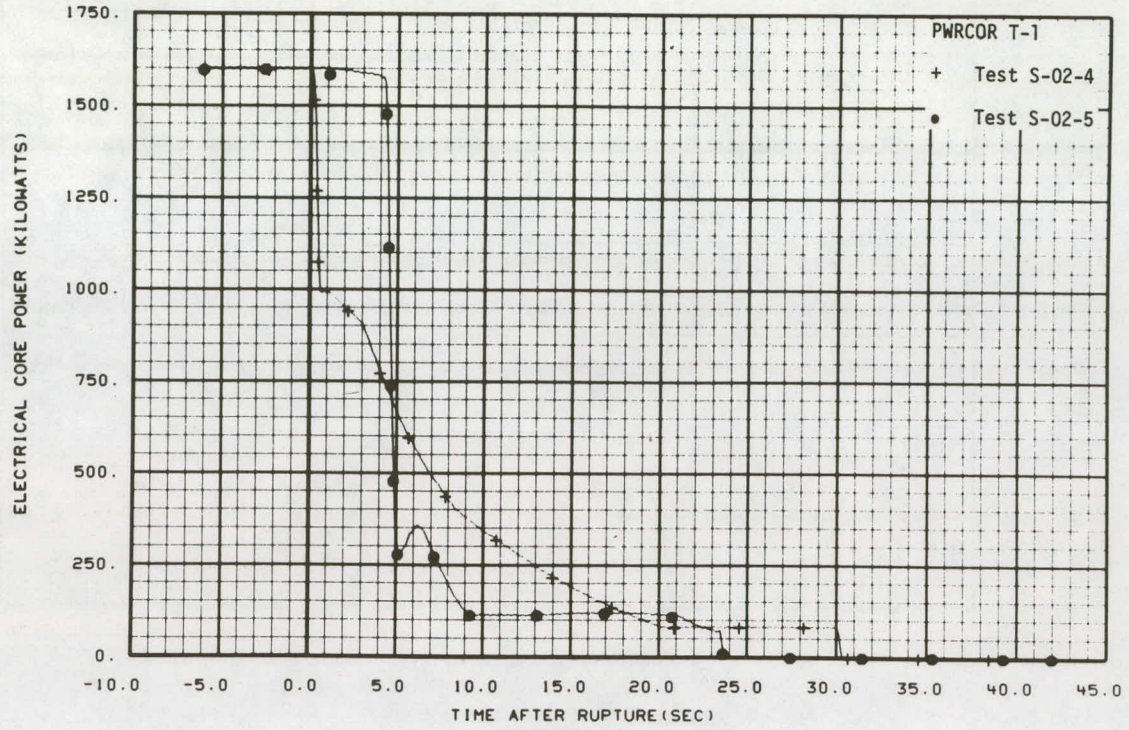

Fig. 32 Electrical core power control – Tests S-02-4 and S-02-5.

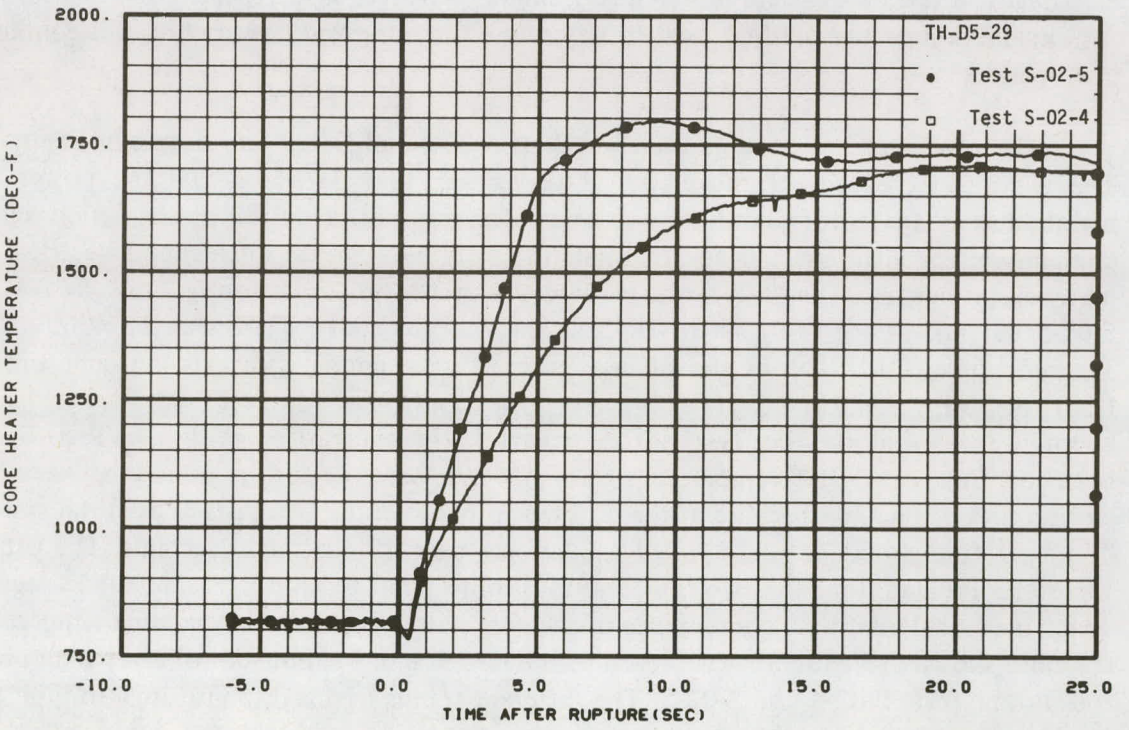

Fig. 33 Response of Thermocouple TH-D5-29 – Tests S-02-4 and S-02-5.

The electrical core power traces used for Tests S-02-7, S-02-9A, and S-02-9 are shown in Figure 34. As was the case in Test S-02-5, the data in Figure 34 show that the power was maintained at 100% for about 2.8 seconds after rupture in Tests S-02-9A and S-02-9. Figure 35 shows a comparison of the response of Thermocouple TH-F2-25 during Tests S-02-7 and S-02-9. The general trends in the differences in rod cladding temperature response are similar to those shown in Figure 33 for Tests S-02-4 and S-02-5. The following generalizations can be made concerning the effect of the improved post-DNB core power control on the rod cladding temperature response:

(1) The temperature change with time was more severe (steeper slope) for the period between one and six seconds after rupture

(2) The cladding temperatures usually reached a maximum between eight and ten seconds after rupture

(3) The cladding temperatures usually turned over after peaking.

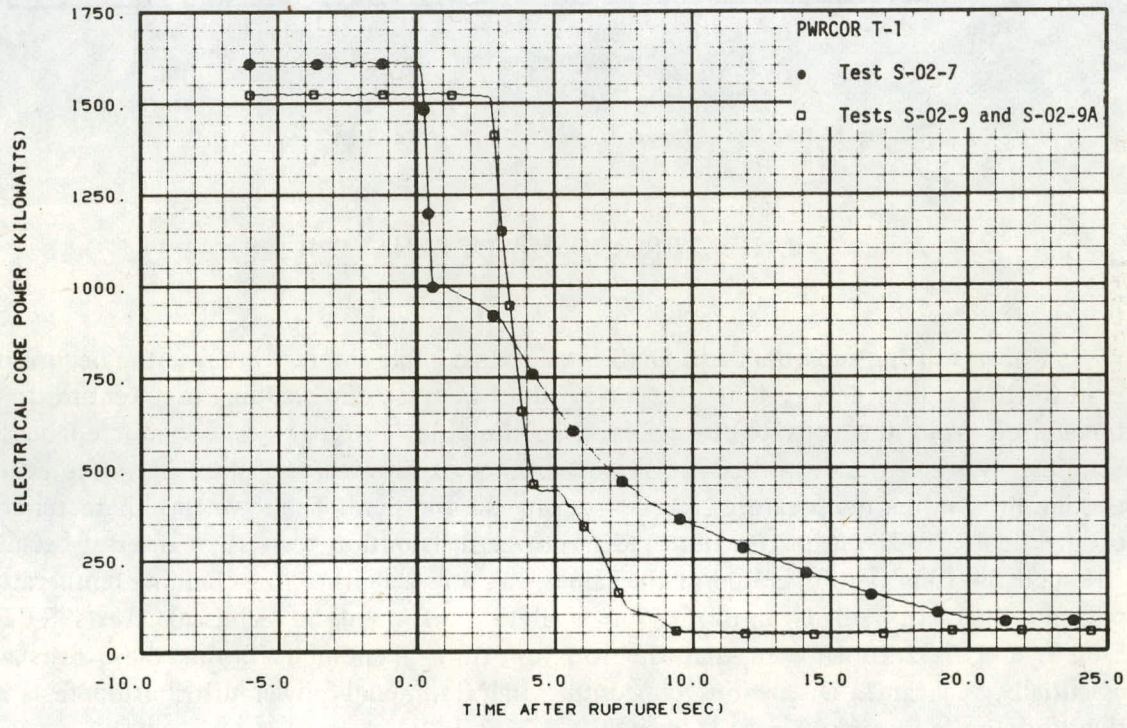

Fig. 34 Electrical core power control – Tests S-02-7, S-02-9, and S-02-9A.

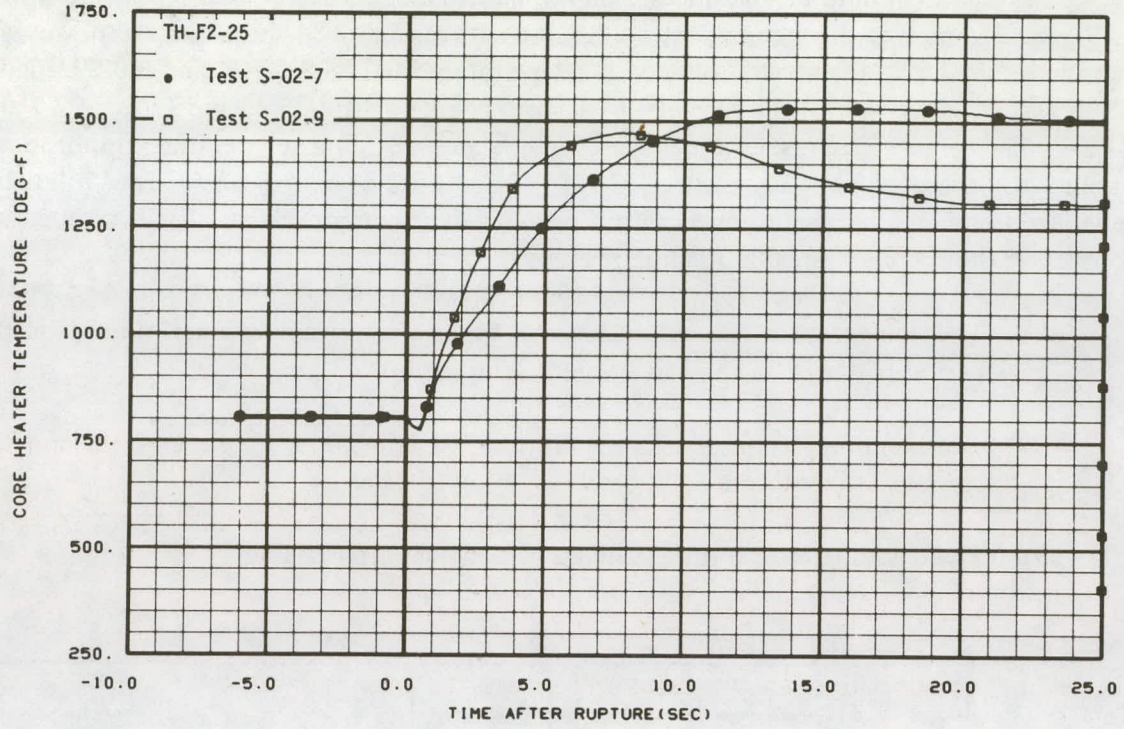

Fig. 35 Response of Thermocouple TH-F2-25 – Tests S-02-7 and S-02-9.

3. HEATER ROD REWET BEHAVIOR

Rod rewetting subsequent to DNB is of considerable interest because the occurrence of rewetting causes energy that otherwise would increase the cladding temperature to be transferred from the rods to the coolant. In the cold leg break tests conducted on the Semiscale system, the occurrence or nonoccurrence of rewetting substantially affected the maximum cladding temperatures reached during the transient. The rewetting characteristics of the heater rods during the flat radial power distribution tests is of interest because, although the rods were operated at the same peak power density, the cladding temperature response was not radially uniform. The analysis performed on Semiscale Tests S-02-7, S-02-9, and S-02-9A showed that the rod rewetting phenomena during these tests was essentially the same. Discussions concerning the flat radial power distribution tests are therefore limited mainly to results from Test S-02-7.

3.1 General Rewet Behavior

Rewetting is the phenomena whereby fluid comes into contact with the heater rod surface after DNB has occurred. The fluid as it contacts the rod surface causes a significant increase in the heat transfer rate from the rod to occur until rod surface dryout again results in a degradation in the heat transfer. The occurrence of rewetting causes the energy that

would otherwise be stored in the rod (consequently causing the rod temperature to rise) to be removed from the rod. Rewetting is then an important consideration because a rewetted condition generally results in lower rod peak cladding temperature.

Results from the flat radial power profile tests indicate that a mixture of rewetting and nonrewetting in the cladding temperature response occurred at the rod high power zones. Some of the cladding thermocouples experienced an early DNB (approximately 0.5 second) with a resultant cladding temperature rise to about 1,500°F, and other thermocouples experienced an early DNB with subsequent rewet. This mixture of response is illustrated by the high power zone thermocouple data shown in Figure 36. A similar variety in cladding temperature behavior occurred at lower elevations in the core as shown in Figure 37. Analysis of the cladding temperature response from heater rods that had thermocouples at both the hot spot and lower core positions does not indicate any relation between the DNB and rewetting characteristics at the two axial locations. In some cases, both the hot spot and lower core thermocouples indicated DNB and rewet; and in other cases, the lower elevation experienced rewet, whereas the hot spot did not (and in other cases, the hot spot experienced rewet, whereas the lower elevation did not).

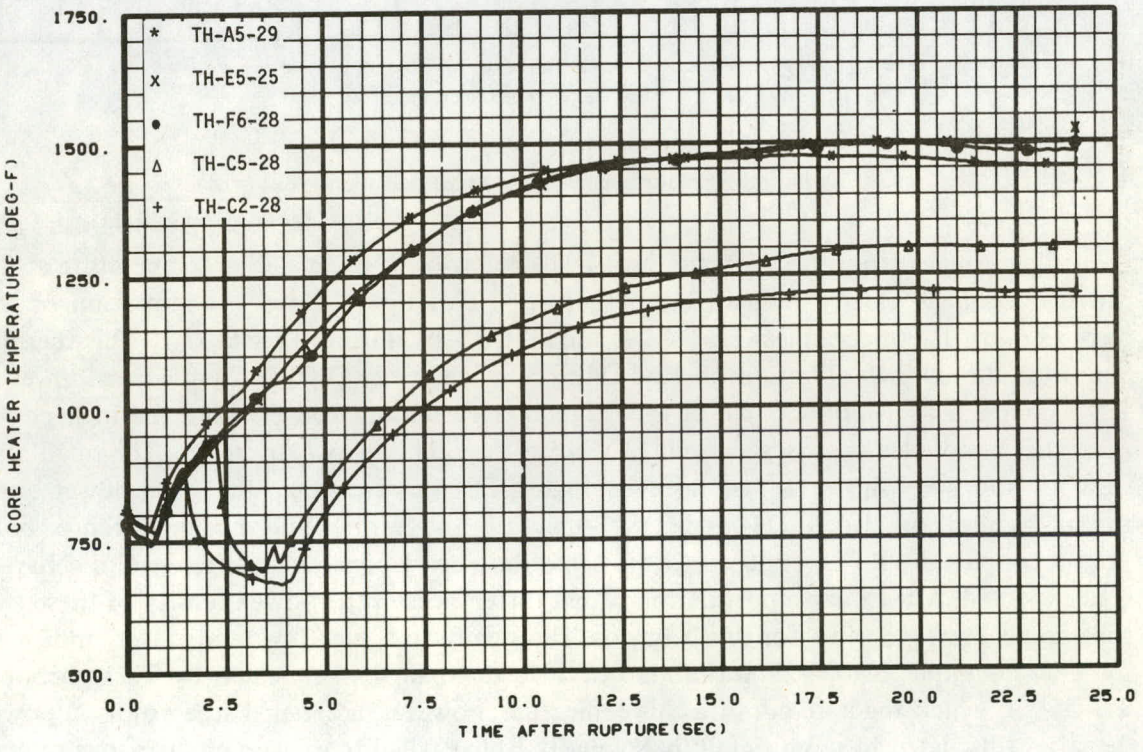

Fig. 36 Cladding temperature response at rod hot spots – Test S-02-7.

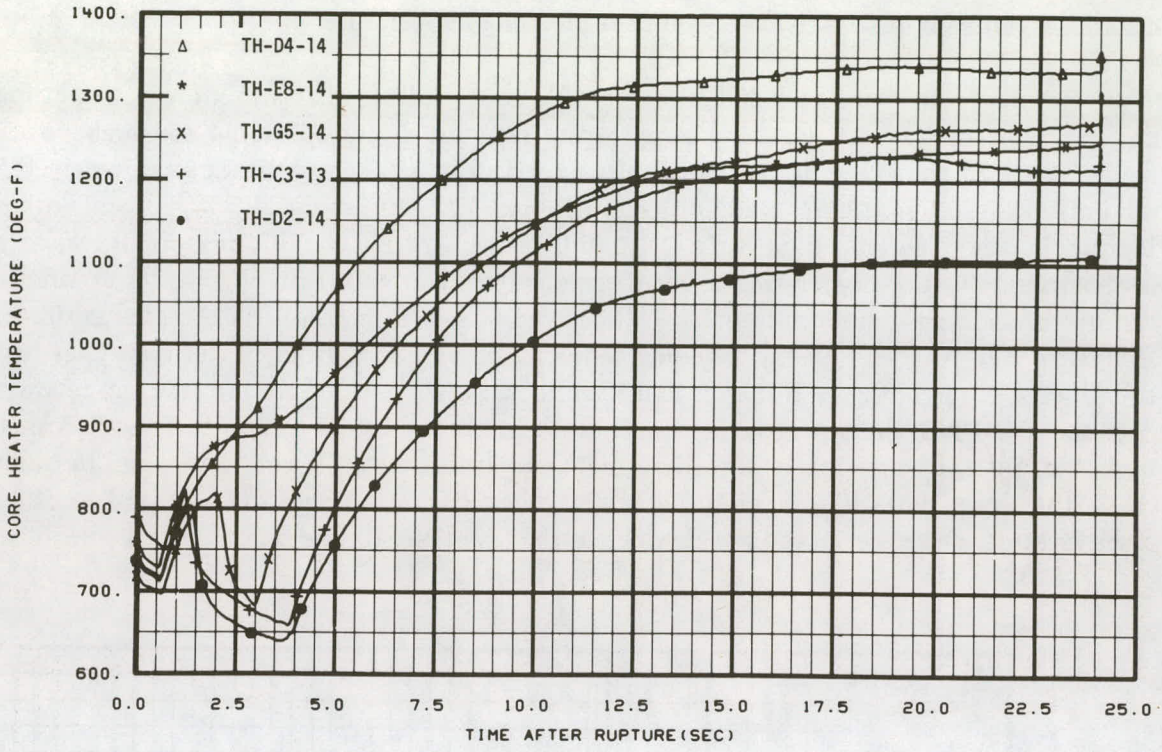

Fig. 37 Cladding temperature response at the 14-inch elevation – Test S-02-7.

The effect of rewetting on the post-DNB behavior of the cladding temperature at the rod hot spots is clearly indicated in Figure 38. This figure shows a comparison of the responses of Thermocouples TH-D4-29 and TH-D5-29 during Test S-02-7. The thermocouple at the 29-inch elevation on Rod D4 experienced early DNB and subsequent rewet at 1.5 seconds. The Thermocouple at the 29-inch elevation on Rod D5 (and the high power zone thermocouples on Rods E4 and E5), however, did not show any rewet. The small plan view of the core shown as an inset in Figure 38 indicates that the high power zone thermocouples on Rods D4 and D5 both face the same fluid channel. Since both thermocouples should be exposed to the same fluid conditions, their difference in behavior is unexpected. A reasonable postulation is that differences in the power density of these two rods could be responsible for this behavior. The steady state cladding temperature indicated by Thermocouple TH-D4-29 was about 10^{o}F lower than that indicated by Thermocouple TH-D5-29, which tends to confirm this conjecture; however, a detailed study of local power densities (discussed in more detail in Appendix B) has failed to explain comparisons such as those for Thermocouples TH-D4-29 and TH-D5-29.

As was stated previously, no rewets occurred at the hot spots of the high power rods during the radially peaked core power tests (Tests S-02-2, S-02-3, S-02-4, and S-02-5). However, some of the low power rods did experience rewetting in all four of these tests. Figures 39 and 40 are plan views of the Semiscale core showing the rewet phenomena at the rod high power zones (21- to 31-inch elevation) for Tests S-02-2 and S-02-3. Figure 39

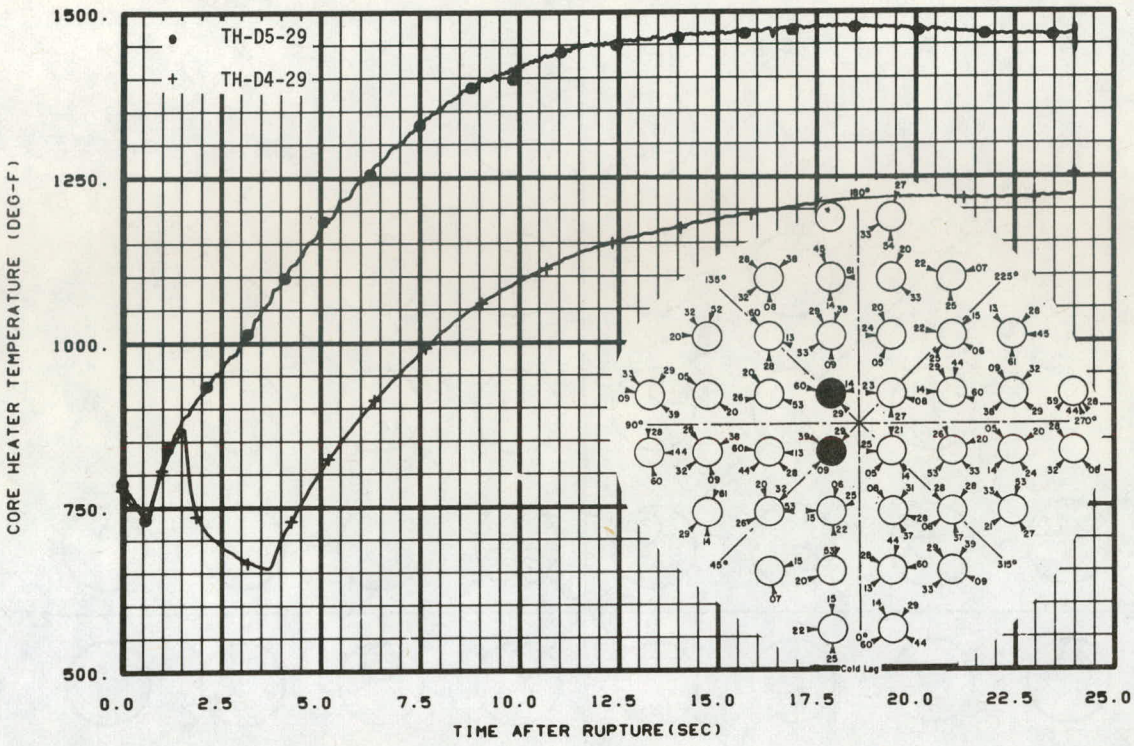

Fig. 38 Comparison of the response of two 29-inch elevation Thermocouples that both face the core central fluid channel – Test S-02-7.

shows the distribution of rewetting at the hot spot of the low power rods during Test S-02-2. Some radial locations experienced DNB at one second and a subsequent rewet (usually at about two seconds), whereas other locations experienced DNB at four seconds. Figure 40 shows that during Test S-02-3, the hot spots of the lower power rods all experienced either delayed DNB (at about four seconds) or delayed DNB with subsequent rewetting.

As was the case for Tests S-02-2 and S-02-3, rewetting occurred at the hot spots of the lower power rods during Tests S-02-4 and S-02-5. The cladding temperature response of the low power rods during Tests S-02-4 and S-02-5 was not radially uniform in behavior. Figures 41 and 42 show the mixture of rewets and nonrewets in the rod hot spot temperature behavior at the rod hot spot and at the 14-inch elevations, respectively, on the low power rods during Test S-02-5. Results from Test S-02-4 showed a similar mixture of rewets and nonrewets.

An interesting consideration shown in Figure 42 is the post-DNB response of Thermocouples TH-E8-14 and TH-F4-14. Neither of these thermocouples experienced rewetting; yet their post-DNB behavior (after two seconds) was considerably different from each other. Figure 43 shows the calculated heat transfer coefficients at the 14-inch elevations on Rod E8 and F4. This figure indicates the existence of radial variation in the post-DNB heat transfer, at this location, even in the absence of any rewetting. Figure 44

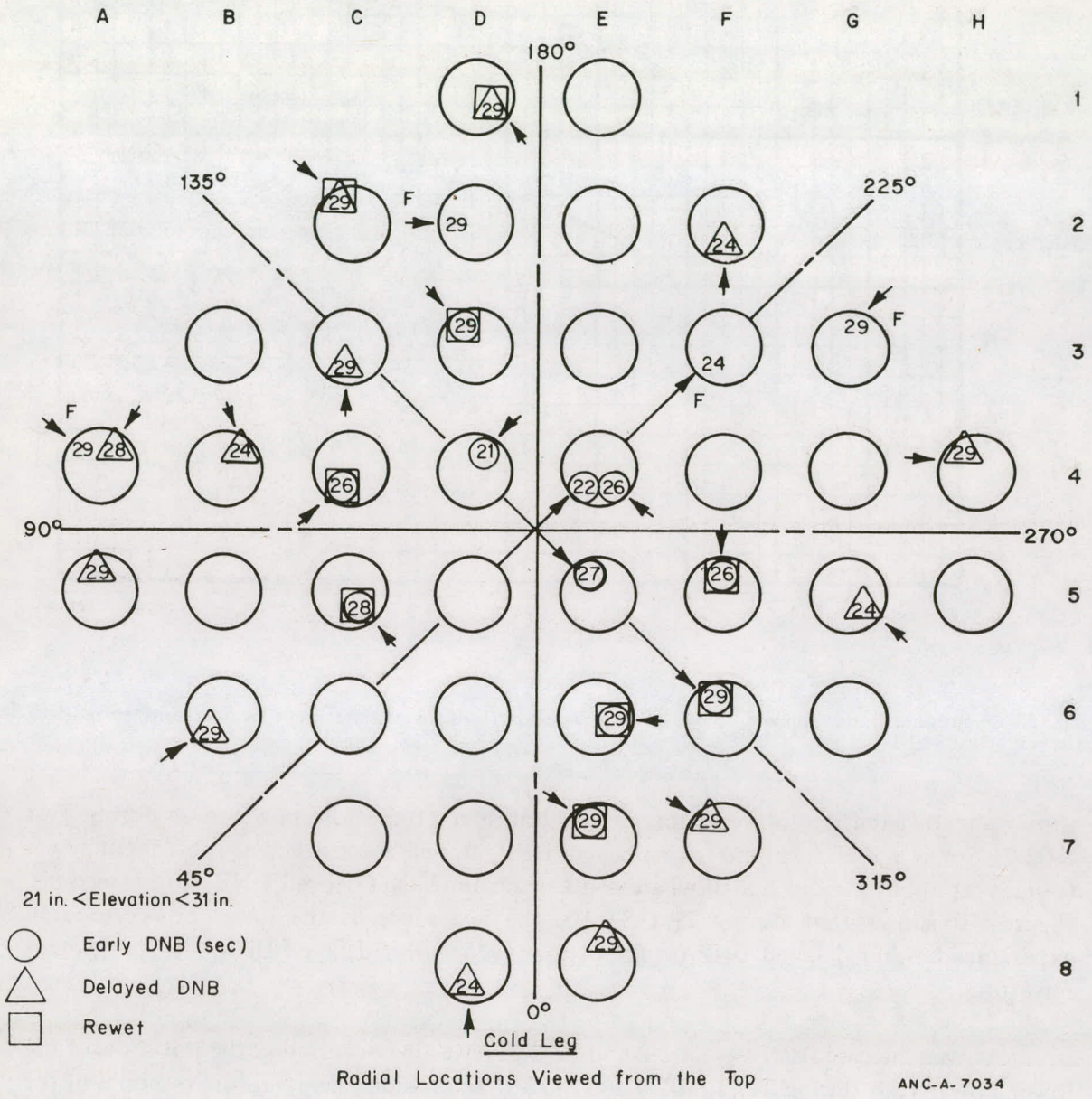

Fig. 39 Plan view of core showing hot spot rewet phenomena -- Test S-02-2.

illustrates the variation in cladding temperature response that occurred on the high power zone of Rod A4 during Test S-02-3. In Test S-02-3, this rod was instrumented with two thermocouples (one at 28 inches and one at 29 inches) on the high power zone. As shown in Figure 44, the 28-inch location experienced DNB and rewet at three and five seconds, respectively, whereas the 29-inch location did not dry out until six seconds. These differences were due primarily to the azimuthal location (Figure 40) of the thermocouples on the rod. The presence of local variations in the fluid conditions is probably the basic cause of the small differences in the behavior of the cladding temperature at the high power zone on Rod A4.

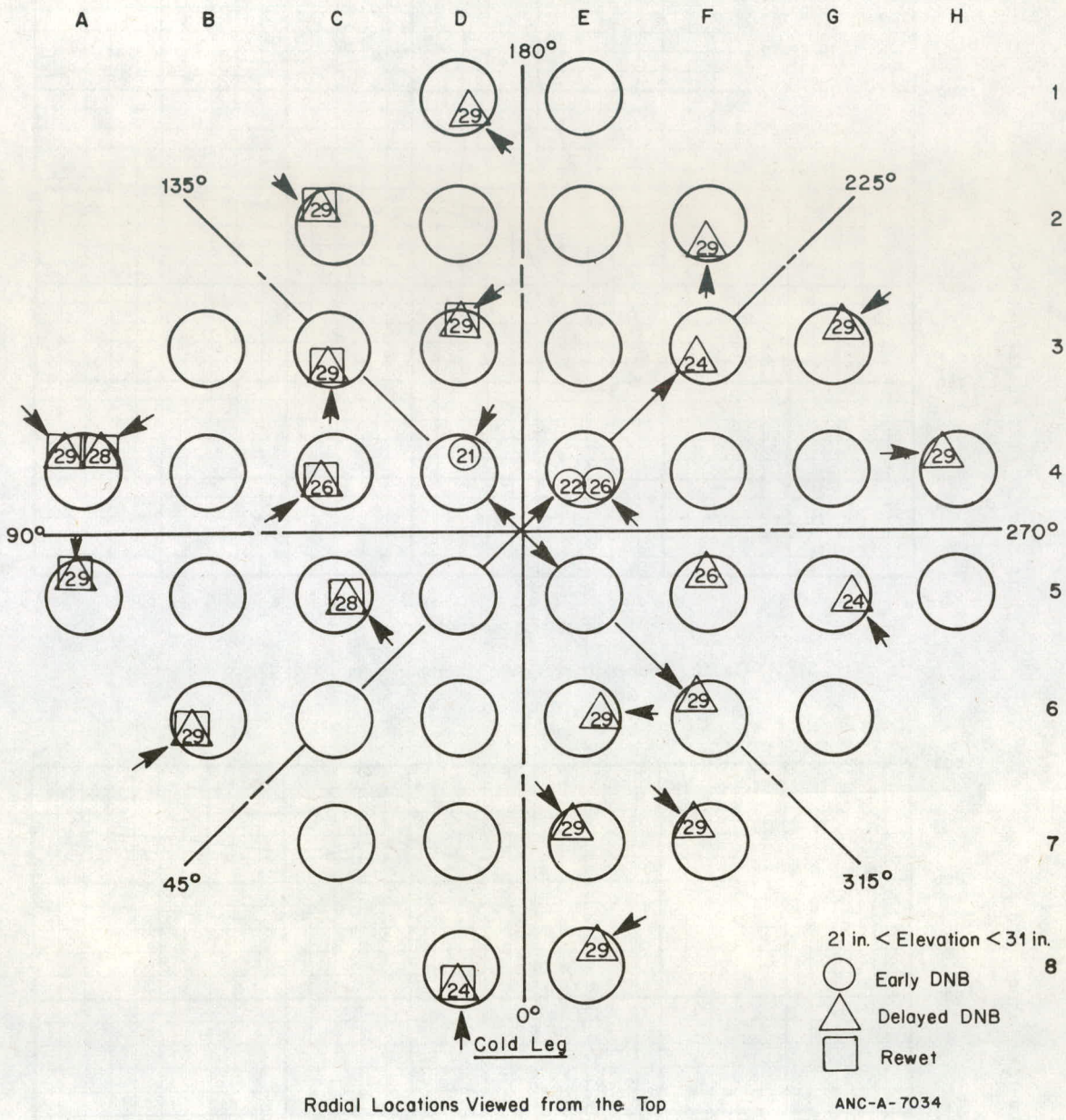

Fig. 40 Plan view of core showing hot spot rewet phenomena – Test S-02-3.

An interesting feature shown in Figure 44 is the rewet (quench) that occurred at about 15 seconds after rupture. Several of the high power zone thermocouples from rods in the upper left portion of the core indicated this quenching during both Tests S-02-2 and S-02-3. The rewets all occurred late in blowdown (10 to 15 seconds). The cause of the quench is attributable to water falling from the intact loop hot leg into the core and impinging upon certain rods. Evidence of the presence of water in the intact loop hot leg was provided by density measurements, as shown in Figure 45, which indicated an increase in density between 9 and 11 seconds after rupture. This increase in density was interpreted to be a slug of water from the steam generator passing by the gamma-densitometer

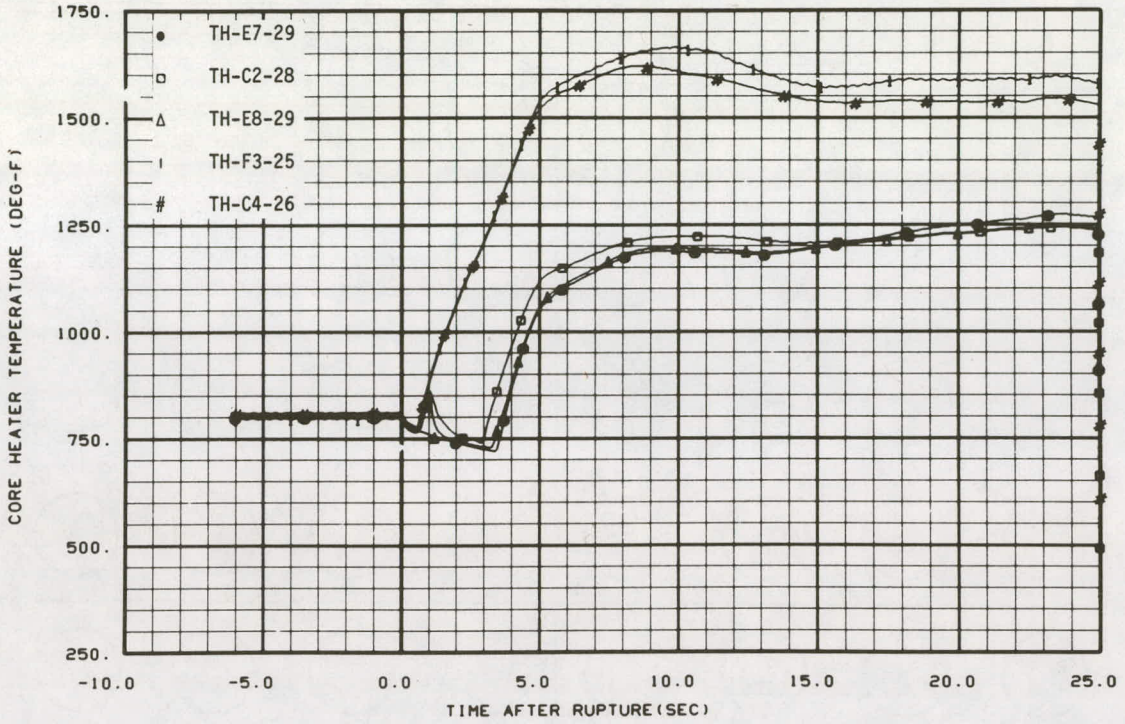

Fig. 41 Cladding temperature response at rod hot spots – Test S-02-5.

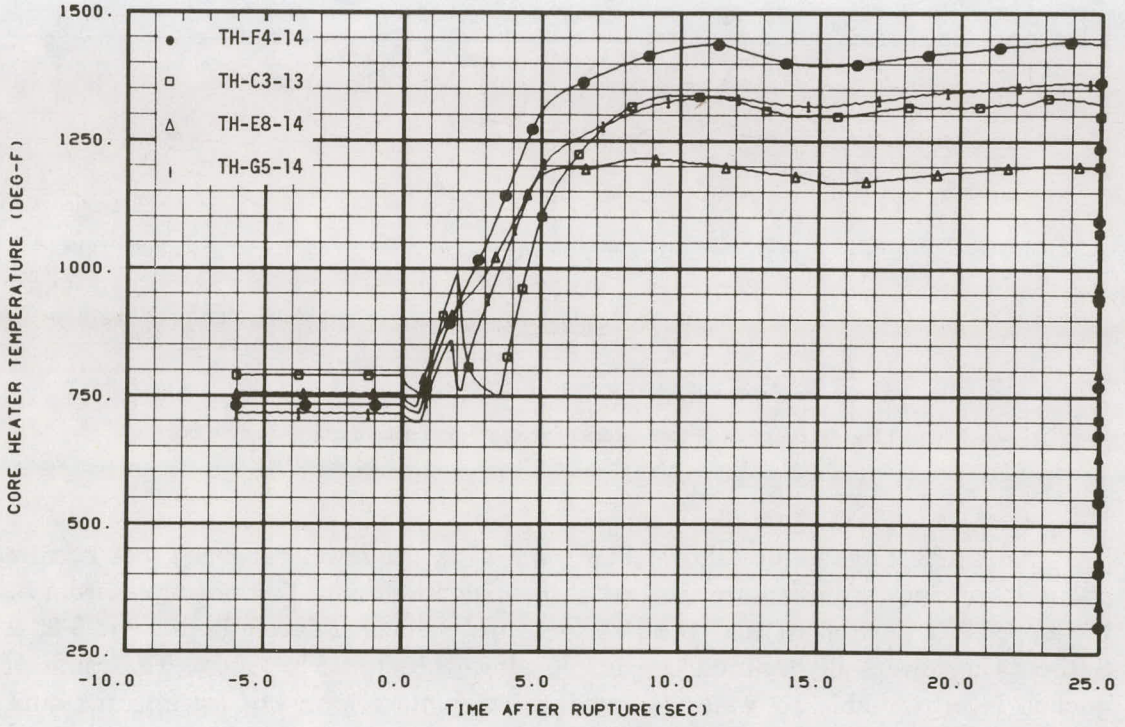

Fig. 42 Cladding temperature response at the 14-inch elevation – Test S-02-5.

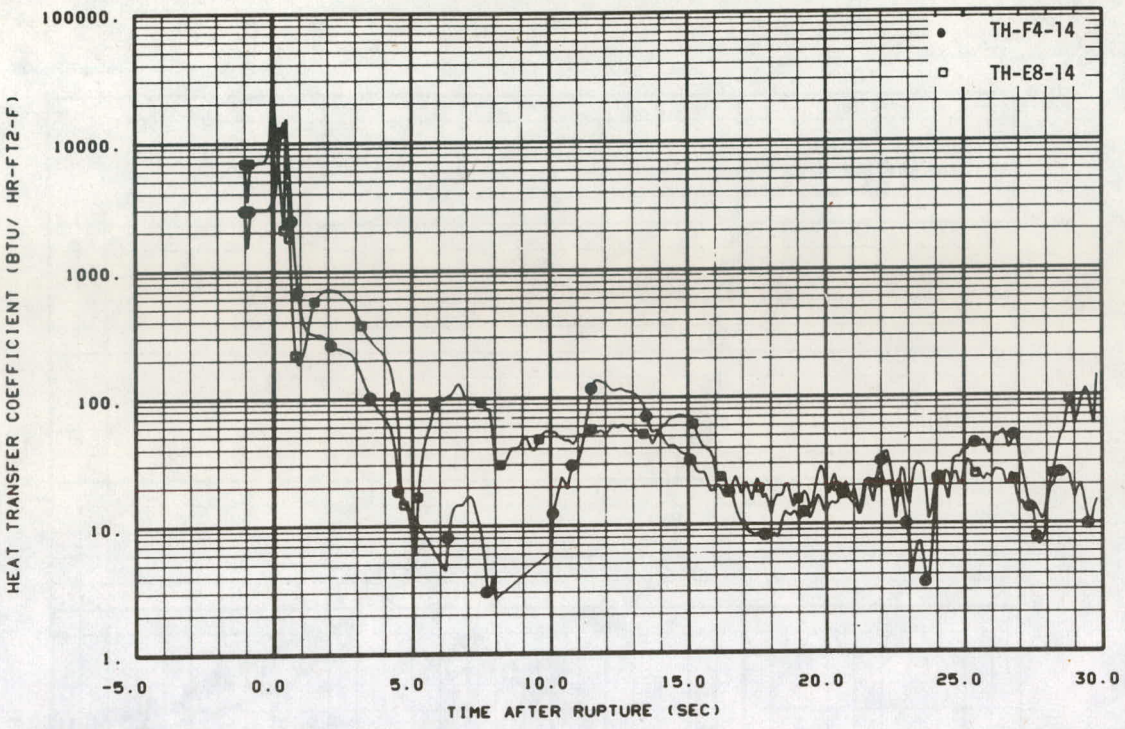

Fig. 43 Comparison of heat transfer coefficients at the 14-inch elevation on rods E8 and F4 – Test S-02-5.

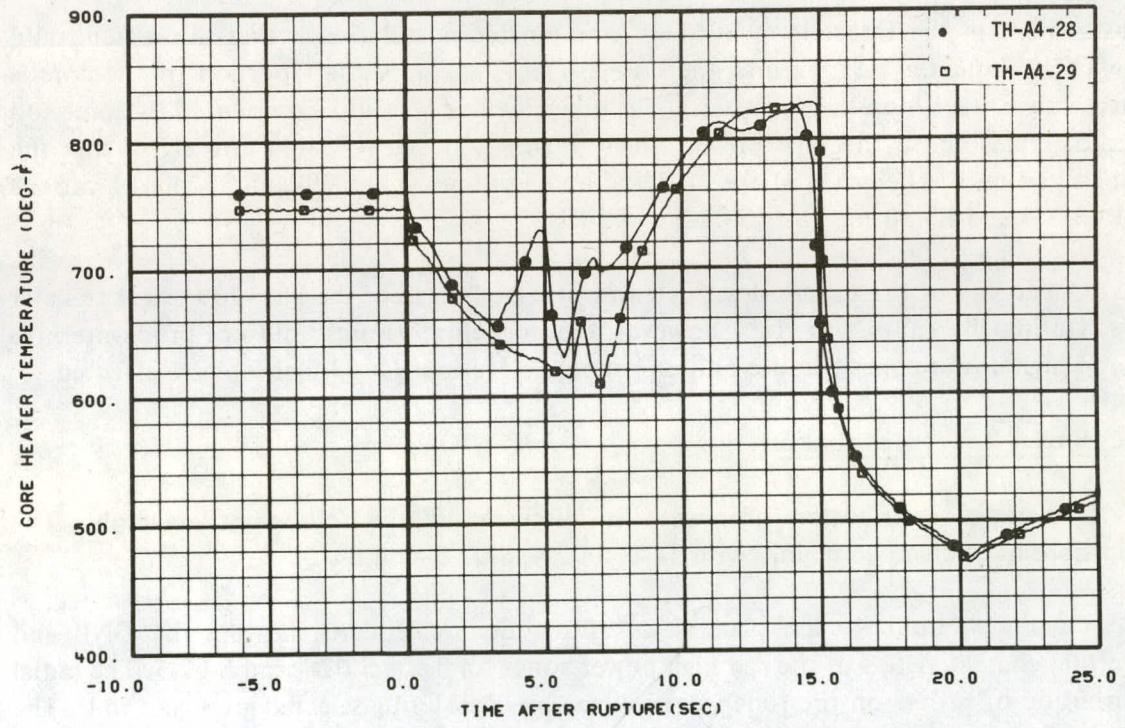

Fig. 44 Comparison of responses of Thermocouples TH-A4-29 and TH-A4-28 – Test S-02-3.

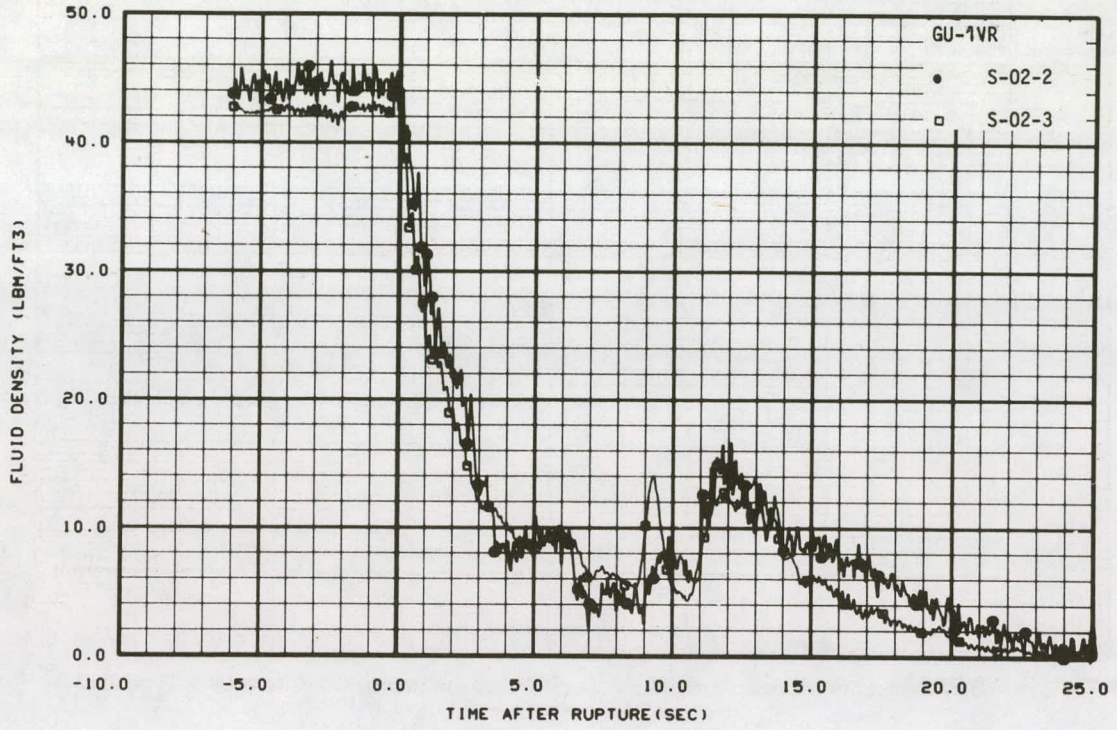

Fig. 45 Fluid density in intact loop hot leg – Tests S-02-2 and S-02-3.

measurement in the intact loop hot leg. A reasonable postulation is that this water could have fallen from the hot leg into the core because the upper left portion of the core is beneath the intact loop hot leg nozzle. The quench event was also experienced by some rod thermocouples above the high power zones. Figures 46 and 47 show the effect that the quench had on the behavior of the cladding temperatures at the 29- and 33-inch elevations on Rods C3 and B3 during Tests S-02-2 and S-02-3.

Quenching of the nature described was observed in all of the blowdown heat transfer tests. During the full power tests, however, the quench apparently did not propagate into the rod high power zones because only upper core elevations ($\geqslant$ 33 inches) were affected.

3.2 Radial Rewet Distribution

The radial distribution of rewets is discussed in the following paragraphs. The discussions are concerned mainly with Tests S-02-4, S-02-5, and S-02-7.

Figures 48 and 49 are plan views of the Semiscale core showing the DNB and rewetting characteristics of the rod high power zones for Tests S-02-4 and S-02-5. The radial distribution of rewets on the rods was analyzed by considering selected groups of rods. The total number of rewets and the total number of high power zone thermocouples were tabulated for each particular group.

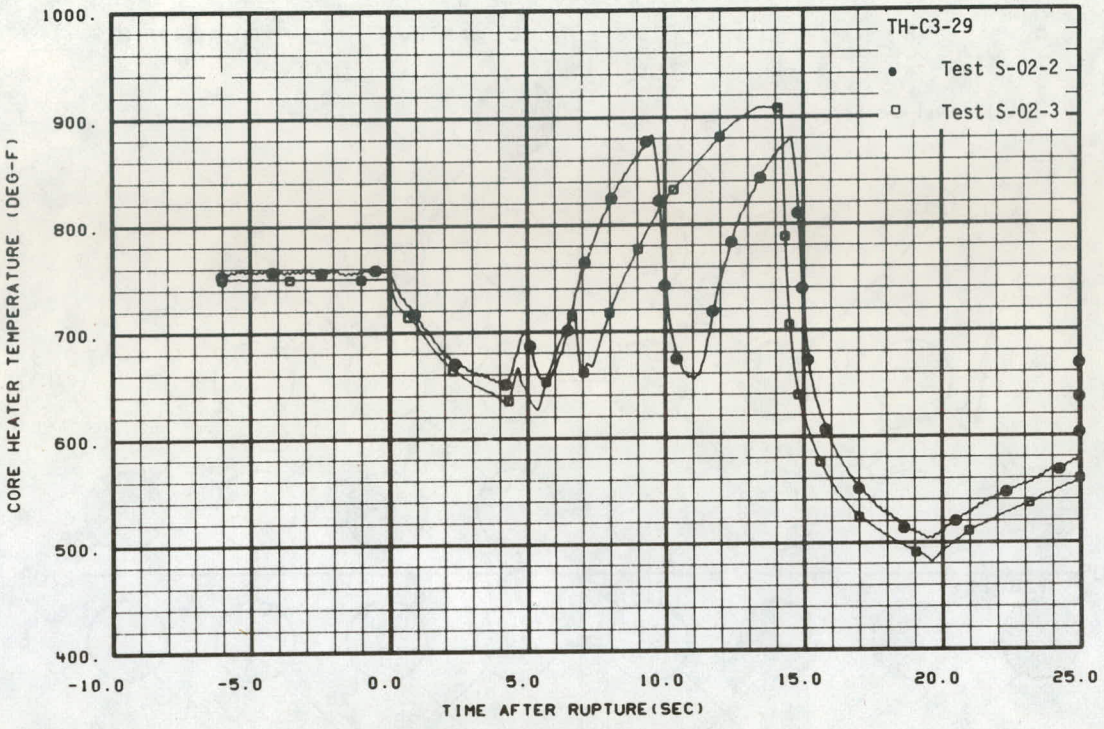

Fig. 46 Response of Thermocouple TH-C3-29 – Tests S-02-2 and S-02-3.

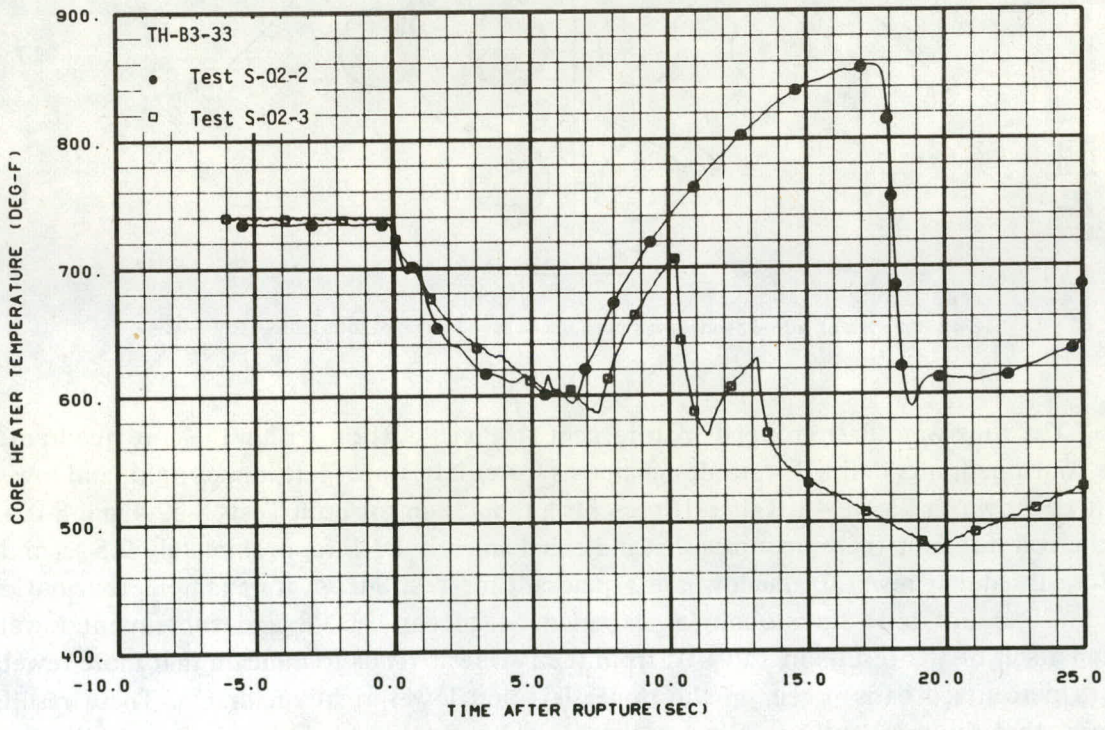

Fig. 47 Response of Thermocouple TH-B3-33 – Tests S-02-2 and S-02-3.

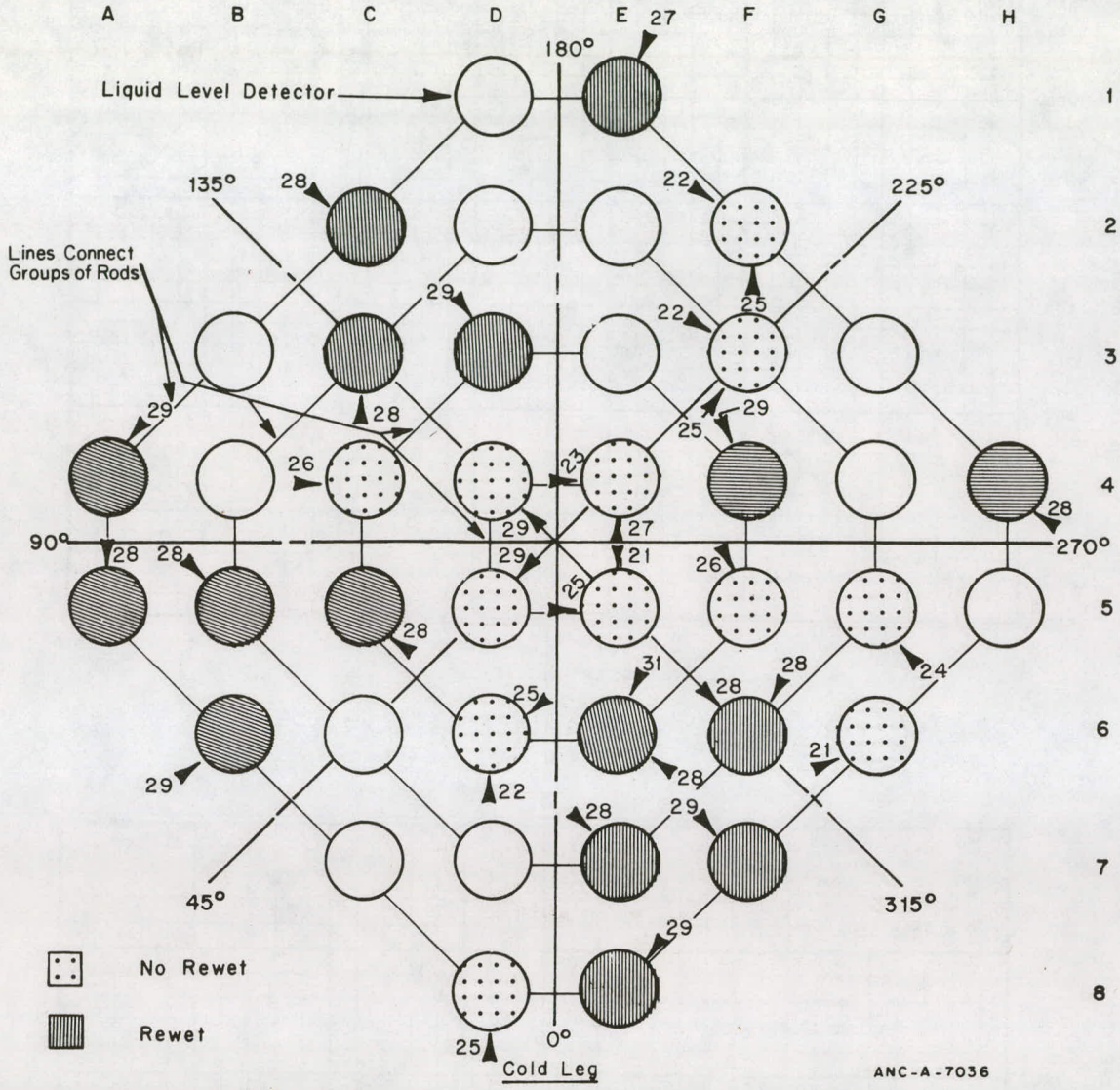

Fig. 48 Plan view of core showing rewet phenomena at rod hot spot locations – Test S-02-4.

The rods were first grouped with respect to their location within the core quadrants. The four quadrants defined were designated as lower left, upper left, upper right, and lower right as shown in Figure 48. Table III presents a tabulation for both Tests S-02-4 and S-02-5 of the rod hot spot thermocouples that indicated an early DNB (approximately 0.5 second) and a subsequent rewet. In the lower left quadrant for Test S-02-4, for example, four out of eight (50%) hot spot thermocouples experienced an early DNB and subsequent rewet. Comparison of the results in Table III from the two tests tends to indicate that more rewets (on a percentage basis) occur in the upper left and lower right quadrants. These results suggest that the transient core flow patterns could have been such that better cooling was provided to the upper left and lower right quadrants. Investigation of the heater rod electrical resistances also suggests that this behavior could be partially attributable to lower

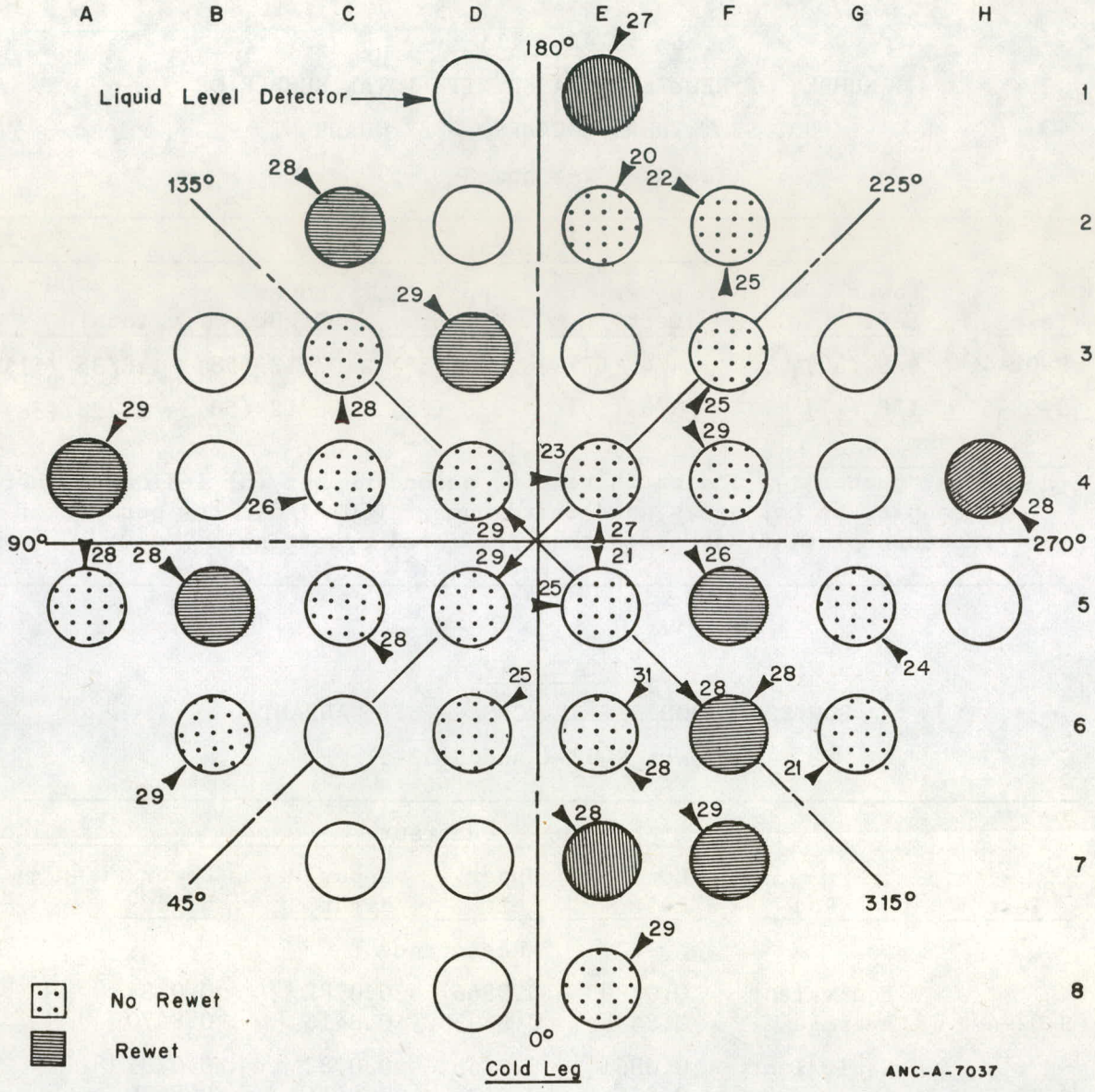

Fig. 49 Plan view of core showing rewet phenomena at rod hot spot locations – Test S-02-5.

power generation in these quadrants. Table IV shows both the equivalent and average resistances of the low power rods in each quadrant for Tests S-02-4 and S-02-5. This table shows that the heater rods in both the upper left and lower right quadrants have slightly higher resistances (consequently, a lower power generation) than the rods in the other two quadrants although the differences are relatively small.

Grouping of the rods was also accomplished by considering circular groups of rods rather than quadrants. The first group of rods considered was the four center (high power) rods. The next group considered was the ring of rods surrounding the center four. Four groups of rods, as shown in Figure 48, were constructed in this manner. Table V indicates the number of rewets and the total number of hot spot thermocouples in each group. These

TABLE III

NUMBER OF REWETS COMPARED WITH TOTAL NUMBER OF HOT SPOT THERMOCOUPLES -- BY QUADRANT

(Tests S-02-4 and S-02-5)

	Quadrant				
Test	Lower Left	Upper Left	Upper Right	Lower Right	Total
S-02-4	4/8 (50)[a]	4/6 (67)	3/9 (33)	7/12 (58)	18/35 (51)
S-02-5	1/6 (17)	3/6 (50)	2/8 (25)	6/12 (50)	12/32 (38)

[a] First number (4) indicates rewets, second number (8) indicates thermocouples at hot spots, and third number (50) indicates percent of thermocouples at hot spots that indicated rewetting.

TABLE IV

LOW POWER ROD RESISTANCES -- BY QUADRANT

(Tests S-02-4 and S-02-5)

		Quadrant			
Test	Rod	Lower Left	Upper Left	Upper Right	Lower Right
		Resistance			
S-02-4	Equivalent	0.0780	0.0866	0.0782	0.0784
	Average	0.8435	0.8496	0.8416	0.8470
S-02-5	Equivalent	0.0861	0.0866	0.0782	0.0784
	Average	0.8456	0.8496	0.8416	0.8470

results do not seem to indicate any radial pattern. Group 1 in both cases had no rewets as was expected because this group is composed of the high power rods. Group 3 in both tests had a large number (on a percentage basis) of rewets. No physical reason is available for the greater number of rewets in this group. Group 4, consisting of those rods adjacent to the core barrel, exhibits more rewets possibly because of an interaction between the flow and the core barrel.

Although no radial patterns appear in the rewet phenomena occurring during Tests S-02-4 and S-02-5, observation of Figures 48 and 49 indicates that any radial patterns may be overshadowed by the effects of axial location of the thermocouples within the high power zone. As indicated in the plan views of the core shown in Figures 48 and 49, rewets, if they occur, are biased to elevations above about 26 inches.

TABLE V

NUMBER OF REWETS COMPARED WITH TOTAL NUMBER OF HOT SPOT THERMOCOUPLES -- BY GROUP

(Tests S-02-4 and S-02-5)

	Group				
Test	1	2	3	4	Total
S-02-4	0/6 (0%)[a]	5/9 (56%)	5/8 (63%)	8/12 (67%)	18/35 (51)
S-02-5	0/6 (0%)	3/8 (38%)	4/8 (50%)	5/11 (45%)	12/32 (38)

[a] First number (0) indicates rewets, second number (6) indicates thermocouples at hot spots, and third number (0%) indicates percent of thermocouples at hot spots that indicated rewetting.

A plan view of the Semiscale Mod-1 core illustrating the DNB and rewet characteristics of all the rod hot spots for Test S-02-7 is shown in Figure 50. This figure shows the aforementioned radial mixture in rewet phenomena that occurred during the flat radial profile tests. Figure 50 shows that the rods in the upper left quadrant of the core experienced more rewets on their high power zones than did the rods in any of the other three quadrants. Table VI shows the frequency of hot spot rewetting compared with the total number of thermocouples at the hot spots in each quadrant of the core. If the same postulation is made that was made in connection with the behavior of the thermocouples on Rods D4 and D5 (a lower initial steady state hot spot temperature may be indicative of a lower power generation on the rod), then core quadrants with low average steady state hot spot temperatures may be expected to exhibit more rewets than a quadrant with a higher steady state temperature. Table VII shows the average steady state hot spot cladding temperatures from each of the core quadrants. The upper left quadrant, as indicated in Table VII, had the lowest steady state temperature value (785°F) in comparison to the other quadrants. Table VI indicates that five of the six hot spot thermocouples in this quadrant experienced rewetting. The values in Tables VI and VII do not indicate any relationship in the other quadrants between the temperature and the number of rewets. The upper right quadrant, for example, had the highest steady state temperature and also had a larger percentage of rewets (25% – two rewets experienced from a total of eight thermocouples) than the lower left and lower right quadrants.

The rods were also arranged by the circular grouping method discussed in connection with Test S-02-4, and comparisons between the steady state hot spot cladding temperature and the rewet phenomena were made. Table VIII lists the cladding temperatures, and Table IX lists the frequency of rewets. These tables show that during Test S-02-7, Group 1 (the four center rods) had the lowest average steady state hot spot temperature (783°F)

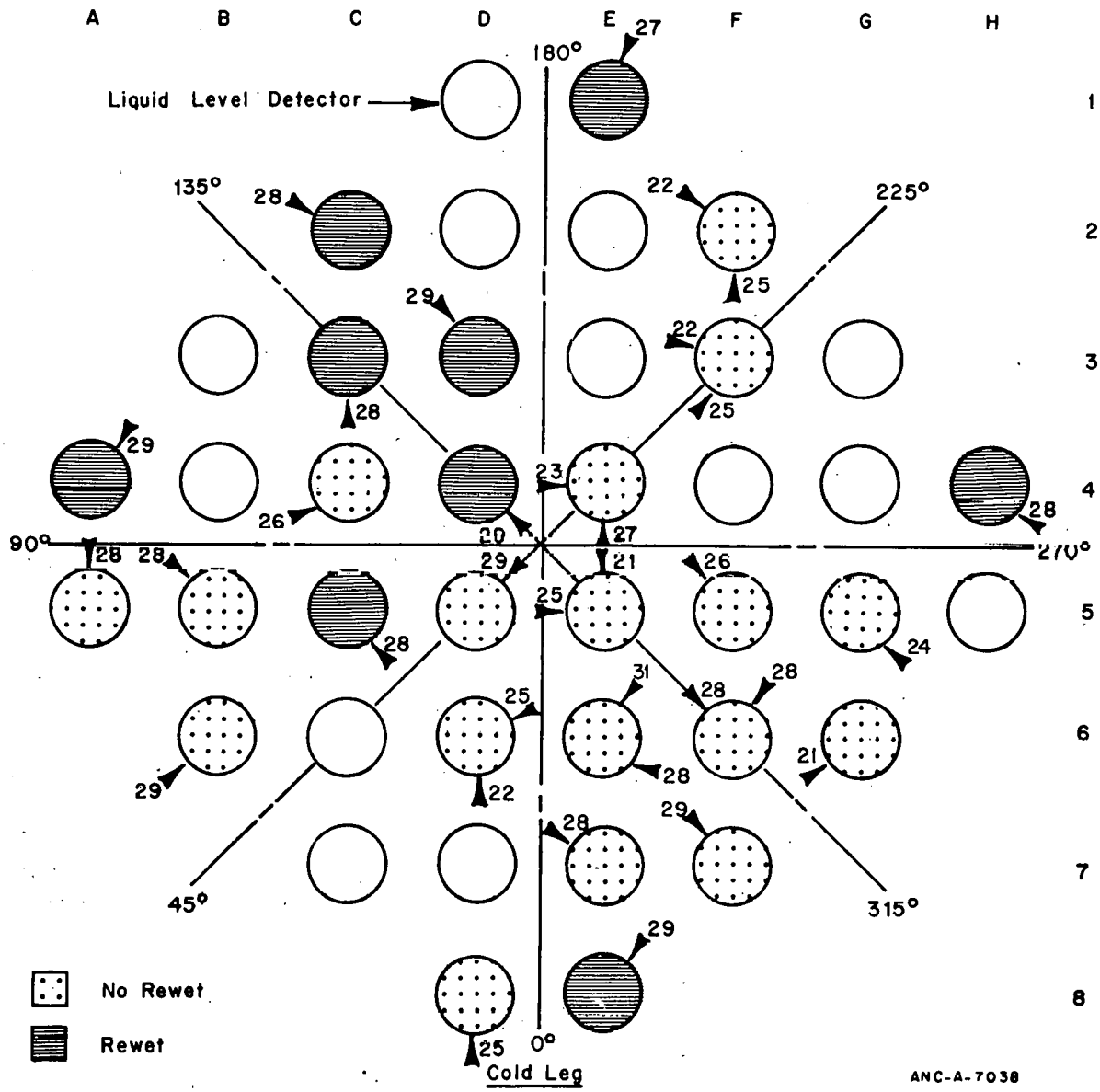

Fig. 50 Plan view of core showing rewet phenomena at rod hot spot locations — Test S-02-7.

TABLE VI

NUMBER OF REWETS COMPARED WITH TOTAL NUMBER OF HOT SPOT THERMOCOUPLES — BY QUADRANT

(Tests S-02-7 and S-02-9)

	Quadrant				
Test	Lower Left	Upper Left	Upper Right	Lower Right	Total
S-02-7	1/8	5/6	2/8	2/12	10/34
S-02-9	1/6	2/6	2/8	3/12	8/32

TABLE VII

AVERAGE STEADY STATE HOT SPOT
CLADDING TEMPERATURES -- BY QUADRANT
(Tests S-02-7 and S-02-9)

Test	Quadrant			
	Lower Left	Upper Left	Upper Right	Lower Right
S-02-7	795	785	797	787
S-02-9	794	783	795	785

TABLE VIII

AVERAGE STEADY STATE HOT SPOT CLADDING TEMPERATURES -- BY GROUP
(Tests S-02-7 and S-02-9)

Test	Group			
	1	2	3	4
S-02-7	783	790	788	797
S-02-9	784	791	786	793

TABLE IX

NUMBER OF REWETS COMPARED WITH TOTAL
NUMBER OF HOT SPOT THERMOCOUPLES -- BY GROUP
(Tests S-02-7 and S-02-9)

Test	Group				
	1	2	3	4	Total
S-02-7	1/6[a]	3/8	1/8	5/12	10/34
S-02-9	1/6	3/8	1/8	3/10	8/32

[a] First number (1) indicates rewets and second number (6) indicates thermocouples at hot spots.

compared to the other groups of rods and also had the lowest frequency of rewets with the exception of Group 3 (one thermocouple experienced rewetting out of the total of six thermocouples at the hot spots in Group 1). Group 4, those rods adjacent to the core barrel, had the highest average hot spot temperature (797°F) in comparison to the other groups and the highest number of rewets (5 rewets out of 12 thermocouples). If a lower average temperature is assumed to reflect a lower average power density on the rods in a particular group and if rods with lower power density are assumed to be more subject to rewetting, then these results are just the reverse of what would be expected. If the ability to rewet were determined only by power density, then more rewets would be expected in Group 1 than in Group 4.

The results obtained from grouping the rods in the manners discussed and comparing the rewet phenomena with the average steady state hot spot cladding temperature tend to indicate either that power density variations among the rods alone do not control the occurrence of rewet or that the steady state temperatures are not an accurate reflection of the power density variations. Extensive analysis of Semiscale steady state and special test data (such as data from power pulse tests and dry core heatup tests) has failed to indicate any correlation between rod power density and rewet behavior. Definition of the special tests conducted and the results obtained from these tests are contained in Appendix B.

Figure 51 shows a comparison on a short time base of several hot spot thermocouples from Test S-02-7. No initial response characteristic difference is observed between those thermocouples which experience rewet and those which do not. Plotted data from Thermocouples TH-D8-25 and TH-H4-28, for example, both had the same slope (temperature change with time) for the period between 0.6 and 2.4 seconds. At 2.4 seconds, however, Thermocouple TH-H4-28 suddenly experienced rewet, whereas Thermocouple TH-D8-25 did not. Similarily, plots of data from Thermocouples TH-C5-28, TH-A4-29, TH-E8-29, TH-H4-28, and TH-C2-28 all had slopes greater than the plot for Thermocouple TH-D5-29. Rewet was not experienced by Thermocouple TH-D5-29, but rewet was experienced by the other five thermocouples. Results of a similar nature were observed from Test S-02-9A and Test S-02-9. The repeatability (repeatability is discussed in detail in Section III-4) of these phenomena suggests that the ability of a rod to rewet may be due to some inherent characteristic of the rod.

3.3 Axial Rewet Distribution

Observation of the DNB and rewet characteristics of all the rod cladding thermocouples from Tests S-02-7, S-02-9, and S-02-9A show a pronounced trend in rewet phenomena as a function of axial position. The heated length of the core can be divided into distinctive axial regions on the basis of DNB and rewet phenomena occurring within these regions. These divisions do not necessarily coincide with the axial power step divisions. The high power zone thermocouple response of Test S-02-7 is a good illustration of this axial dependence. Figure 50, for example, indicates that none of the thermocouples on the peak power step below an elevation of 27 inches indicates rewet. Those thermocouples between 27 and 31 inches, however, show a mixture of responses. Some of the thermocouples in this region experienced DNB and rewet, whereas others did not rewet. The heated length of the core can thus be categorically divided into the following regimes:

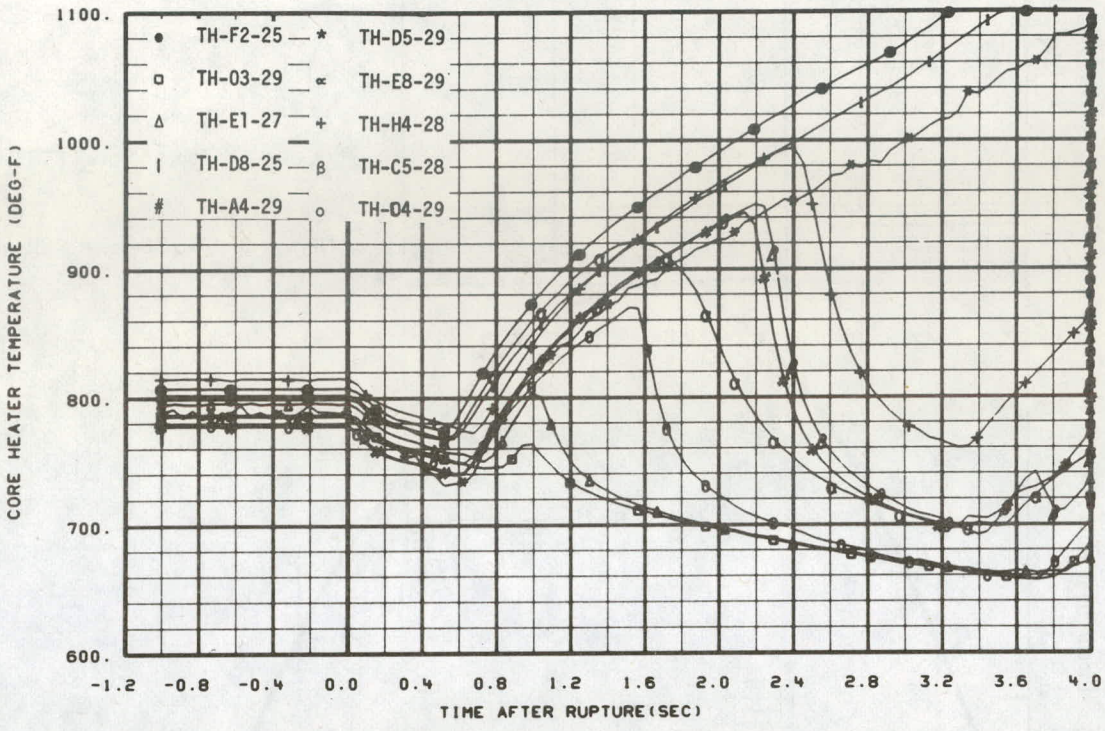

Fig. 51 Short term cladding temperature response at rod hot spot locations – Test S-02-7.

(1) Early DNB without rewet

(2) Early DNB without rewet and early DNB with rewet

(3) Delayed DNB and early DNB with rewet.

The axial distribution of rewet behavior is shown in Figure 52. The different shaded regions on this figure correspond to the regimes discussed.

Figure 52 shows that a definite axial pattern exists in the Semiscale core rewet phenomena. This axial dependence existed for all of the flat radial power profile tests (Tests S-02-7, S-02-9A, and S-02-9). The existence of this axial pattern indicates a strong relationship between local power density, fluid conditions, and whether or not a rod is able to rewet. Apparently, two definite regions exist (approximately 0 to 11 inches and 17 to 26 inches above the bottom of the heated length) in which rewets do not occur. Apparently, the quality and power density here are such that rewetting is prohibited. Thermocouples available at elevations between 13 and 15 inches and between 27 and 31 inches, however, contain a mixture of rewets and some nonrewets. The quality-power-density relationship here must be such that rewetting is possible but not certain. Upper core thermocouples between 32 and 39 inches indicated a variety of responses including delayed DNB and early DNB with rewets. Elevations above 39 inches indicated either delayed DNB or no DNB. The

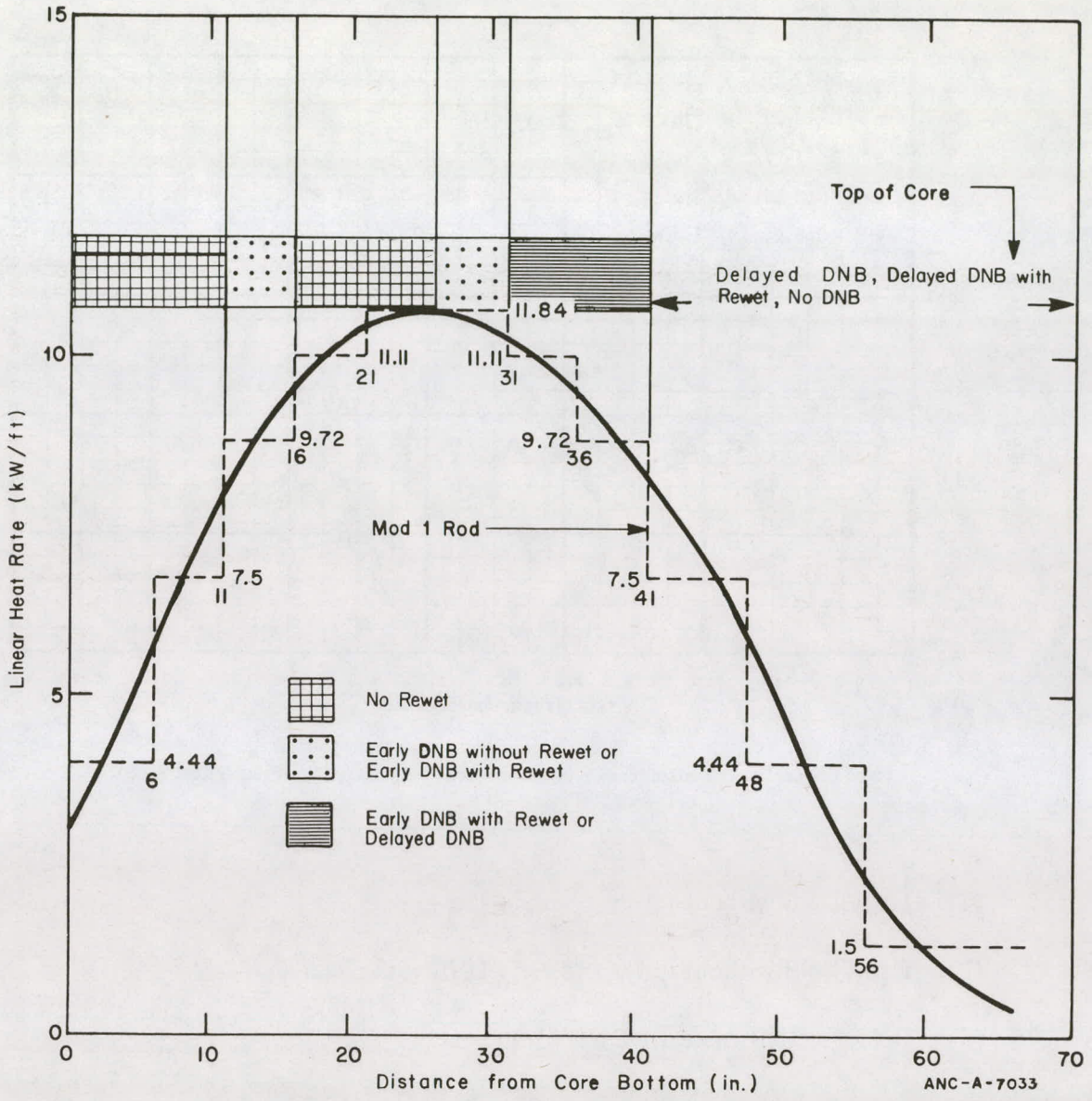

Fig. 52 Axial distribution of rewet behavior – Test S-02-7.

variation in thermocouples responses seen in the upper core elevations was probably due to radial variations in fluid conditions. Appendix C presents the thermocouple response used to determine the axial regions.

In addition to the suspected strong relationship between rod power density and fluid quality in relation to the rod rewet phenomena, flow maldistributions in the core due to the grid spacer locations could possibly influence the occurrence of rewetting. Three grid spacers are located along the heated length of the rods at elevations of 17.4, 34, and 50.6 inches above the core bottom. The grids at 17.4 and 34 inches are located directly above the two zones in the core in which a mixture of both rewets and nonrewets occurred. The

presence of the grids could possibly bias the flow in a reverse core flow situation in such a manner as to affect the rewetting characteristics for some distance downstream of the actual location of the grid spacer. A reasonable additional postulation is that, if the proper combination of fluid conditions and heater rod surface conditions exist (such as surface flux and surface roughness), rewetting could propagate axially from upper core elevations to lower core elevations. Figures 53 and 54 show the temperature response on two rods that were instrumented with thermocouples at the 29- and 33-inch elevations during Test S-02-7. The thermocouples on Rod A4, for example, indicate that the good cooling at the 33-inch elevation could have influenced the cladding temperature at the 29-inch elevation. The thermocouples on Rod F7, however, do not show the same relationship as those on Rod A4. The lack of a sufficient number of rods in the Semiscale core with thermocouples at both the 29- and 33-inch elevation probably prevents any definitive statements concerning the axial propagation of rewets at this time.

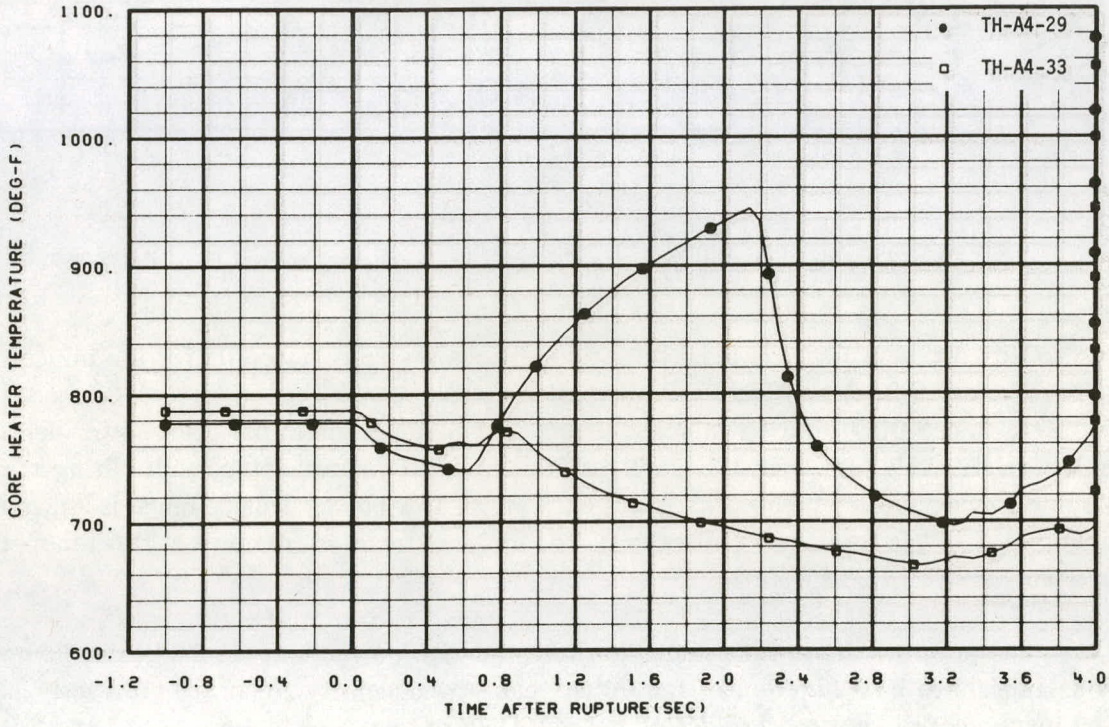

Fig. 53 Cladding temperature response at 29- and 33-inch elevations on Rod A4 – Test S-02-7.

Tests S-02-4 and S-02-5 rod cladding temperature results also conform to the axial pattern shown in Figure 52. Results from Tests S-02-2 and S-02-3 do not, however, fit into the pattern at the hot spot location. As was noted previously, all of the high power zone thermocouples on the low power rods experienced either delayed DNB or rewetting during Tests S-02-2 and S-02-3. The low power rods were operated at a substantially lower peak power density during these two tests than they were during any of the other cold leg break

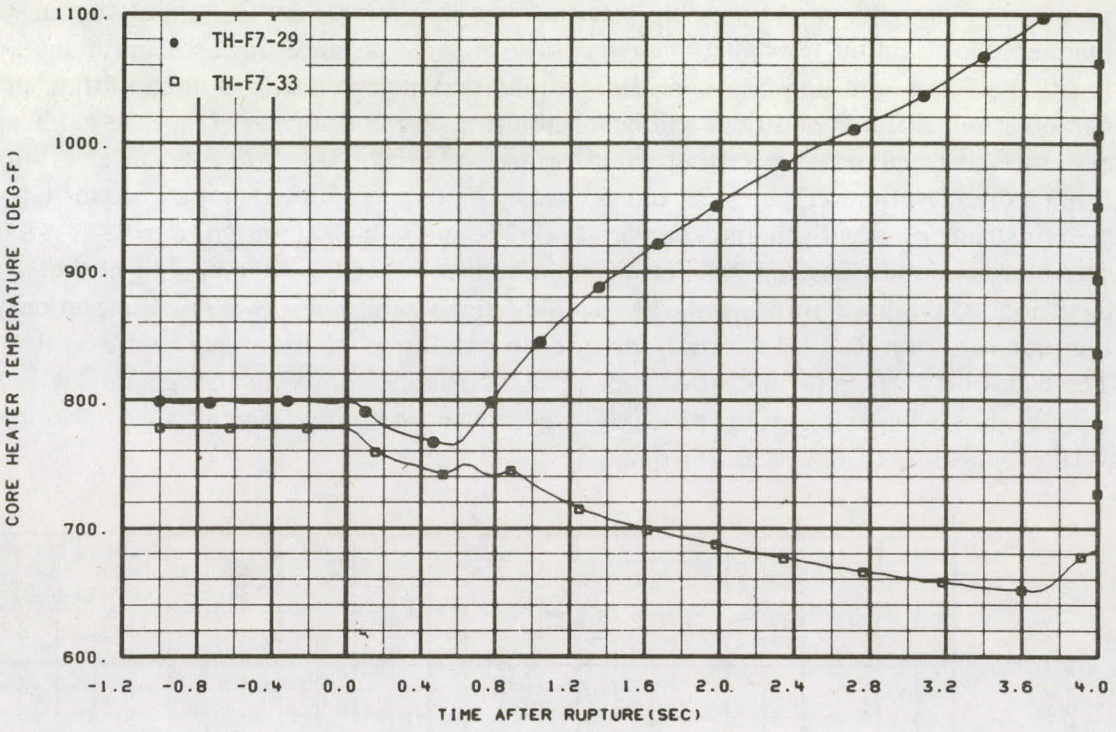

Fig. 54 Cladding temperature response at 29- and 33-inch elevations on Rod F7 – Test S-02-7.

tests. This difference in rod axial power conditions probably accounts for the nonconformity of Test S-02-2 and Test S-02-3 results. Results from Tests S-02-4, S-02-5, S-02-7, S-02-9A, and S-02-9 tend to indicate that a certain range of initial peak power densities exists on the rods for which the axial pattern shown in Figure 52 will result during a 200% double-ended cold leg break. The lower extreme of this power density range is apparently about 11.5 kW/ft (peak power location). The upper extreme is unknown at this time, but is probably above 14.25 kW/ft.

The point of the rewet penetration into the high power zone on the Semiscale heater rods appears to be a function of the initial peak power density. As noted previously, all of the low power rod hot spots indicated delayed DNB or rewetting in Tests S-02-2 and S-02-3, whereas the high power rods did not experience any rewets. In Tests S-02-4 and S-02-5, no rewets were observed below the 26-inch elevation; and in Tests S-02-7, S-02-9A, and S-02-9 no rewets were observed below the 27-inch elevation. If peak power density is plotted against the high power zone elevation below which rod rewetting does not occur, the result is a straight line as shown in Figure 55. This result again tends to indicate that the relationship between power density and quality plays an important role in determining whether or not a rod will rewet. The axial quality gradient is not expected to be significantly different for any of the 100% power tests; however, as shown in Figure 55, differences in the peak power density have a noteworthy effect on the rewet behavior in the rod peak power step.

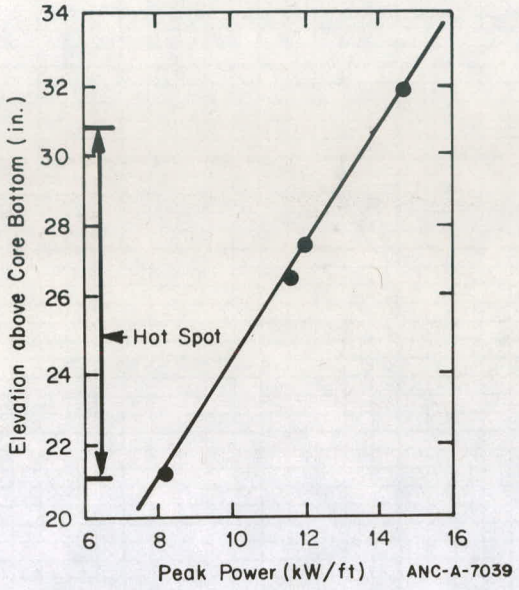

Fig. 55 Axial penetration of rewets into high power zone versus rod peak power density.

4. DATA REPEATABILITY

Data repeatability is an important aspect of the blowdown heat transfer test results because should wide variations occur in core thermal response during tests that had similar initial conditions, such variations would tend to limit the usefulness of the data. Two different aspects of data repeatability are examined in this section. In the first section, repeatability of the rod cladding temperature behavior is examined by comparing results from Tests S-02-9A and S-02-9. In the second section, repeatability of the rewet phenomena is examined by comparing the results from Tests S-02-7, S-02-9A, and S-02-9.

4.1 Cladding Temperature Repeatability

The following paragraphs contain discussions concerning the cladding temperature repeatability during two of the blowdown heat transfer tests. The two tests considered, Tests S-02-9A and S-02-9, were conducted from identical initial conditions. The core inlet mass flow rate and density are virtually identical for Tests S-02-9A and S-02-9 as shown in Figures 56 and 57. Since the flow and density are so similar, the core thermal response was also expected to be very similar during the two tests.

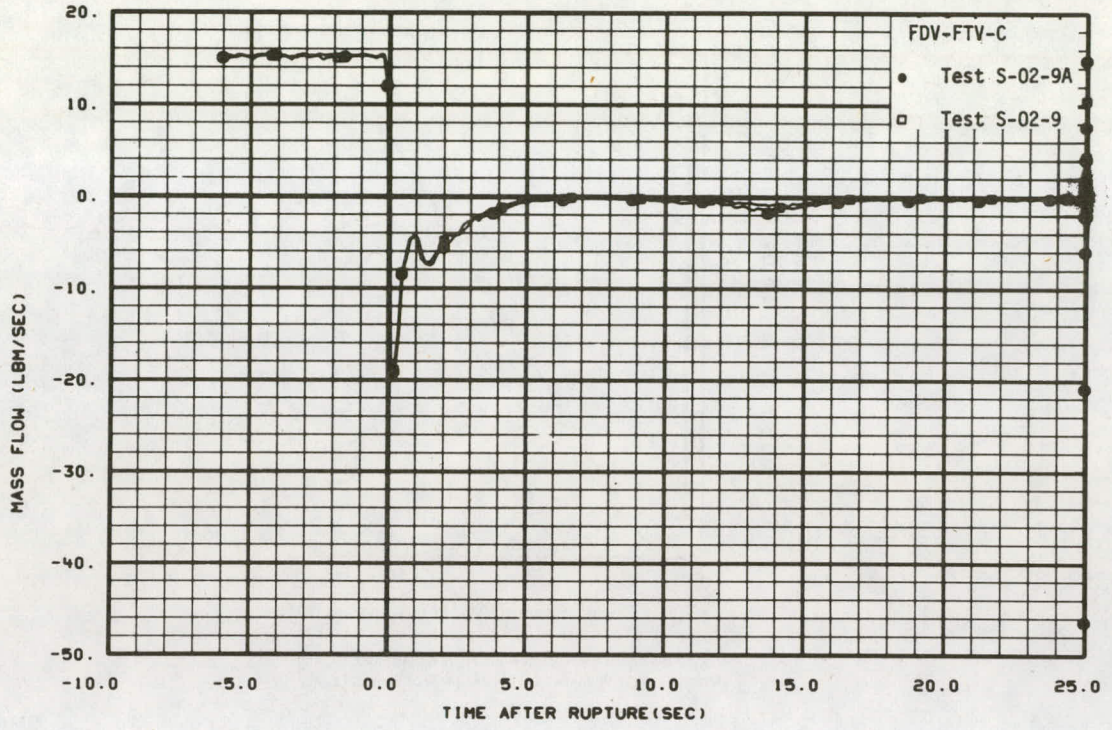

Fig. 56 Comparison of core inlet mass flow rates – Tests S-02-9A and S-02-9.

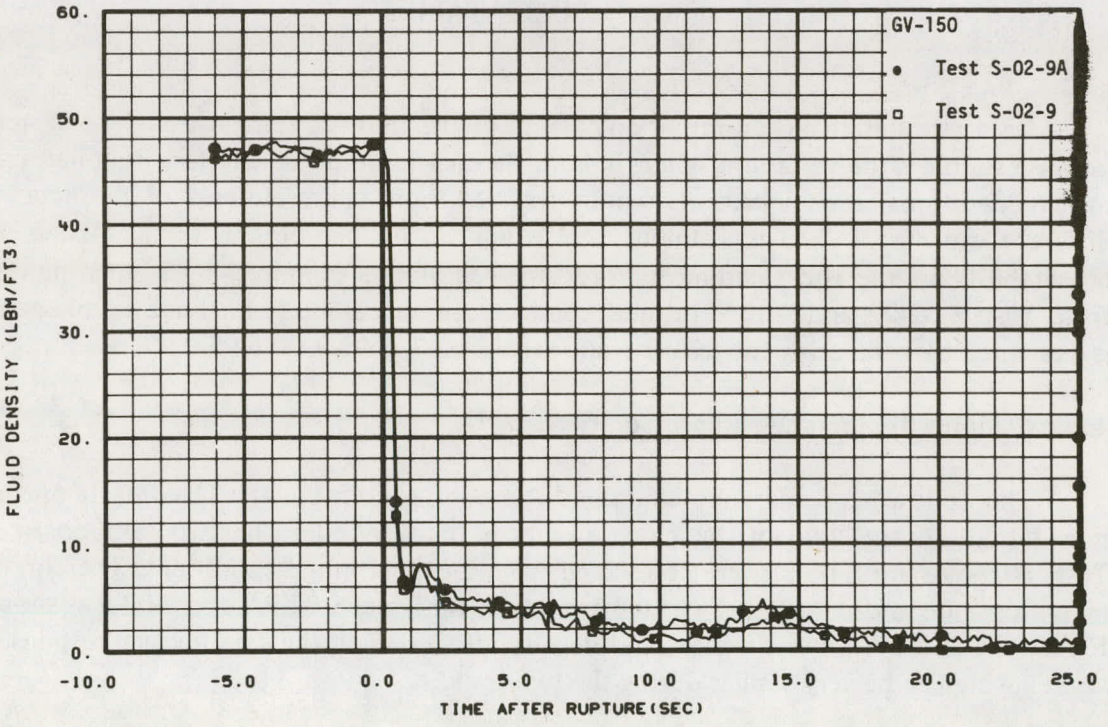

Fig. 57 Comparison of core inlet density – Tests S-02-9A and S-02-9.

Comparison of the rod cladding temperatures from the two tests under consideration indicated that, for the large part, the temperatures were in excellent agreement during the period considered in this report (6 to 25 seconds). Figures 58 and 59 show typical temperature comparisons for the rod high power zone and for the 14-inch elevation, respectively. Only two thermocouples in the high power zone (Thermocouples TH-E1-27 and TH-C2-28) showed different responses when compared between Tests S-02-9A and S-02-9. These differences were minor in nature and usually consisted of slight variations in rewetting phenomena. Some of the thermocouples on the heater rod cladding in the 37- to 44-inch elevation range also showed some variation. Differences in this elevation range usually consisted of differences in the behavior subsequent to ten seconds. Figures 60 and 61 show the variations noted at the 44-inch location on Rod E7 and the 39-inch location on Rod D5. These variations are probably related to radial variations in the fluid conditions in the upper core. Comparisons of the axial variation in temperatures on Rod F5 and D4 for the two tests are shown in Figures 62 and 63. These figures show the excellent reproducibility of both the trends and magnitudes of the data from the two tests.

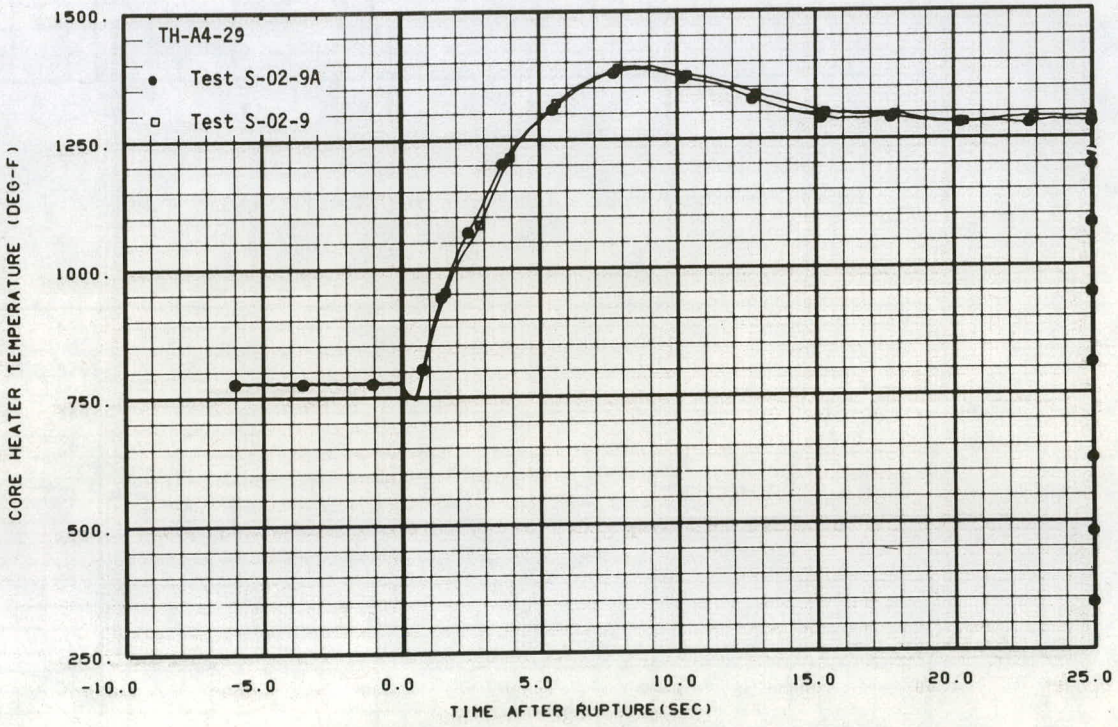

Fig. 58 Temperature response at high power zone – Tests S-02-9A and S-02-9.

The figures shown indicate in general that the cladding temperatures measured during Tests S-02-9A were in excellent agreement with those cladding temperatures measured during Test S-02-9. The few response differences noted in the upper core were attributed to fluid condition differences between the two tests. Small variations in the fluid conditions are expected because of the complex nature of the two-phase flow environment.

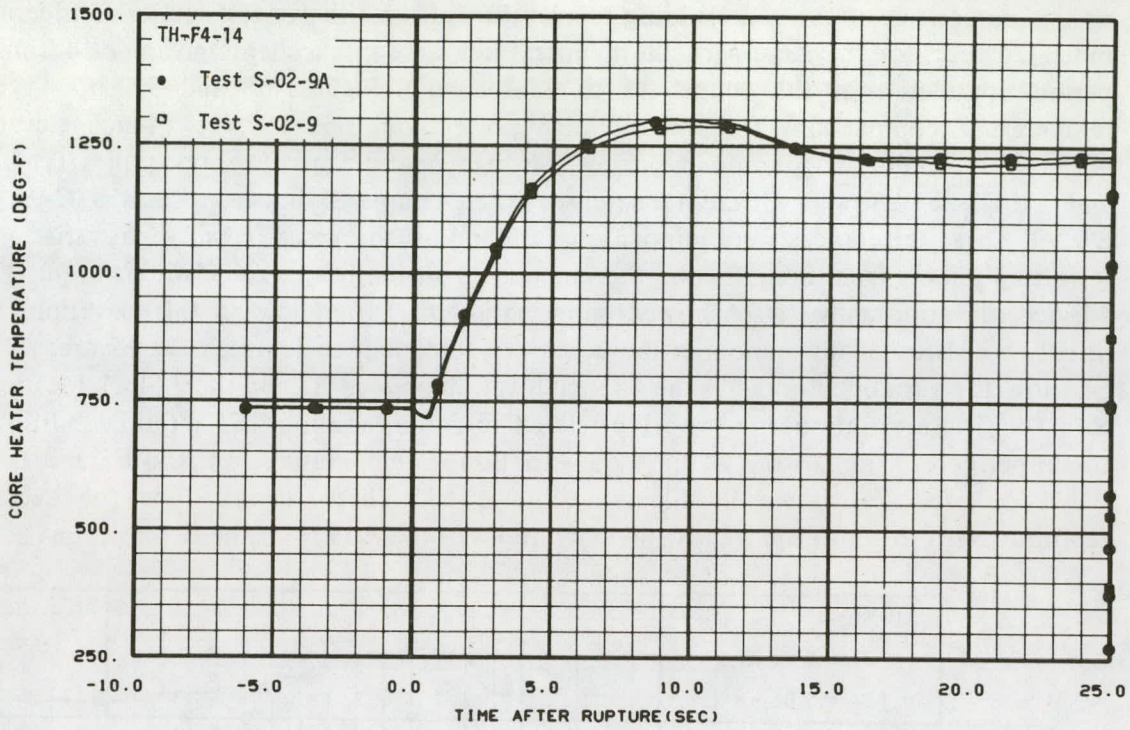

Fig. 59 Temperature response at 14-inch elevation – Tests S-02-9A and S-02-9.

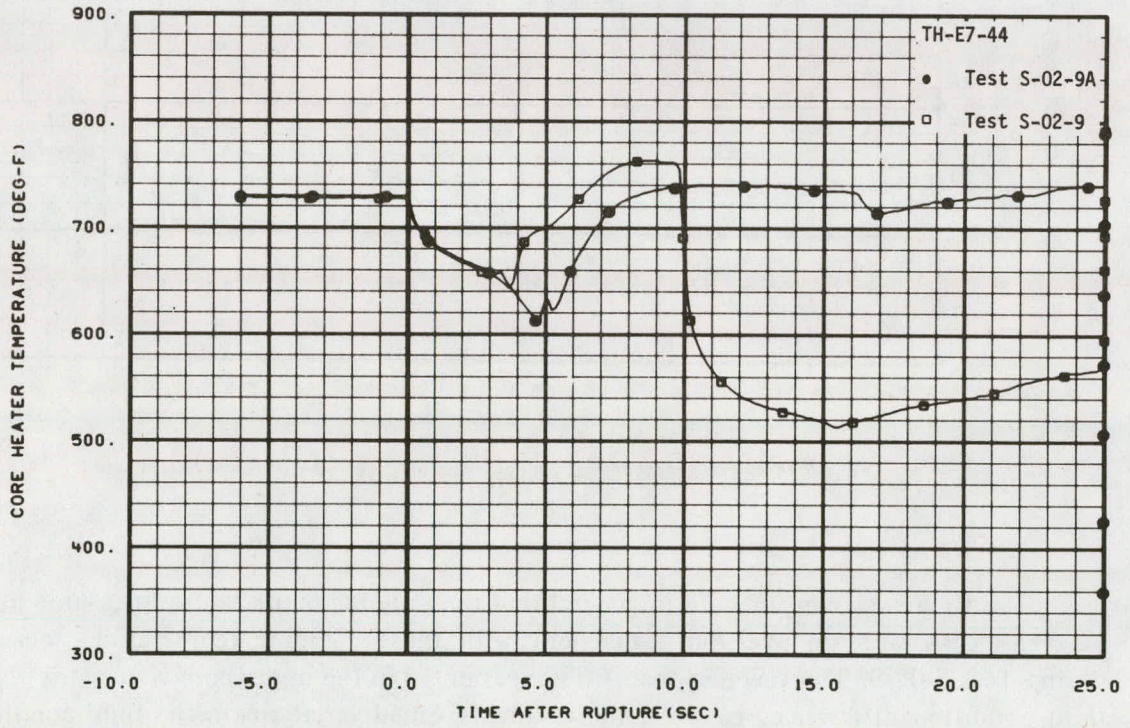

Fig. 60 Temperature response at 44-inch elevation – Tests S-02-9A and S-02-9,

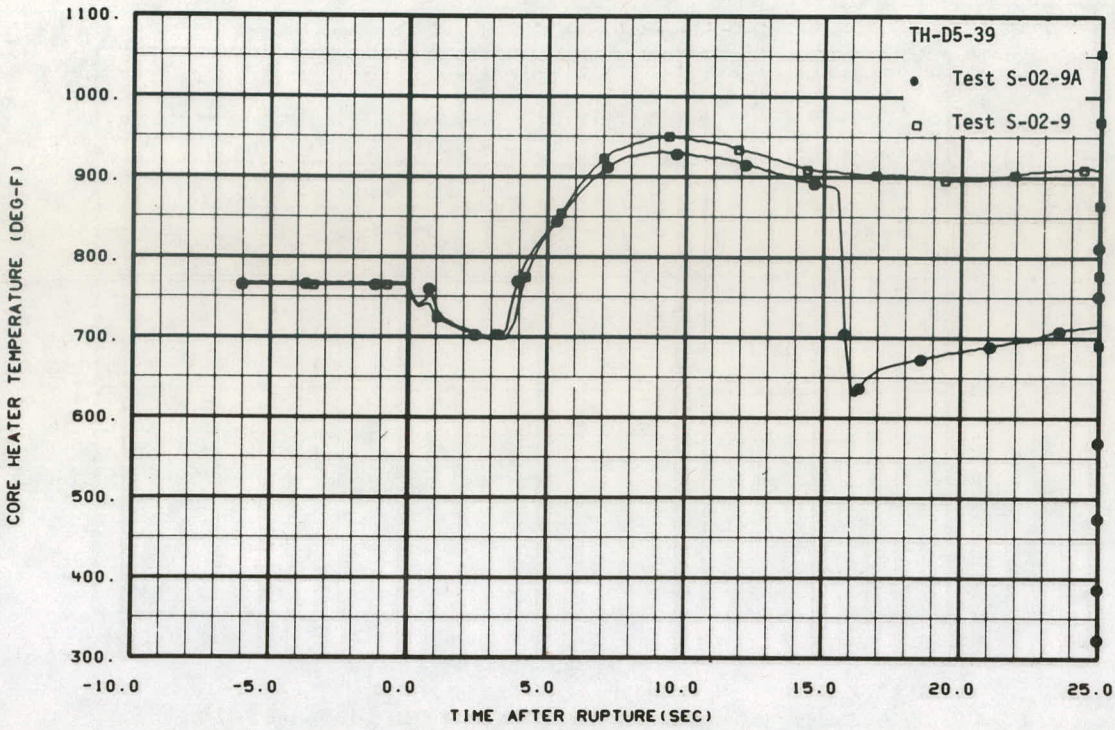

Fig. 61 Temperature response at 39-inch elevation – Tests S-02-9A and S-02-9.

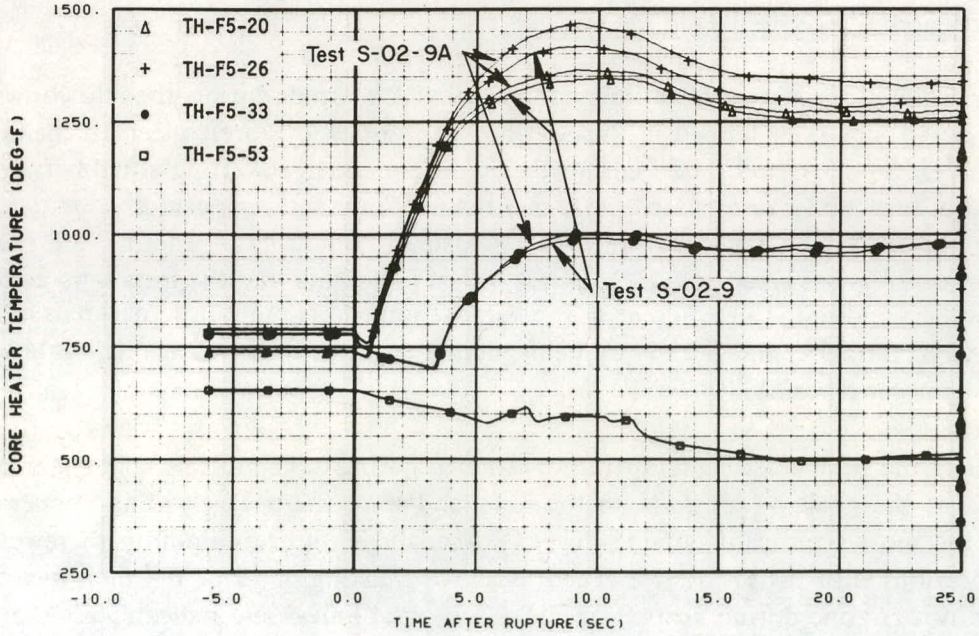

Fig. 62 Cladding temperature response of Rod F5 – Tests S-02-9A and S-02-9.

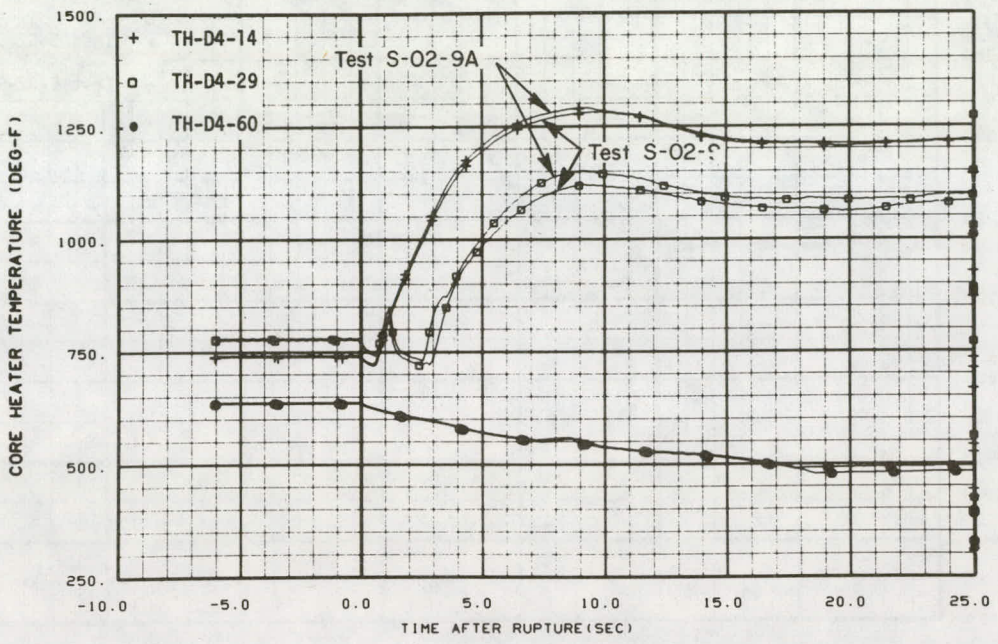

Fig. 63 Cladding temperature response of Rod D4 – Tests S-02-9A and S-02-9.

4.2 Repeatability of the Rewet Phenomena

Repeatability of the rewet phenomena that occurred during the blowdown heat transfer test series is examined in this section. The discussions are concerned mainly with Tests S-02-7, S-02-9A, and S-02-9 although the differences in rewetting noted between Test S-02-4 and Test S-02-5 results are briefly mentioned. Since the peak cladding temperature is strongly influenced by the occurrence of rewetting, to determine whether the rewetting noted on certain rods is repeatable from test to test (assuming that the tests were conducted from similar conditions) or whether the rewet phenomena is random in nature is desirable. Tests S-02-7, S-02-9A, and S-02-9, all being similar tests, provide an excellent data base for examining rewet repeatability.

Since the peak cladding temperature attained during the Semiscale cold leg break tests occurred at the peak power zone on the rods, and since the peak cladding temperature is one of the most significant variables for LOCA analysis, the repeatability of rewetting at these locations is of major interest. Table X shows a listing of all of the thermocouples in the high power zone during Tests S-02-7, S-02-9A, and S-02-9 and indicates whether or not the thermocouples experienced rewetting. (All the hot spots experienced early DNB.) As previously discussed in connection with the axial rewet patterns, the results indicated in Table X show that none of the thermocouples in the high power zone below an elevation of 27 inches experienced rewet.

TABLE X

INDICATIONS OF REWETTING AT ROD HOT SPOTS

	Test		
Thermocouple	S-0-27	S-02-9A	S-02-9
TH-E5-21			
TH-G6-21			
TH-F2-22			
TH-F3-22			
TH-E4-23			
TH-F2-25			
TH-F3-25			
TH-E5-25			
TH-G5-25			
TH-D6-25			
TH-C4-26			
TH-F5-26			
TH-E1-27	Rewet	Rewet	Rewet
TH-E4-27			
TH-C2-28	Rewet	Rewet	Rewet
TH-C3-28	Rewet		
TH-C5-28	Rewet		Rewet
TH-E6-28			
TH-F6-28J			
TH-FJ-28P			
TH-D3-29	Rewet	Rewet	Rewet
TH-A4-29	Rewet		
TH-D4-29	Rewet	Rewet	Rewet
TH-A5-29			
TH-B5-29			
TH-D5-29			
TH-B6-29			
TH-E7-29		Rewet	Rewet
TH-F7-29		Rewet	Rewet
TH-E8-29	Rewet	Rewet	Rewet
TH-E6-31	Rewet	Rewet	Rewet

Twelve thermocouples were used in the region between 21 and 26 inches from the bottom of the core, and none of them showed rewetting for any of the three tests under consideration. The response of these twelve thermocouples was then exactly reproducible in Tests S-02-7, S-02-9A, and S-02-9. Differences in rewet behavior at the hot spot among the three tests occurred only in the 27- to 31-inch elevation region. Table X shows that five thermocouples in the 27- to 31-inch elevation range did not respond in the same manner for each test. No pattern existed in the differences. Thermocouples TH-E7-29 and TH-F7-29, for example, did not rewet during Test S-02-7; they did, however, experience rewet during both Tests S-02-9A and S-02-9. Thermocouples TH-C3-28 and TH-A4-29 rewetted in Test S-02-7 but did not during Tests S-02-9A and S-02-9. Of the 19 thermocouples in the 27- to 31-inch-elevation range common to all three tests, 14 behaved similarily. Six of these 14 thermocouples experienced rewet and eight did not. Of the 31 hot spot thermocouples common to the hot spot location on the rods for Tests S-02-7, S-02-9A, and S-02-9, 26 responded in the same fashion for all three tests and five did not. A statistical analysis performed with these data (Appendix D) indicates that the probability of these events being random is less than 0.02. Two different conclusions can be reached from this analysis: (a) the behavior of a given thermocouple (rewet, no rewet) is really random from tests to test and the results observed in Tests S-02-7, S-02-9A, and S-02-9 constitute an extremely rare event, and (b) the behavior of a given thermocouple is generally not random and is dependent on many things possibly including elevation within a rod power step (fluid conditions), rod surface conditions, azimuthal location of the thermocouples with respect to the rod heating element, etc. The axial rewet pattern discussed previously suggests that elevation of a thermocouple within the high power zone may be the major factor controlling the occurrence or nonoccurrence of rewetting. Consequently, the behavior of thermocouples in the upper section ($>$ 26 inches) of the hot spot may not be as repeatable as the behavior in the lower section (21 to 26 inches) because of larger variation in the fluid conditions in the upper section.

Comparisons of results from thermocouples that were comparable in Tests S-02-4 and S-02-5 indicated, in general, similar rewetting characteristics. Of the 73 cladding thermocouples common to both tests, only eight thermocouples experienced different rewet phenomena in the two tests. The usual difference was that rewetting occurred during Test S-02-4 but did not during Test S-02-5. As discussed in Section III-2.3, these differences were probably due to the post-DNB core power control. Specific discussions concerning the particular rewetting differences noted between Tests S-02-4 and S-02-5 are contained in Appendix D.

In summary, the test comparisons presented indicate that the repeatability of the core thermal response during the blowdown heat transfer test series was good. The cladding temperature response was shown to be repeatable with a few exceptions at all axial elevations in the heated core. Although some exceptions were noted along the upper four inches of the high power zones, the rewet phenomena occurring at the rod hot spots during Tests S-02-7, S-02-9A, and S-02-9 were also shown to be highly repeatable.

IV. COMPARISON BETWEEN CALCULATED CORE THERMAL RESPONSE AND TEST DATA

The following section contains an evaluation of the agreements and differences between the measured and calculated core thermal response for Test S-02-2. The first section discusses the problems associated with the test prediction and is also concerned with the modeling changes that resulted in an improved core thermal response calculation relative to the data. The second section discusses results calculated with a model of the core and vessel.

Both a complete Semiscale system model and a separate core model were used to calculate the Semiscale core thermal response presented in the following sections. A complete description of the basic system model is contained in Reference 11. The core model and the assumptions associated with its use are described in Appendix E. Results calculated with the core model, because it was driven with boundary conditions derived from measured test data, are insensitive to errors in the core thermal calculations induced by incorrect hydraulic calculations in the system model. These calculations then provide an opportunity in view of the Semiscale data to evaluate the models used to predict the core thermal response.

The heater rod temperature comparison plots presented in the following sections represent cladding surface temperatures. The surface temperature was calculated from the measured test data using the inversion technique previously mentioned.

1. CALCULATIONS WITH THE SYSTEM MODEL

The following section discuss the pretest calculation of the Semiscale Mod-1 core thermal response for Test S-02-2. Problem areas and differences between the calculated and measured reponses are noted. Changes made to the models in attempts to improve the correlation between predictions and data are also discussed.

1.1 Pretest Calculations

A pretest calculation of the thermal hydraulic response for Test S-02-2 was done using the RELAP4 MOD3 (Update 75) computer code. The RELAP4 model utilized in this calculation had a single volume lower plenum and a single fluid channel representing the heated core length as discussed in Reference 11.

Comparison of test data with pretest calculations indicated several differences in the core hydraulic and thermal response. Differences were apparent in the following areas:

(1) Core inlet flow

(2) Core inlet density

(3) Heater rod high power zone cladding temperature response.

The response of Thermocouple TH-E5-27 (a high power rod hot spot thermocouple) and the predicted high power rod hot spot temperature are compared in Figure 64. The data in this figure show that, although the time to DNB is predicted accurately, the initial temperature rise of Rod E5 is larger than the calculated temperature rise, and the calculated temperature turns over too soon relative to the test data. Further evaluation of the calculated and measured data indicate that differences in the core hydraulics comparisons were responsible in part for the underprediction of the heater rod cladding temperature. The predicted and measured core inlet flow rate comparison shown in Figure 65, for example, indicates that the initial core flow reversal during the test was much larger in magnitude (almost a factor of four) than the calculated value and also that the predicted flow was larger than the measured flow between two and three seconds. The incorrect calculation of the core inlet flow affects both the core inlet density and possibly the location of any calculated low flow or flow stagnation points within the core. Comparison of the measured and calculated core inlet density shows that the density was overpredicted for the first 2.5 seconds of the transient. As discussed in Reference 11, the incorrect calculation of the core hydraulics was due mainly to inadequacies in the hydraulic calculations in other parts of the system (lower plenum, break flow, etc.). Consequently, the differences in the heater rod cladding temperature response shown in Figure 64 can be attributed primarily to hydraulic effects rather than to the core heat transfer models used in the calculation because the thermal and hydraulic effects are coupled.

1.2 Posttest Calculations

Evaluation of the comparisons of Test S-02-2 data and pretest calculations led to a better understanding of the Semiscale system response to blowdown and also indicated areas in which the physical effects were not being properly represented with the calculation methods. The following paragraphs address the changes made to the models and nodalization schemes in an attempt to improve the calculation techniques so that they more closely represent the actual physical phenomena occurring in the Semiscale system.

The results presented in the previous section suggest the need for improvement in the core hydraulics calculations. The details of the modeling changes and improvements made in order to better represent Semiscale data, however, are not the subject of this report; the discussion here is limited primarily to the effects of the modeling changes on the calculation of the core thermal response. Detailed discussion of the model nodalization changes can be found in Reference 11.

Four basic changes to the analytical model were made. These were:

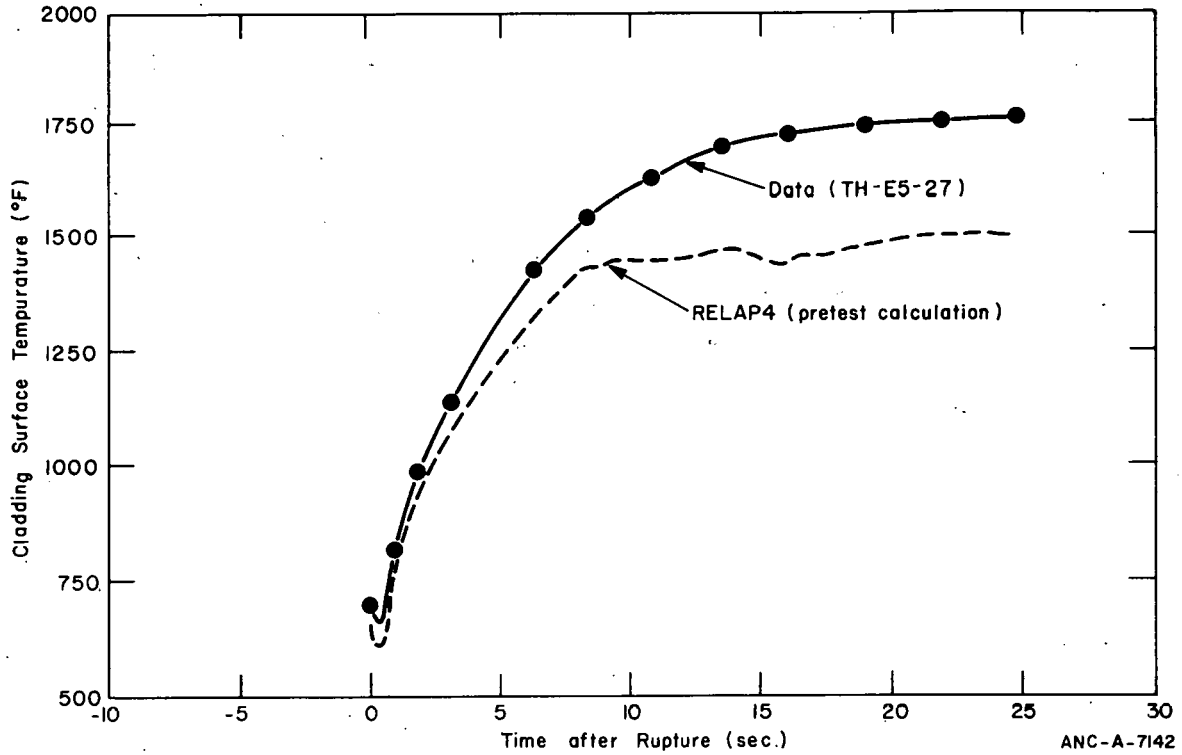

Fig. 64 Comparison of high power rod hot spot surface temperature response – RELAP4 pretest prediction and Thermocouple TH-E5-27 – Test S-02-2.

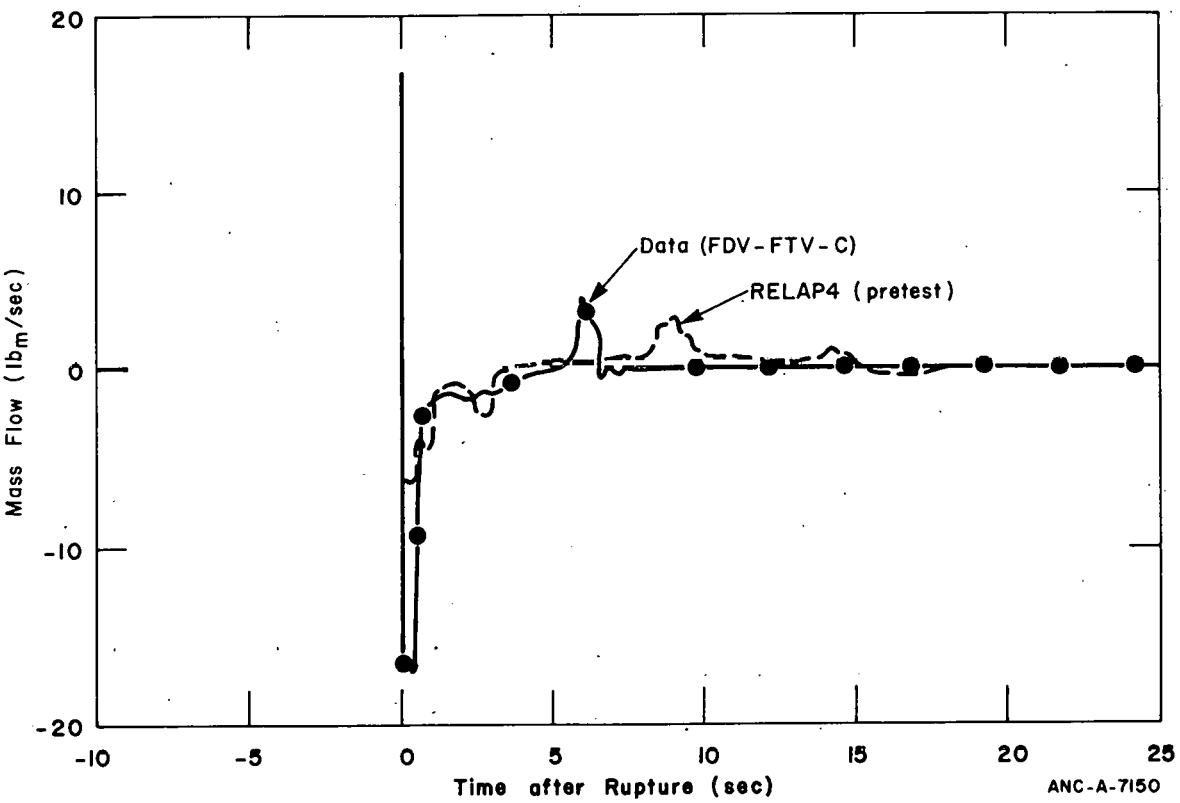

Fig. 65 Comparison of predicted and measured core inlet flow rates – RELAP4 test prediction and Test S-02-2 data.

(1) Addition of a new break flow model

(2) Addition of parallel fluid channels in the core region

(3) More detailed nodalization in the vessel lower plenum and downcomer region

(4) Replacement of the existing pool boiling heat transfer correlation with a constant value of 25 Btu/hr-ft^2-^{o}F.

An experimental version of the RELAP4 code (MOD E, Update 26) was used to provide posttest calculations of the Semiscale system response for Test S-02-2. This version of the code allowed the use of an improved break flow model, which in turn resulted in a significant improvement in the core inlet flow calculation. Figure 66 shows the improvement in the core inlet flow calculation relative to both the pretest calculation and the measured data. The improved core flow calculation resulted in some improvement in the cladding temperature response calculation, but the calculated maximum vaue is still 200^{o}F lower than the measured value. Figure 67 shows the calculation of the high power rod hot spot temperature response relative to the pretest calculation and the data.

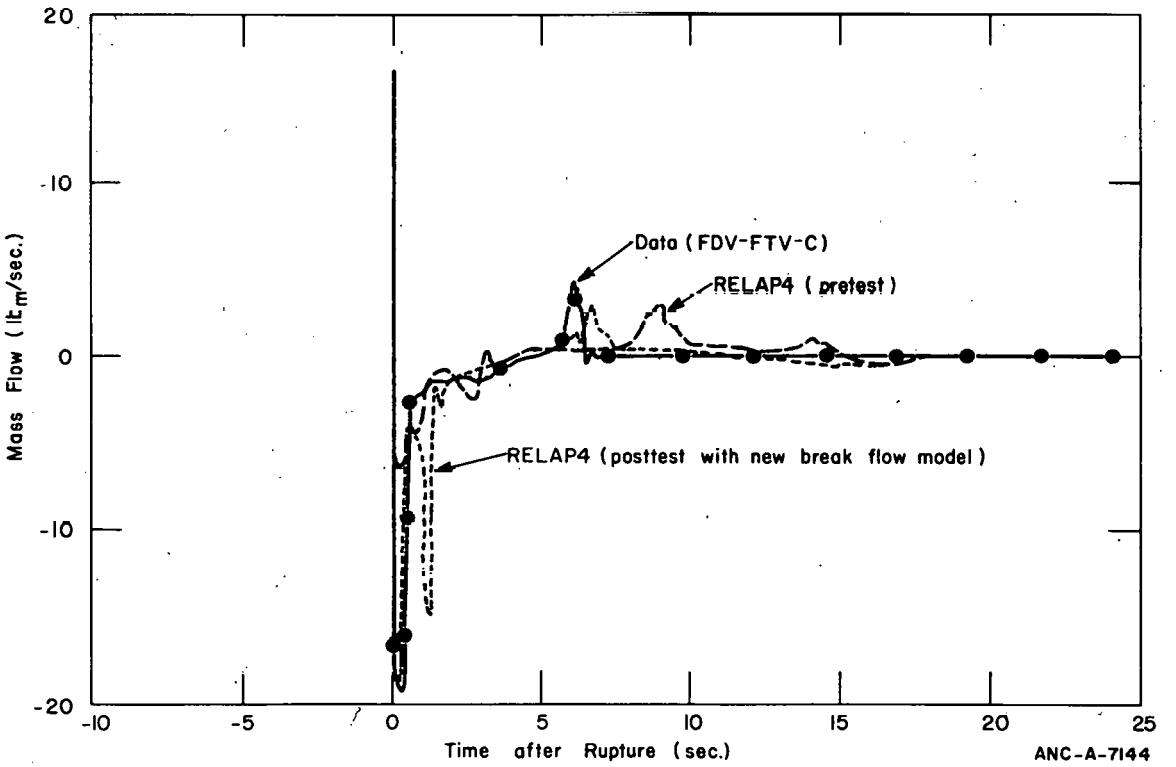

Fig. 66 Comparison of predicted and measured core inlet flow rates — pretest calculation, posttest calculation with improved break flow model, and Test S-02-2 data.

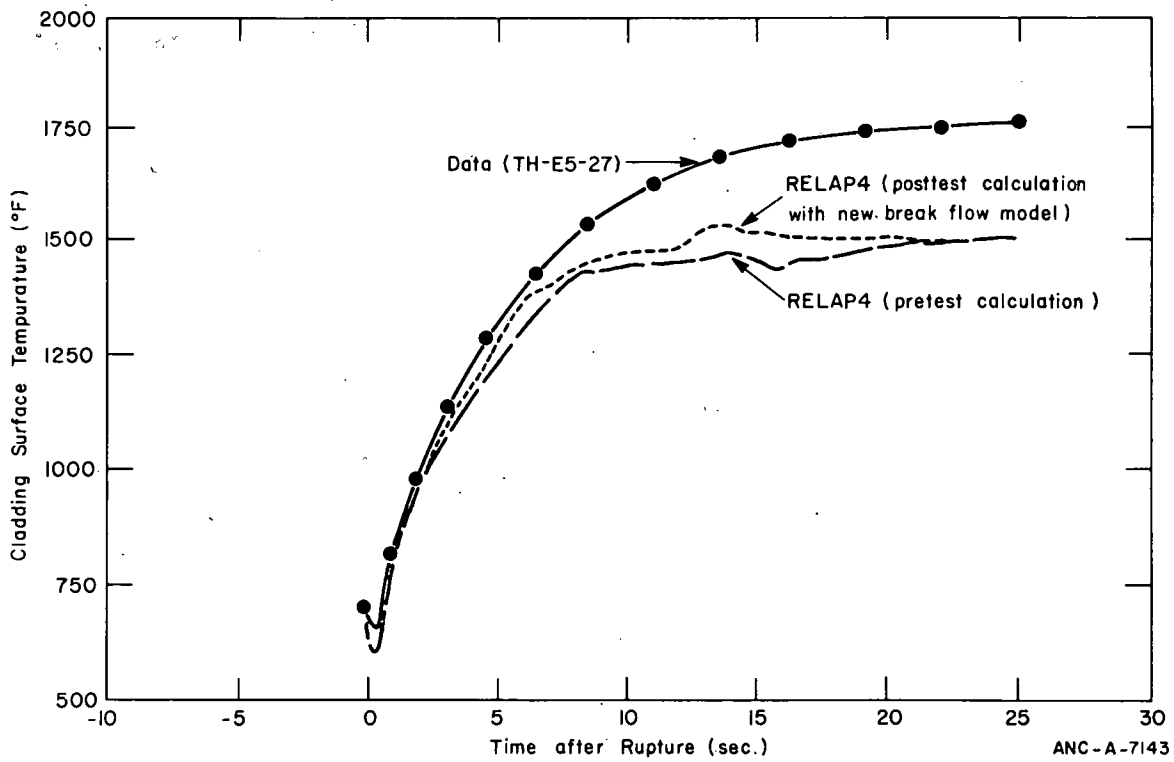

Fig. 67 Comparison of high power rod hot spot surface temperature response – posttest calculation, posttest calculation with improved break flow model, and Test S-02-2 data.

The addition of parallel fluid channels into the heated length of the core resulted in the calculation of DNB about 0.2 second earlier than indicated by the data. The parallel channels were added into the model to better represent the hot and cold fluid channels formed by the high and low power heater rods, respectively. The earlier prediction of DNB caused the calculated rod temperature to be higher than the data until about six seconds after rupture. At six seconds, the predicted and measured temperature crossed over. Prior to six seconds, the heatup rate of the calculated temperature response was lower than the heatup rate indicated by the test data. This difference is again believed to be due partially to differences between the calculation and the data in the core inlet flow and density (both were overpredicted).

Changes in the nodalization representing the vessel lower plenum and downcomer (Reference 11) improved both the calculation of the core inlet flow and density. The cladding temperature calculation was also improved slightly, although the peak temperature was still underpredicted. Figure 68 shows the improvement in the calculated temperatures attributed to the addition of the parallel fluid channels in the core and changes in the model nodalization scheme.

Changes in the heat transfer models used in the calculation in addition to the above mentioned changes caused the calculated high power rod hot spot temperature to be overpredicted. The heatup rate indicated by Thermocouple TH-E5-27 was also overpredicted, as shown in Figure 69. The heat transfer model change included deletion of the

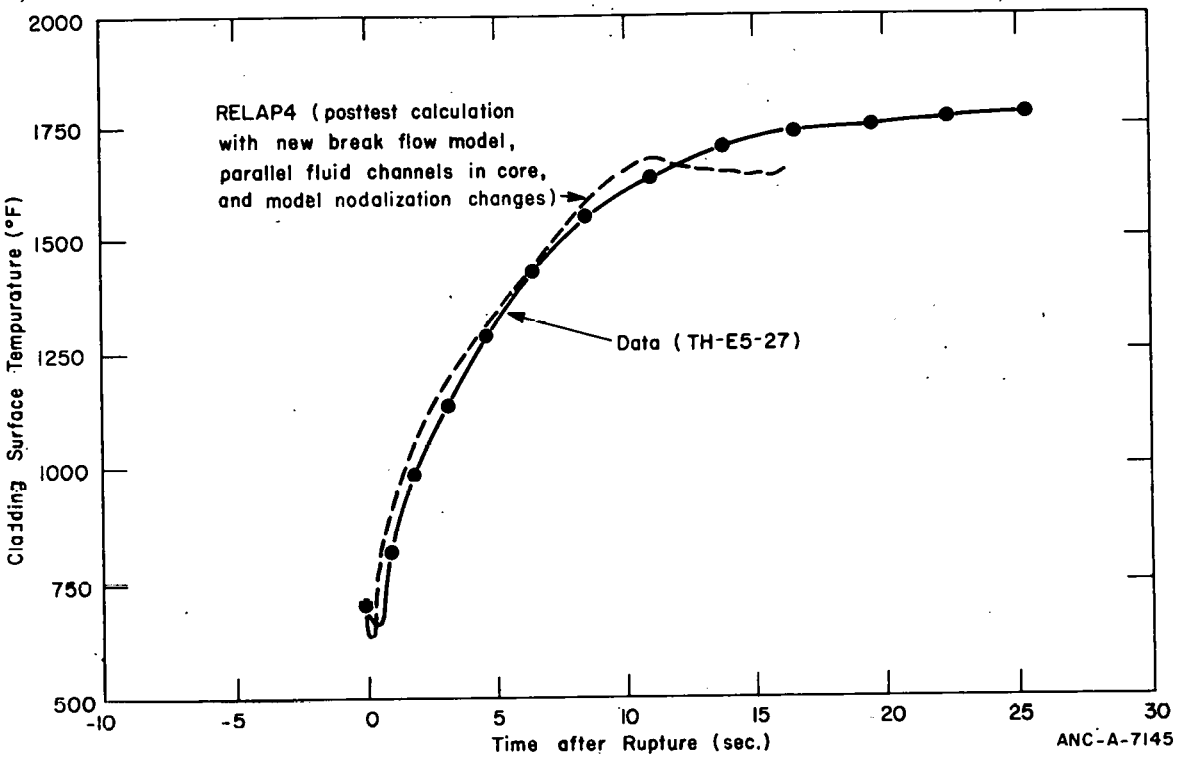

Fig. 68 Comparison of high power rod hot spot surface temperature response – posttest calculation with improved break flow model, parallel fluid channels in the core, and vessel nodalization changes and Test S-02-2 data.

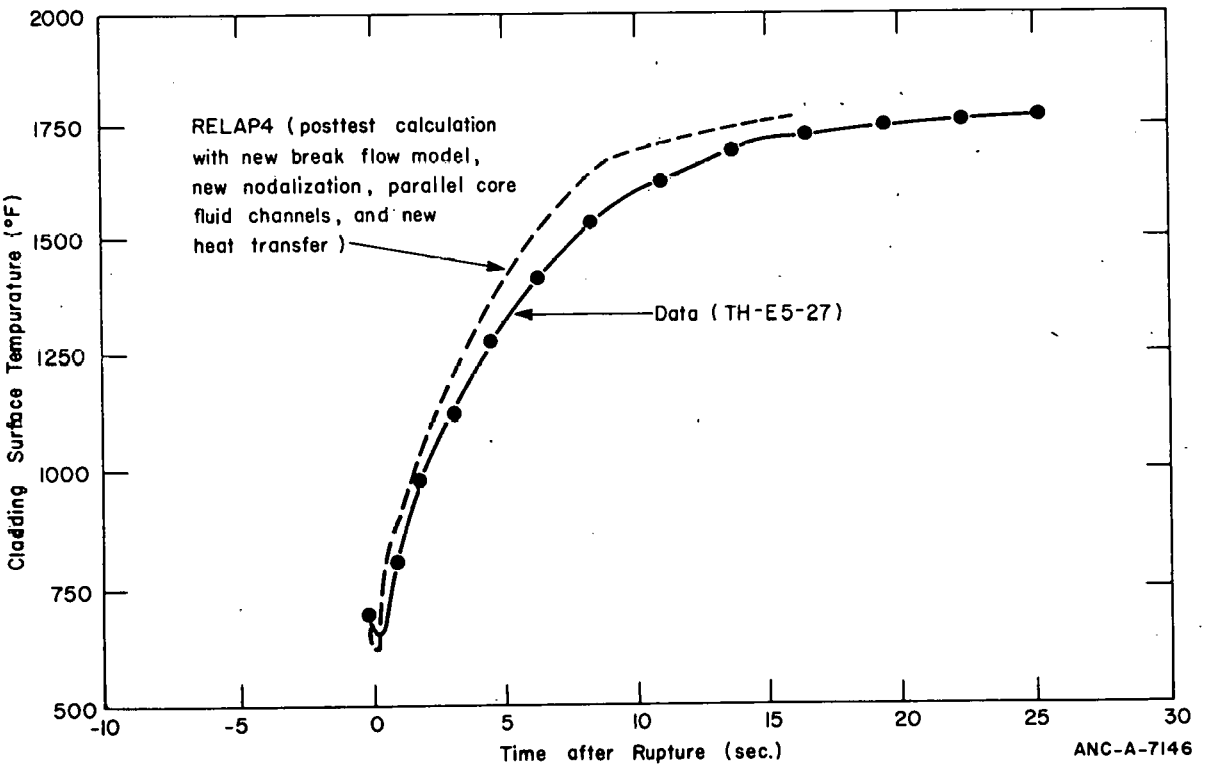

Fig. 69 Comparison of high power rod hot spot surface temperature response – posttest calculation with improved break flow model, parallel fluid channels in the core, vessel nodalization changes, and new heat transfer model and Test S-02-2 data.

Berenson[13] pool film boiling correlation and substitution of a constant value of 25 Btu/hr-ft^2-^{o}F for the heat transfer coefficient in its place. This change was made because test data indicated that the Berenson correlation overpredicted the value of the heat transfer coefficient.

2. CALCULATIONS WITH THE CORE MODEL

Calculations conducted with the core model provide an opportunity to examine the heat transfer correlations used in the RELAP4 code more effectively than do calculations with the system model. Use of the measured test data as input boundary conditions for the core model allows elimination, to a large extent, of the core hydraulic errors that affected the core thermal response in the system model calculations. A description of the core model and associated boundary conditions is contained in Appendix E.

Figure 70 shows comparisons of the high power rod hot spot cladding surface temperatures calculated with the core model and the cladding surface temperature calculated from the response of Thermocouple TH-E5-27 during Test S-02-2. The two predicted temperatures shown in Figure 70 were calculated with the Berenson heat transfer correlation replaced by a constant value of 25 Btu/hr-ft^2-^{o}F. Convective film boiling was, however, treated differently in the two predictions. The Groeneveld 5.9[14] correlation was used in one case and the Dougall–Rohsenow[15] correlation was used in the other case. The results in Figure 70 indicate that the Groeneveld correlation, in conjunction with replacement of the Berenson correlation with a constant value of 25, overpredicted the data.

The calculations in Figure 70 were conducted with RELAP4 MOD E, Update 15. In the most recent version of the code (RELAP4 MOD 005, Update 1), the Berenson correlation has been replaced with a slightly modified version of the Bromley[16] correlation. Figure 71 shows the comparison of the calculated heater rod hot spot surface temperature with the surface temperature calculated from the response of three different hot spot thermocouples (Thermocouples TH-B6-29, TH-D5-29, and TH-D4-29) during Test S-02-9. As shown in Figure 71, the heat transfer models reasonably predict the cladding temperature of the rods on which rewetting did not occur.

In summary, the comparisons presented in these sections illustrate the importance of accurately calculating the core hydraulic response in order to provide accurate calculations of the core thermal response. The core model calculations showed that, given the correct input hydraulic boundary conditions, use of a value of 25 Btu/hr-ft^2-^{o}F instead of the Berenson correlation resulted in a better calculation of the heater rod hot spot temperature response. The core model calculations also showed that use of the Groeneveld 5.9 flow film boiling correlation resulted in better predictions than did use of the Dougall-Rohsenow correlation. The calculations performed with the core model indicate that both hot and average fluid channels should be included in the core to properly predict the occurrence of

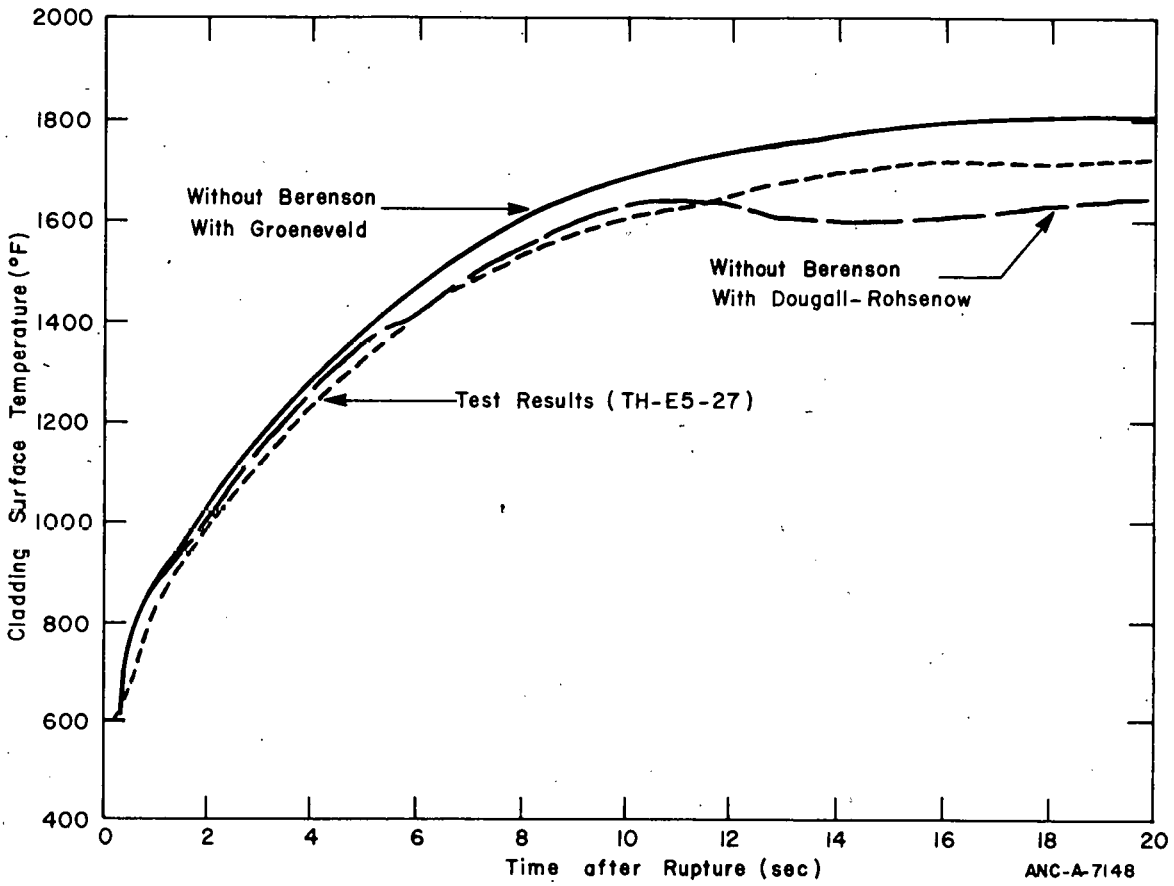

Fig. 70 Comparison of high power rod hot spot surface temperature response – core model calculations and Test S-02-2 data.

DNB. Use of both hot and average fluid channels in the system model resulted in a prediction of DNB that was about 0.2 second earlier than the data indicated. This early prediction of DNB could, however, be due to the existence of errors in the core hydraulic calculations, or perhaps the surface temperature calculated from the test data is in error. Satisfactory predictions of the hot spot cladding surface temperature were obtained using the latest version of the RELAP4 code. In this version, a modified version of the Bromley correlation has replaced the Berenson heat transfer correlation. The occurrence of rewetting at some of the high power zone thermocouple locations (such as occurred during Tests S-02-7 and S-02-9) was not predicted by the analytical models. This may be a result of the nodalization used in the models (one fluid volume was used to simulate the fluid adjacent to the rod high power zones) and the inability to simulate the effects of the grid spacers on the core flow patterns.

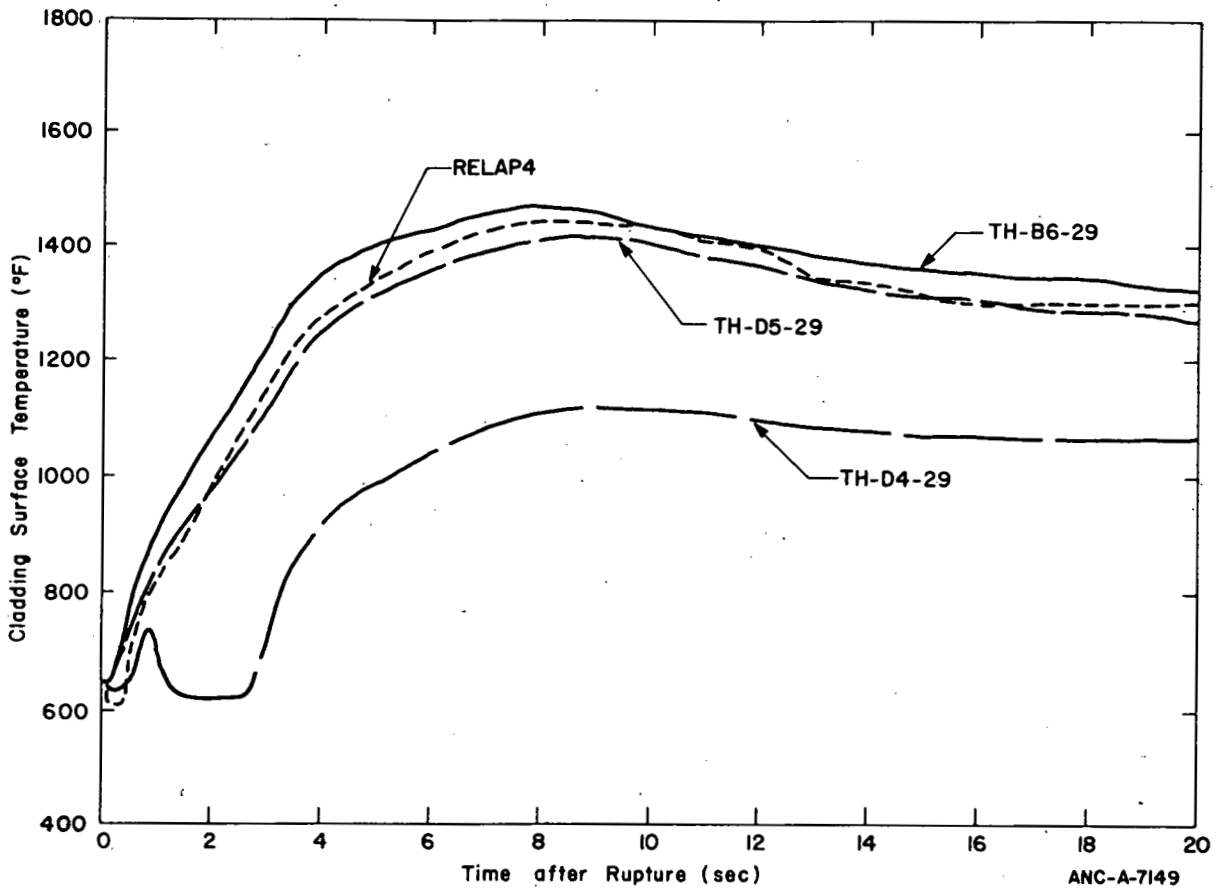

Fig. 71 Comparison of heater rod hot spot surface temperature core model calculations and Test S-02-9 data.

V. CONCLUSIONS

The following conclusions have been reached in analyzing the response of the Semiscale heater rods during the blowdown heat transfer test series.

1. GENERAL CORE RESPONSE TO CORE FLOW

During blowdown, the core thermal response was heavily dependent on the core flow direction. The core flow direction was in turn controlled by the break location. The hot leg break caused the transient core flow to remain in the normal (upward) direction. The combination of the high core inlet fluid density and flow during the hot leg break resulted in a quasi-steady heat transfer process in which excellent cooling was provided to the core heater rods. Consequently, no DNB occurred, and the rod cladding temperatures continually declined from their steady state values. The core thermal response during a cold leg break test was entirely different. In response to the break flow, the core flow immediately reversed at the occurrence of rupture. Core flow stagnation occurred between 3 and 5 seconds after rupture. Departure from nucleate boiling at the rod high power zones occurred between 0.4 and 4 seconds after rupture, depending on rod power density. DNB caused severe degradation in heat transfer at the rod surfaces which resulted in sharp cladding temperature increases. Rod rewetting subsequent to DNB occurred in some cases and greatly reduced the maximum cladding temperatures attained.

Variations in the measured reverse core flow magnitude and duration during the cold leg breaks were noted to affect the time to DNB on some of the low power rods in the core. The high power rods were relatively unaffected.

2. INFLUENCE OF SPECIFIED OPERATING CONDITIONS

The different core fluid temperature distributions imposed on the system during the blowdown heat transfer tests indirectly affected the core cladding temperatures. The fluid temperature distribution was shown to affect the magnitude of the transient core flow, which in turn altered the time to DNB on some of the rods.

The different power densities and radial power distributions imposed on the rods during the blowdown heat transfer test series seemed to affect only the peak cladding temperatures attained during the transient. The cladding temperature response was no more radially uniform during the flat radial power distribution tests than it was during the tests with the peaked radial power distribution.

3. HEATER ROD REWET BEHAVIOR

No definite radial patterns existed in the rod hot spot rewetting phenomena. More rewets were, however, noted to occur in the upper left and lower right quadrants of the core for some of the tests. No correlation could be found between the rewetting phenomena and local rod power density variations.

A definite axial pattern in the rewet phenomena was noted. Rewets were observed to occur in certain regions of the core that were not necessarily defined by the rod power steps. This axial pattern existed for all of the full power tests. The implication of this axial distribution is that the close interaction between both quality and power density controls rewetting. The axial pattern in rewets holds for rod peak power densities between about 11.5 and 14.25 kW/ft.

4. DATA REPEATABILITY

In general, the core thermal results from essentially identical tests were quite repeatable. The data were reproducible in terms of both the post-DNB cladding temperature response and the rewet behavior.

5. COMPARISON BETWEEN CALCULATED CORE THERMAL RESPONSE AND TEST DATA

The core hydraulic response must be calculated accurately in order to provide an accurate calculation of core thermal response. Given the correct hydraulic boundary conditions, calculations showed that use of a value of 25 Btu/hr-ft^2-^{o}F instead of the Berenson correlation results in a more nearly accurate prediction of the heater rod hot spot temperature response. The Groeneveld 5.9 flow film boiling correlation produced better prediction than did the Dougall–Rohesenow correlation.

The most recent version of the RELAP4 code, in which the Berenson correlation has been replaced with a modified version of the Bromley correlation, provided satisfactory calculations of the rod hot spot cladding surface temperature response.

VI. REFERENCES

1. H. S. Crapo, M. F. Jensen, K. E. Sackett, *Experimental Data Report for Semiscale Mod-1 Test S-02-1 (Blowdown Heat Transfer Test),* ANCR-1231 (July 1975).

2. H. S. Crapo, M. F. Jensen, K. E. Sackett, *Experiment Data Report for Semiscale Mod-1 Test S-02-2 (Blowdown Heat Transfer Test),* ANCR-1232 (August 1975).

3. H. S. Crapo, M. F. Jensen, K. E. Sackett, *Experiment Data Report for Semiscale Mod-1 Test S-02-3 (Blowdown Heat Transfer Test),* ANCR-1233 (September 1975).

4. H. S. Crapo, M. F. Jensen, K. E. Sackett, *Experiment Data Report for Semiscale Mod-1 Test S-02-7 (Blowdown Heat Transfer Test),* ANCR-1237 (November 1975).

5. H. S. Crapo, M. F. Jensen, K. E. Sackett, *Experiment Data Report for Semiscale Mod-1 Test S-02-4 (Blowdown Heat Transfer Test),* ANCR-1234 (November 1975).

6. H. S. Crapo, M. F. Jensen, K. E. Sackett, *Experiment Data Report for Semiscale Mod-1 Test S-02-5 (Blowdown Heat Transfer Test),* ANCR-1235 (January 1976).

7. H. S. Crapo, M. F. Jensen, K. E. Sackett, *Experiment Data Report for Semiscale Mod-1 Tests S-02-9 and S-02-9A (Blowdown Heat Transfer Test),* ANCR-1236 (January 1976).

8. J. V. Beck, "Nonlinear Estimation Applied to the Nonlinear Inverse Heat Conduction Problem", *International Journal of Heat and Mass Transfer, 13* (1970) pp 703-716.

9. K. V. Moore and W. H. Rettig, *RELAP4 – A Computer Program for Transient Thermal-Hydraulic Analysis* ANCR-1127, Rev. 1 (March 1975).

10. E. M. Feldman and D. J. Olson, *Semiscale Mod-1 Program and System Description for the Blowdown Heat Transfer Tests (Test Series 2),* ANCR-1230 (August 1975).

11. J. M. Cozzuol, *Thermal Hydraulic Analysis of the Semiscale Mod-1 Blowdown Heat Transfer Test Series,* ANCR-1287 (June 1976).

12. D. S. Rowe, *COBRA3C: A Digital Computer Program for Steady State and Transient Thermal-Hydraulic Analysis of Rod Bundle Nuclear Fuel Elements,* BNWL-1695 (March 1973).

13. P. J. Berenson, "Film-Boiling Heat Transfer from a Horizontal Surface", *Journal of Heat Transfer,* 83 (August 1961) pp 351-358.

14. D. C. Groeneveld, *An Investigation of Heat Transfer in the Liquid Deficient Regime,* AECL-3281, Rev. 1 (December 1968, revised August 1969).

15. R. S. Dougall and W. M. Rohsenow, *Film Boiling on the Inside of Vertical Tubes with Upward Flow of the Fluid at Low Qualities,* MIT-TR-9079-26 (1963).

16. L. A. Bromley, "Heat Transfer in Stable Film Boiling", *Chemical Engineering Progress* (1950) pp 221-227.

THIS PAGE

WAS INTENTIONALLY

LEFT BLANK

APPENDIX A

CORE POWER CONTROL

THIS PAGE

WAS INTENTIONALLY

LEFT BLANK

APPENDIX A

CORE POWER CONTROL

The purpose of this appendix is to explain the need for use of a transient electrical core power control during the Semiscale blowdown tests that is different from the standard nuclear core power decay curve[A-1]. The analytical technique used to determine an appropriate electrical power control is also described.

The material property differences between the Semiscale electrical rod and a nuclear rod and the lower peak temperature limit on the electrical rod result in a somewhat different thermal performance. Since the thermal diffusivity of a UO_2 rod is much lower than that of boron nitride (principal composition by volume of the electrical rod), the nuclear rod will contain a greater amount of stored energy at a given condition that will an electrical rod at the same conditions. Therefore, in order for the electrical rods to adequately model a nuclear core during blowdown, the transient electrical power must be adjusted to account for differences in the stored energy of the rods.

The criterion for selecting an electrical rod power control is that it causes the surface temperature of an electrical rod to approach as closely as possible the surface temperature calculated for a nuclear rod. This criterion was met by matching the transient surface heat flux calculated for an electrical rod with the transient surface heat flux calculated for a nuclear rod, assuming that both rods were subjected to the same transient boundary conditions. These calculations were performed using one-dimensional analytical heat conduction models of the electrical and nuclear rods. The power decay curve applied to the nuclear rod in all cases was the proposed standard power decay discussed in Reference A-1. Since the Semiscale electrical heater rods have a fixed axial peaking factor of 1.58, use of the technique described to specify the core power control allows the matching of electrical and nuclear rod surface heat fluxes at only one axial location. The rod axial location of peak power generation (the hot spot) was the point at which the nuclear and electrical fluxes were matched because the cladding temperature response at this location was of prime concern during the blowdown heat transfer test series.

The power profile shown in Figure 7 of the main body of this report and in Figure A-1 of this appendix was derived using the above described method of heat flux matching, assuming that the heat transfer mechanism at both rod surfaces was nucleate boiling for the entire blowdown transient. As a result of this assumption, the power profile causes the electrical rod response to correctly simulate a nuclear rod only up until the time at which DNB occurs. To provide better representation of a nuclear rod, improved post-DNB core power controls were used for Test S-02-5 and for Tests S-02-9 and S-02-9A. In the case of Test S-02-5, measured data (core fluid temperature, rod heat transfer coefficients, etc.) from Test S-02-4 were used as transient input boundary conditions for the analytical models. In the case of Tests S-02-9A and S-02-9, measured data from Test S-02-7 were used as boundary conditions for the analytical models. Two improved post-DNB core power controls were thus defined using the surface heat flux matching technique. The power

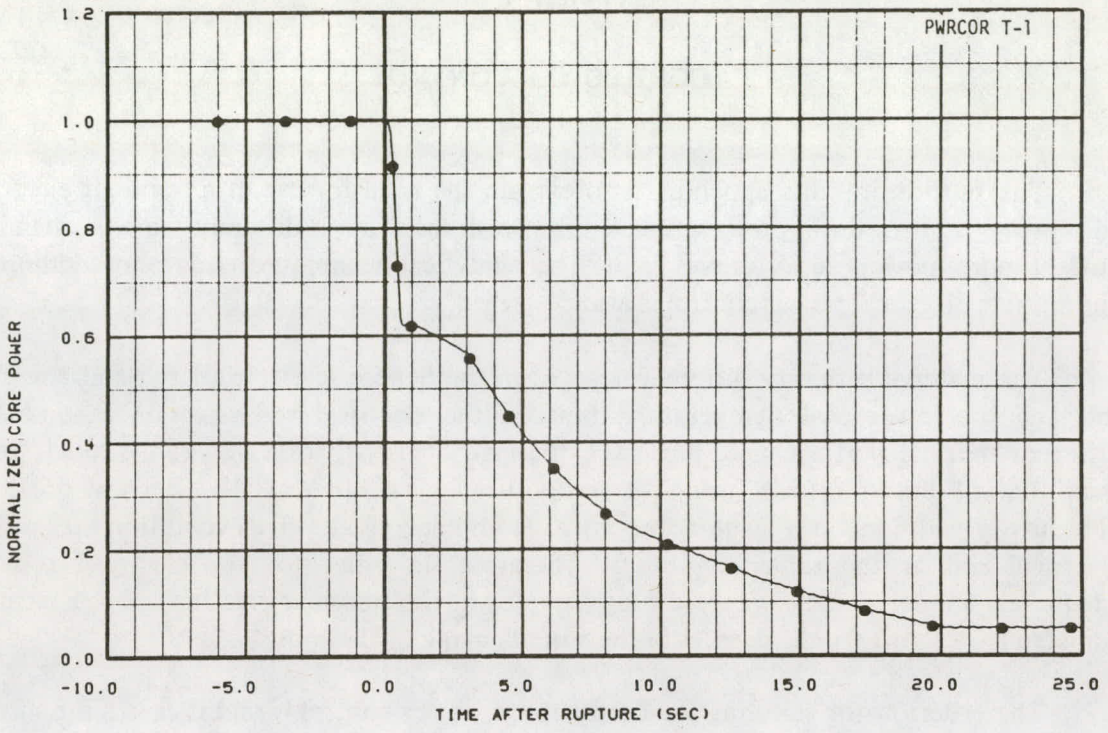

Fig. A-1 Normalized transient core power.

defined for Tests S-02-9A and S-02-9 is different from that defined for Test S-02-5 only because of the radial peaking in the core in Test S-02-5. Because of this peaking, the rod hot spot power densities were different (14.25 kW/ft for Test S-02-5 versus 11.84 kW/ft for Tests S-02-9A and S-02-9). Consequently, the same core power control specification could not be used in all three tests.

REFERENCE

A-1. Proposed ANS Standard, *Decay Energy Release Following Shutdown of Uranium-Fueled Thermal Reactors,* ANS-5-1, (October 1971).

APPENDIX B

ANALYSIS OF ROD LOCAL POWER DENSITY

THIS PAGE

WAS INTENTIONALLY

LEFT BLANK

APPENDIX B

ANALYSIS OF ROD LOCAL POWER DENSITY

During the course of the blowdown heat transfer test series, several special tests were conducted on the system. Some of these tests were conducted as part of the established warmup procedure for each blowdown, and others were conducted in attempts to answer specific questions concerning the system response. The purpose of this appendix is to describe these special tests and present results from special test data and other Semiscale test data that were used in conjunction with the question of heater rod power density variation.

The data used in the analysis of the Semiscale heater rod power density variations included the following:

(1) Steady state cladding temperature values

(2) Power pulse test data

(3) Heater rod infrared scan profiles

(4) Heater rod X-ray photographs

(5) Dry core heatup data.

The response of Thermocouple TH-D4-29 which experienced rewetting in relation to that of Thermocouple TH-D5-29 which did not experience rewetting during Test S-02-7 prompted the analysis of the Semiscale special test data in search of reasons to explain these differences in behavior. Comparison of the steady state cladding temperatures from all the thermocouples at a given core elevation indicated some variation in the initial values of the temperature from rod to rod. The initial values of the cladding temperature during Test S-02-7 are shown plotted versus core elevation in Figure B-1. The temperature variations shown on this figure, although relatively small, seem to imply that differences do exist in the characteristics of individual rods. However, many possible reasons exist for the variation shown in Figure B-1. A few possibilities are:

(1) Radial location of the thermocouple beneath the cladding surface

(2) Local power density variations

(3) Thermocouple contact resistance

(4) Azimuthal location of the thermocouple in relation to the heater coils

(5) Thermocouple measurement errors

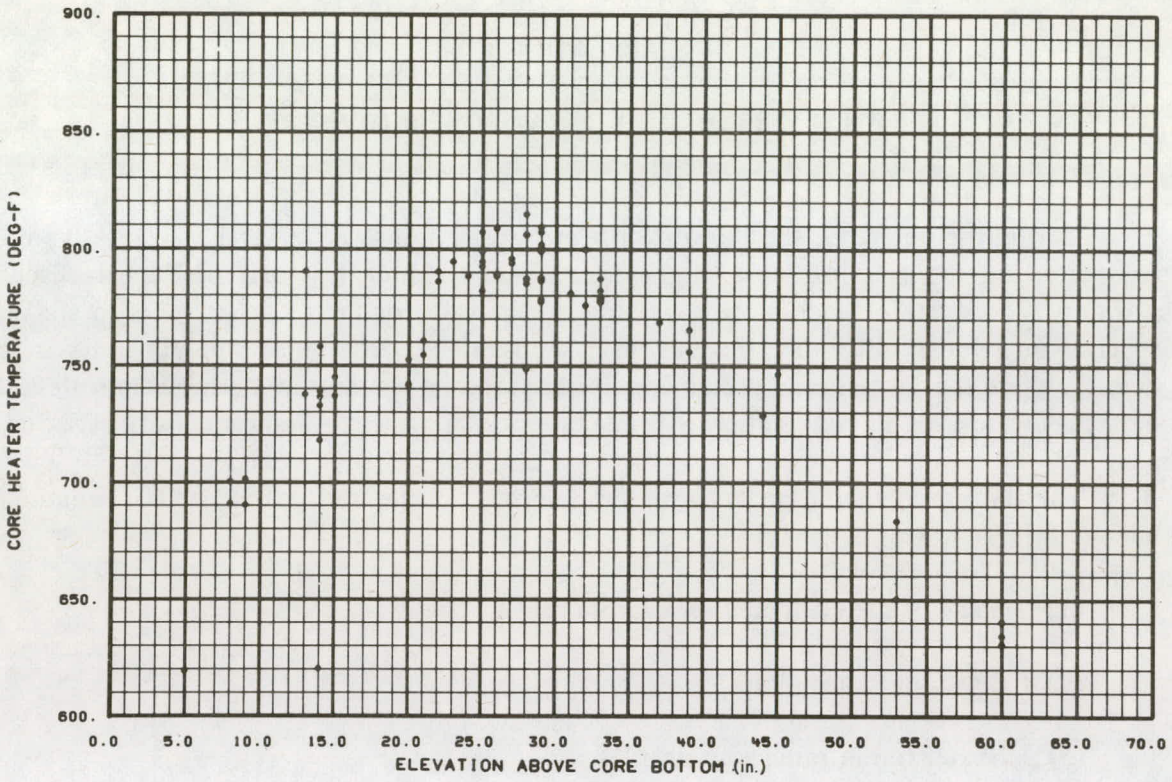

Fig. B-1 Preblowdown steady state cladding temperature versus elevation – Test S-02-7.

(6) Flow maldistribution within the core

(7) Errors in the actual thermocouple elevation

(8) Changes in the individual rod material thermal properties.

1. POWER PULSE TEST DATA ANALYSIS

Special tests prior to each blowdown were conducted on the electrical core in an attempt to detect changes in the rod material thermal properties. These tests were termed "power pulse" tests. The tests were conducted by applying a step change to the core voltage, maintaining the voltage for about ten seconds, and then returning the voltage to its initial value. These tests were conducted while the core was operating at low power (about 150 kW), and the peak power applied to the core was generally about 550 kW. Figure B-2 shows the response of Thermocouples TH-D5-29 and TH-D4-29 to the pulse test conducted prior to Test S-02-7. Also shown on the figure is the predicted response of the high power zone. The predicted response was calculated with a one-dimensional conduction model of the Semiscale eletrical rod. The prediction agrees quite well with the behavior of the thermocouple on Rod D5. The power input to the model had to be reduced by about 13%

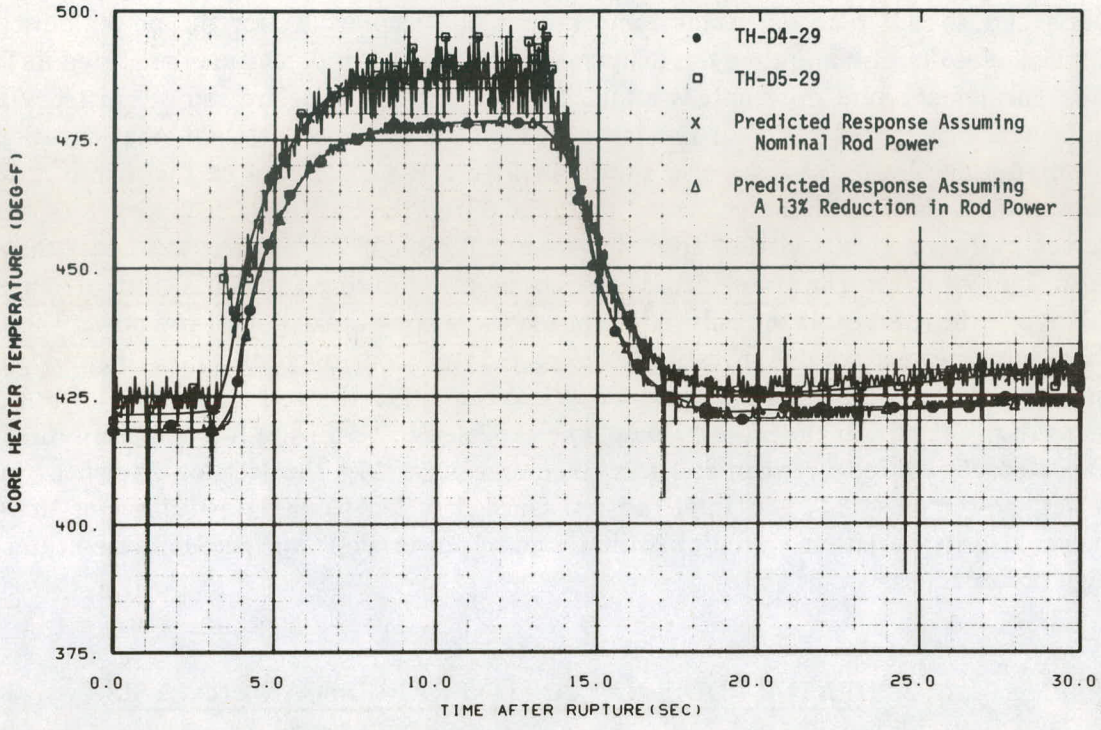

Fig. B-2 Measured and predicted response of Thermocouples TH-D4-29 and TH-D5-29 during pulse test.

in order to duplicate the measured behavior of Thermocouple TH-D4-29. However, the power generation of Rod D4 was not necessarily 13% lower than that of Rod D5. In applying the conduction model, the assumption was made that the two rods were identical as far as material properties, thermocouple location, and thermocouple contact resistance were concerned. This assumption probably does not exactly represent the true conditions. The difference in response of Rods D4 and D5 during the pulse test was, however, in agreement with the behavior of the rods as indicated by Thermocouples TH-D4-29 and TH-D5-29 during the Test S-02-7 blowdown (Thermocouple TH-D5-29 did not experience rewet).

The response of the hot spot to the power pulse tests was analyzed by computing the maximum temperature differential attained during the course of the pulse test. The following equation was used to calculate the temperature differential:

$$\Delta T = [T_{TC} - T_f(Z)]_1 - [T_{TC} - T_f(Z)]_2 \qquad \text{(A-1)}$$

where

T_{TC} = measured thermocouple temperature

$T_f(Z)$ = fluid temperature at the thermocouple elevation.

The subscripts 1 and 2 refer, respectively, to the time prior to application of the power pulse and to the time when the temperatures had stabilized after the power pulse was applied. Results of computing the temperature differential in this manner are listed in Table B-I. The temperature differentials attained at the rod hot spots are shown plotted against individual heater rod electrical resistance in Figure B-3. Those hot spots that experienced rewet during Test S-02-7 are also shown in Figure B-3. The data of this figure indicate substantial variation in the values of the pulse ΔT of the individual rods. Seven of the 24 values plotted had a deviation from the mean ΔT value ($57.5^{\circ}F$) that was larger than 1σ. Also, four of the thermocouples that experienced rewet during Test S-02-7 indicated a pulse ΔT above the average. If the pulse ΔT response was a good indication of rod power variation, then more rewets would probably be expected to occur on rods whose thermocouples indicated a lower-than-average pulse ΔT. Also, the larger the rod resistance (lower power generation), the lower the pulse ΔT would be expected to be. Figure B-3 does not reflect this expected correlation between rod resistance and pulse ΔT. The lack of agreement in the rewet, power pulse ΔT, and total rod resistance data led to an investigation of the local power density variation (variation within a given power step) on the Semiscale heater rod high power zones.

2. HEATER ROD X-RAY AND INFRARED SCAN ANALYSIS

Both X-rays and infrared scans of the Semiscale heater rods were utilized in investigating the existence of local power density variations on the Semiscale rods. The infrared scan tests were conducted as part of the heater rod acceptance test. The test was conducted by taking a series of infrared photographs of the heater rod while power pulses were applied to the rod which was in an air environment. Figure B-4 is an infrared scan of one of the heater rods. Locations where abnormalities on the infrared scans were detected, such as that indicated in Figure B-4, were then investigated on the X-rays of the rods. In many instances, variations on the infrared scans could be correlated with differences in the local pitch on a given rod power step. Figure B-4, for example, illustrates the infrared scan of Rod E5 (Serial Number A88112 – used in the core for Test S-02-1, S-02-2, and S-02-3). Examination of the X-ray for this rod revealed that the pitch of the resistance wire in the rod varied about 6% in the vicinity indicated by the hump on the scan. Table B-II indicates the variation in effective coil wire length based on the measured pitch variations. Similar results were noted on other rods that were analyzed in this manner. Table B-III compares the pitch and wire lengths of the high power zone resistance wire for several of the high power rods. The variations noted in the resistance wire pitch are not intolerable as far as the Semiscale tests are concerned. An important concern in application of the analytical technique used to calculate rod heat transfer coefficients, surface fluxes, and surface temperatures from the measured data is the axial location of the thermocouples in relation to the power density variations. If the power input to the analytical model does not accurately reflect the rod power density, then incorrect results are obtained for the calculated rod surface flux and surface heat transfer coefficients. Attempts to improve on the power input values for the analytical technique and perhaps partially account for thermocouple locations relative to power density variations required a special Semiscale dry core heatup test.

TABLE B-I

RESPONSE OF ROD HOT SPOT THERMOCOUPLES TO POWER PULSE TEST CONDUCTED DURING WARMUP FOR TEST S-02-7

Thermocouple	ΔT	$\Delta T/\overline{\Delta T}$	$>1\sigma$	Rewet
TH-G6-21	40.5	0.71	X	No
TH-E5-21	45.5	0.79	X	No
TH-F2-22	60.5	1.05		No
TH-D6-22	53.5	0.93		No
TH-E4-23	53.5	0.93		No
TH-G5-24	51.5	0.90		No
TH-F3-25	55.5	0.97		No
TH-E5-25	51.5	0.90		No
TH-D6-25	54.4	0.95		No
TH-D8-25	60.5	1.05		No
TH-F2-25	56.5	0.98		No
TH-C4-26	62.5	1.09		No
TH-F5-26	53.5	0.93		No
TH-E4-27	53.5	0.93		No
TH-E1-27	63.5	1.11		Yes
TH-C5-28	55.5	0.97		Yes
TH-H4-28	66.5	1.16	X	Yes
TH-C2-28	68.5	1.19	X	Yes
TH-F6-28J	55.5	0.97		No
TH-E6-28	55.5	0.97		No
TH-F6-28P	60.5	1.05		No
TH-D4-29	53.5	0.93		Yes
TH-A5-29	65.5	1.14	X	No
TH-B5-29	53.5	0.93		No
TH-E8-29	64.5	1.12	X	Yes
TH-E7-29	59.5	1.04		No
TH-A4-29	55.5	0.97		Yes
TH-B6-29	71.5	1.25	X	No
TH-D5-29	57.5	1.00		No
TH-F7-29	66.5	1.16	X	No
TH-D3-29	53.5	0.93		Yes

$n = 31$

$\overline{\Delta T} = 57.4$

$s = 6.66$

$s/\overline{\Delta T} = 0.12 = 1\sigma$

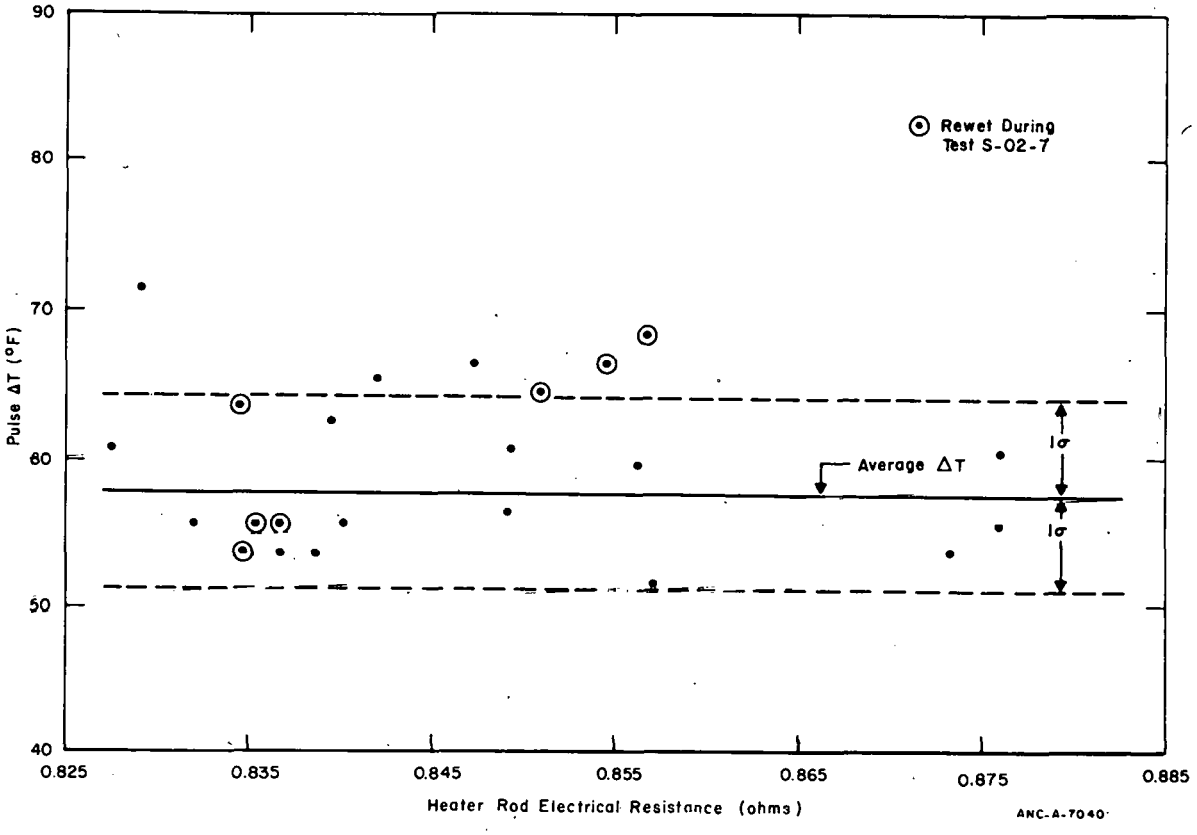

Fig. B-3 Heater rod hot spot temperature differential versus rod electrical resistance during pulse test.

3. DRY CORE HEATUP TEST ANALYSIS

The dry core heatup was conducted on the Semiscale system by stepping the core power from a low value to a higher specified value, maintaining the power for a short time, and then shutting the power off. This test was conducted with air as the medium surrounding the heater rods. The test was then essentially an adiabatic heatup of the core. The core was also reflooded at a very low flood rate subsequent to the power shutdown. The reflood portion of this test allowed quench times of the thermocouples to be compared for verification of their elevation in the core. Figure B-5 shows the typical response of the rod cladding to the dry heatup test. New power factor multipliers were calculated by evaluating the slope ($\Delta T/\Delta t$) for each hot spot temperature measurement during the heatup portion of the test and then normalizing the individual slopes to the average slope. Consequently, a new power multiplier of less than 1.0 would indicate that according to the thermocouple response during the dry heatup, the power density on that particular rod was somewhat less than the nominal desired power density. Similarly, a power multiplier larger than 1.0 would indicate a power density larger than nominal. The power multipliers calculated in this manner were verified by using them in conjunction with the analytical inversion calculations to determine whether essentially zero rod surface heat fluxes were

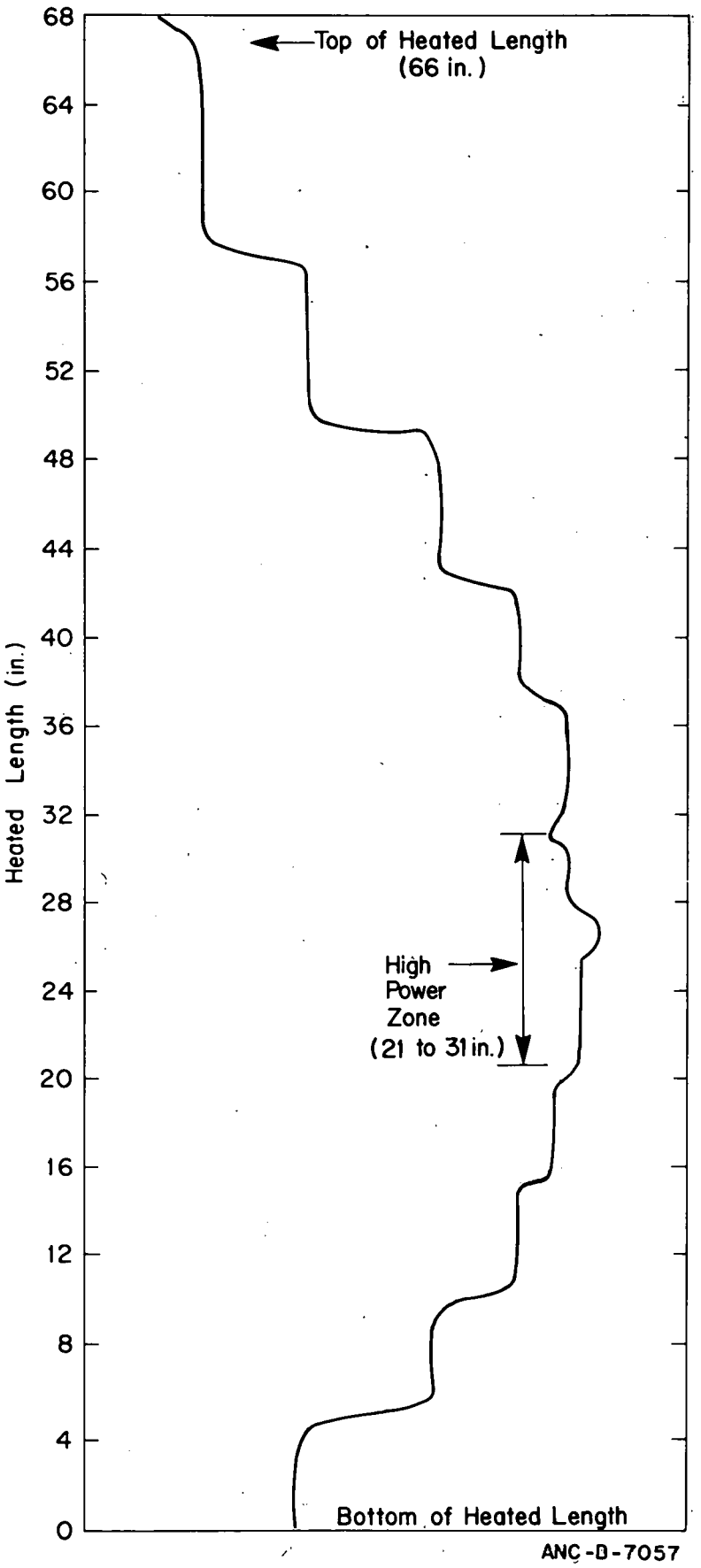

Fig. B-4 Infrared scan of Rod E5.

TABLE B-II

RESISTANCE WIRE LENGTH VARIATIONS ON
ROD E5[a] HIGH POWER ZONE

Pitch (in. of rod/coil turn)	Length (in. of wire/in. of rod)
0.1600	3.2782
0.1639	3.2075
0.1560	3.3544
0.1661	3.1692

[a] Serial No. (88112)

TABLE B-III

COMPARISON OF AVERAGE PITCH AND RESISTANCE WIRE LENGTHS
FOR THE HIGH POWER RODS

Rod (Serial No.)	Pitch (in. of rod/coil turn)	Length (in. of wire/ in. of rod)
E4(88102)[a]	0.1531	3.4125
D5(8890)[a]	0.1614	3.2524
E5(88112)[a]	0.1604	3.2708
D4(88107)[a]	0.1623	3.2361
D5(88118)[b]	0.1574	3.3274
E5(88114)[b]	0.1605	3.2696

[a] Used during Tests S-02-1, S-02-2, and S-02-3.

[b] Used during Tests S-02-4, S-02-5, S-02-7, S-02-9A, and S-02-9.

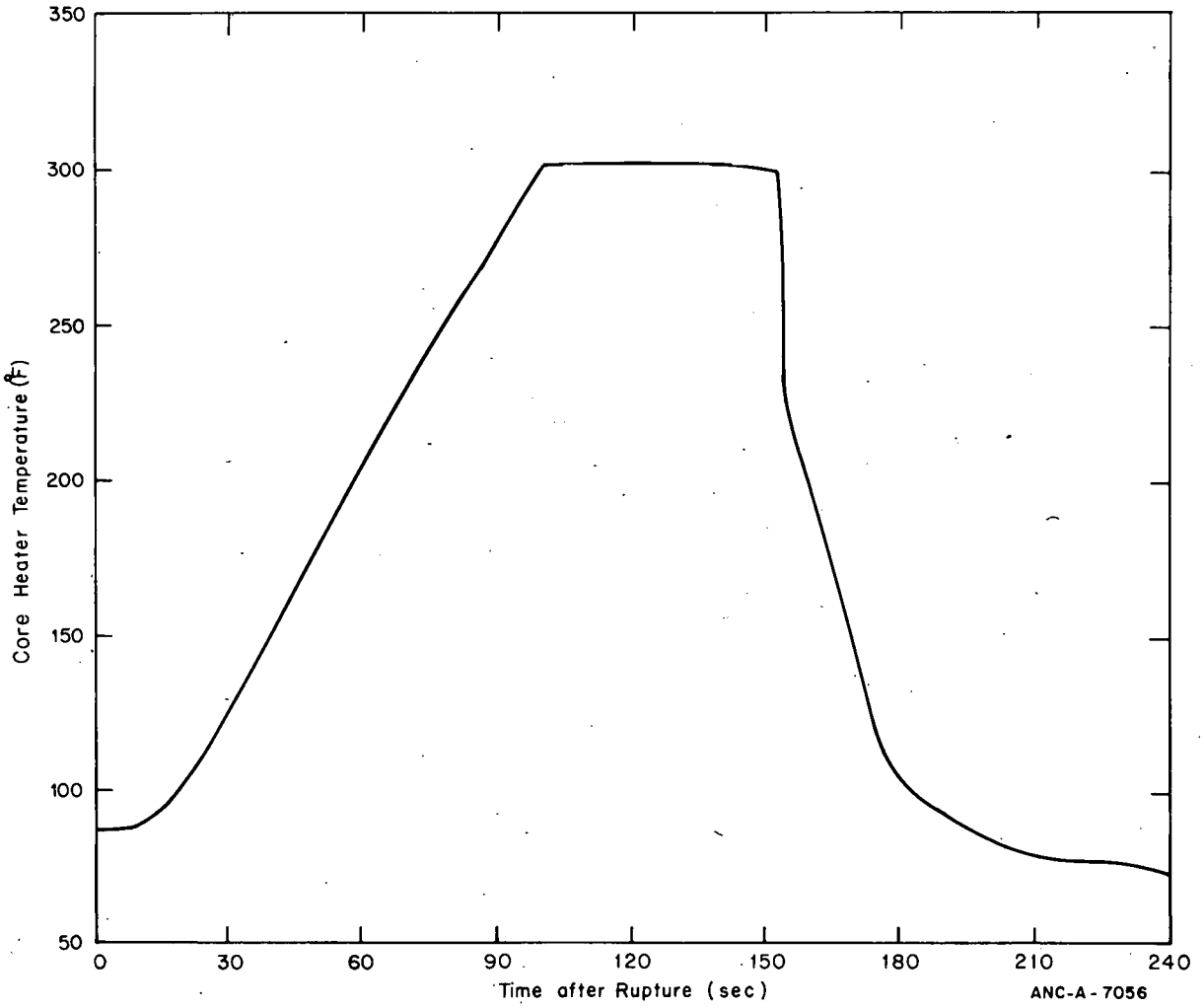

Fig. B-5 Response of Thermocouple TH-D6-25 to the dry core heatup test.

calculated as they should be because the heatup was essentially adiabatic. Table B-IV lists the new power multipliers calculated. Also listed in Table B-IV Is whether or not the thermocouple experienced rewet during the transient portion of Test S-02-7. Comparison of the data in the table does not indicate any correlation between the new power multipliers and the rewet characteristics. For example, some of the rewets occurred on zones that had power multipliers larger than 1.0, and many rods that had calculated power multipliers less than 1.0 did not experience any rewetting.

The data taken during the core flooding conducted subsequent to the heatup tests verified with only three possible exceptions the axial location of the thermocouples. Figure B-6 shows the thermocouple quench times versus core elevation for the flood test.

In summary, the special tests conducted and analyzed thus far have qualitatively substantiated the existence of power density variations both within the high power zone on a given rod and among the high power zones on all the rods. New power multipliers for the rod high power zones were developed using data from the dry core heatup test. The new

TABLE B-IV

POWER FACTOR MULTIPLIERS FOR TEST S-02-7

Thermocouple	Power Factor	Rewet
TH-E5-21	0.90	No
TH-F3-22	0.9908	No
TH-F2-22	0.9825	No
TH-E4-23	0.9481	No
TH-G5-24	1.0263	No
TH-E5-25	0.9687	No
TH-D6-25	1.0126	No
TH-F3-25	1.0256	No
TH-C4-26	1.0220	No
TH-F5-26	1.0331	No
TH-E4-27	0.9766	No
TH-C3-28	1.0296	Yes
TH-E6-28	1.0057	No
TH-F6-28J	1.0370	No
TH-C2-28	0.9838	Yes
TH-C5-28	1.0401	Yes
TH-D3-29	1.0258	Yes
TH-F7-29	1.0161	No
TH-A4-29	0.9989	Yes
TH-D5-29	0.9774	No
TH-B6-29	0.9964	No
TH-E8-29	1.0301	Yes
TH-A5-29	1.0016	No
TH-B5-29	1.0360	No
TH-D4-29	0.9476	Yes
TH-E6-31	0.9781	Yes

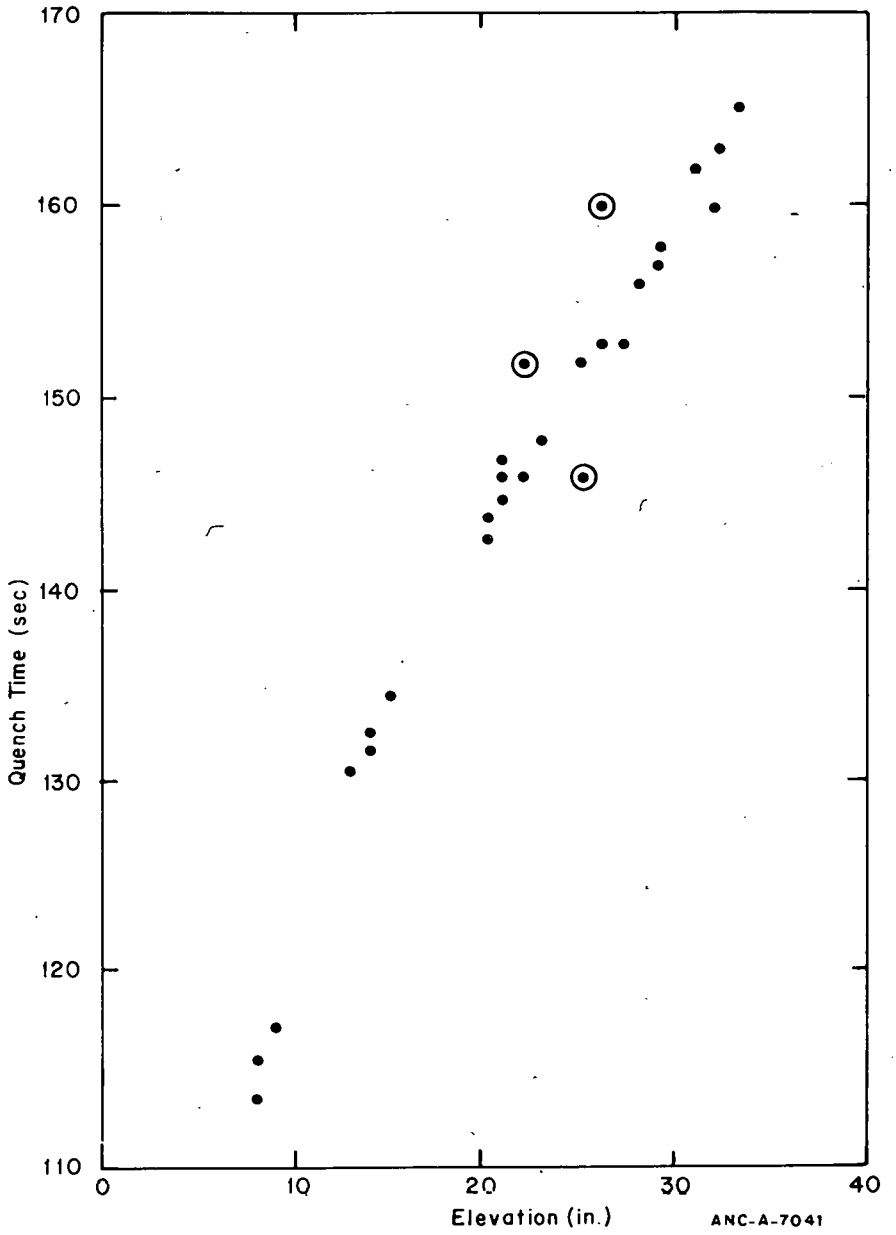

Fig. B-6 Thermocouple quench time versus elevation.

power multipliers, when used in conjunction with the analytical technique used to calculate rod heat transfer quantities, did improve the results, but neither the pulse test differential temperatures or the new power multipliers seemed to correlate with the occurrence of rewetting on the rod high power zones. The reflood test conducted on the system verified that all but three of the high power zone thermocouples were located (axial position) where they were thought to be.

THIS PAGE

WAS INTENTIONALLY

LEFT BLANK

APPENDIX C

AXIAL REWET PHENOMENA IN THE SEMISCALE MOD-1 CORE FOR TEST S-02-7

THIS PAGE

WAS INTENTIONALLY

LEFT BLANK

APPENDIX C

AXIAL REWET PHENOMENA IN THE SEMISCALE MOD-1 CORE FOR TEST S-02-7

The axial representation of the heater rod rewet phenomena discussed in Section III-3.3 in connection with Test S-02-7 indicates a noteworthy relationship between the heater rod power density and the local core fluid conditions with respect to the occurrence of rewetting. The purpose of this appendix is to present the rod cladding thermocouple behavior that verifies the discussion in Section III-3.3.

The heated length of the Semiscale core can be divided into distinct axial regions on the basis of DNB-rewet patterns. These divisions are not synonymous with the axial power density steps on the heater rods. The figures presented in this appendix show how these axial divisions were selected for Test S-02-7. Each figure shows overlays of the transient temperature response of locations at essentially the same elevation in the core.

Figure C-1 shows the thermal response at the 8- and 9-inch elevations during Test S-02-7. The behavior at the 8- and 9-inch elevations is extremely uniform relative to that shown in Figure C-2 for the 13- to 15-inch elevations. No rewetting was observed at the lower elevation, whereas the behavior at the 13- to 15-inch locations was varied. Figures C-3 and C-4 show the behavior at the 20-inch and the 21- to 26-inch elevations, respectively. The data shown in these figures indicate the absence of any rewetting. The response at the 27- to 31-inch elevations is shown in Figure C-5. The response shown in Figure C-5 is similar (with the exception of magnitudes of the temperatures) to that indicated at the 13- to 15-inch elevations in that both rewetting and nonrewetting occur. Figures C-6 and C-7 show the cladding temperature behavior at the 32- to 33-inch elevations and the 37- to 39-inch elevations, respectively. Some of the thermocouples at the 32- to 33-inch elevations indicated early DNB with immediate rewet, and others showed that DNB was delayed until about four seconds after rupture. The 37- to 39-inch and 44- to 45-inch elevations all experienced delayed DNB (four seconds) as shown in Figures C-7 and C-8. The behavior at these two elevations is seen to be quite uniform radially. The 39-inch elevation on Rod A4 is an exception in that it experienced quenching at about 13.5 seconds. Thermocouple behavior at the 53- and 60-inch core elevations is shown in Figures C-9 and C-10, respectively. Successive DNB and rewetting is observed at the 53-inch core elevation, whereas no DNB is experienced at the 60-inch elevation.

The preceding figures show that different types of response are observed in the heated core depending on the particular elevation. Table C-I summarizes the thermocouple behavior with respect to elevation.

Results from Tests S-02-4, S-02-5, S-02-9A, and S-02-9 indicate that the cladding thermal behavior during these tests can be categorized in a similar fashion to that shown here for Test S-02-7. Results from Tests S-02-2 and S-02-3, however, show some deviation

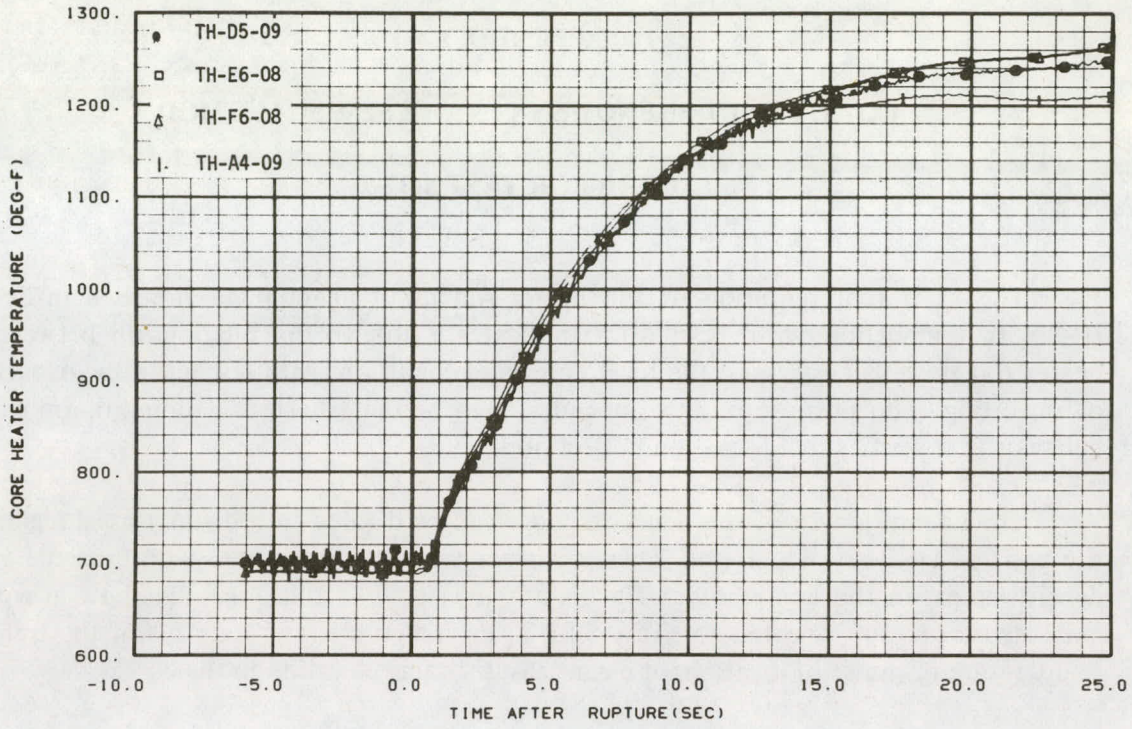

Fig. C-1 Cladding temperature response at 8- to 9-inch elevation – Test S-02-7.

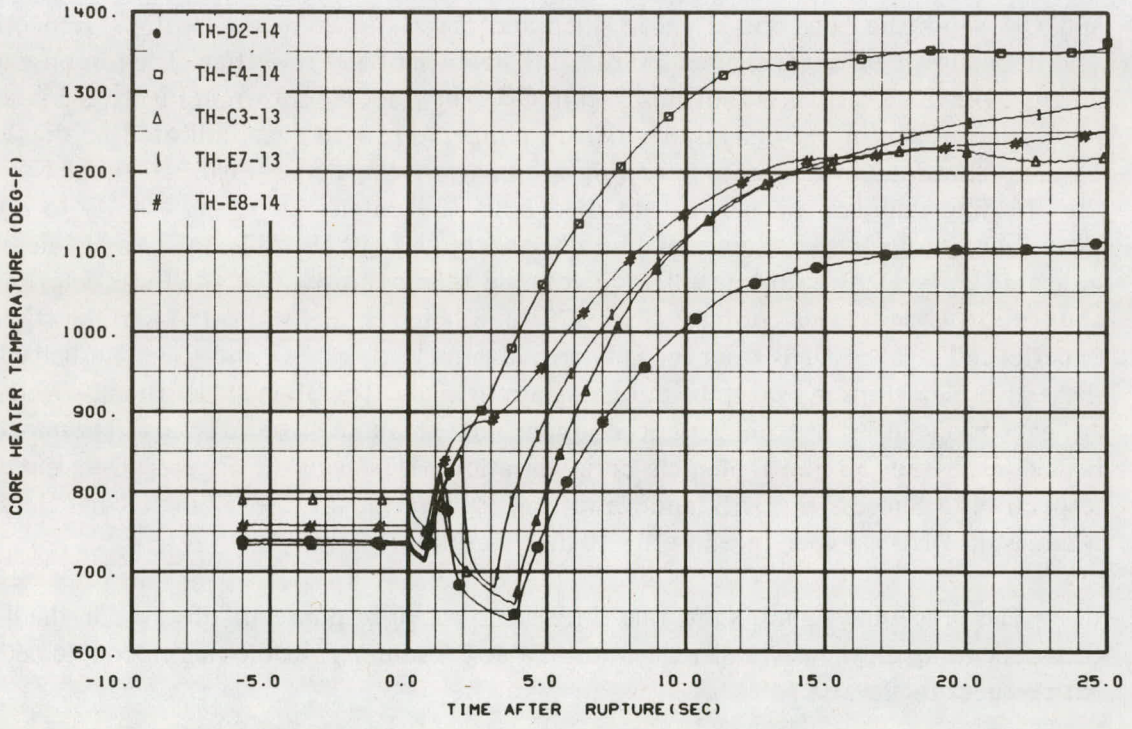

Fig. C-2 Cladding temperature response at 13- to 15-inch elevation – Test S-02-7.

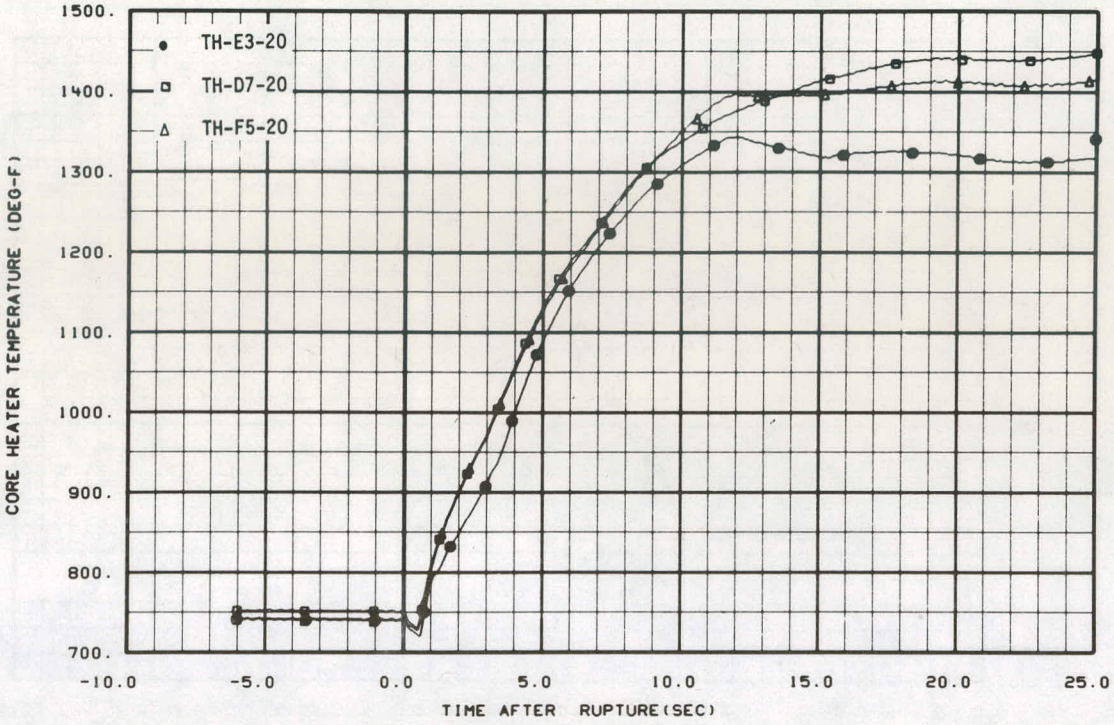

Fig. C-3 Cladding temperature response at 20-inch elevation – Test S-02-7.

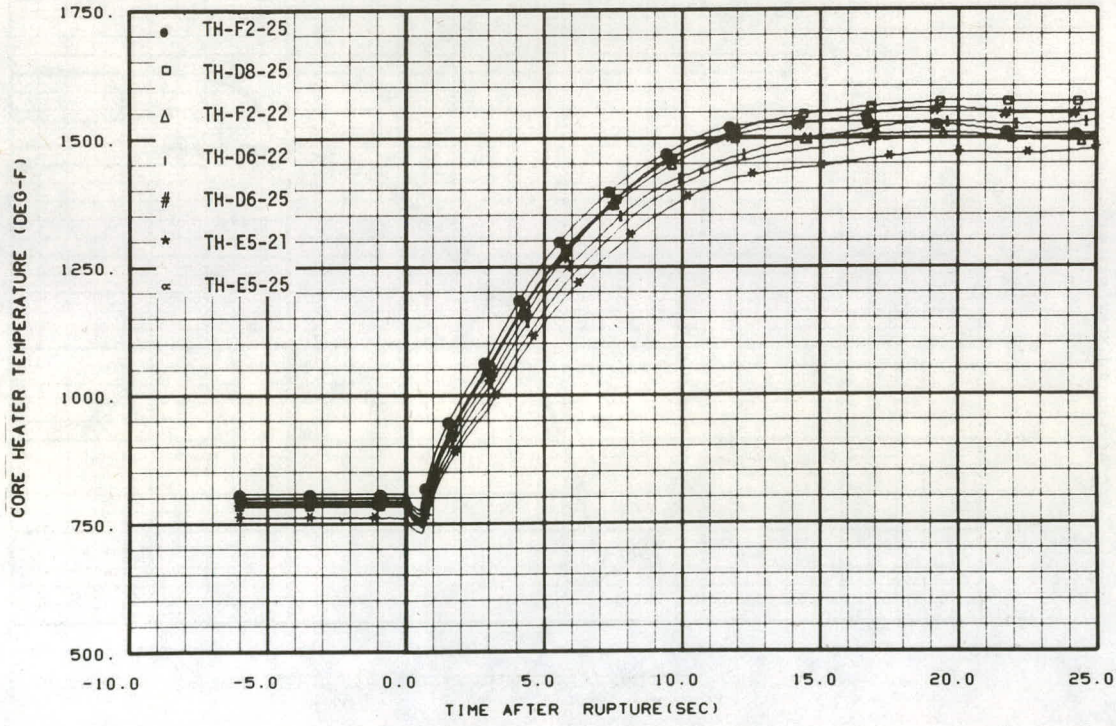

Fig. C-4 Cladding temperature response at 21- to 26-inch elevation – Test S-02-7.

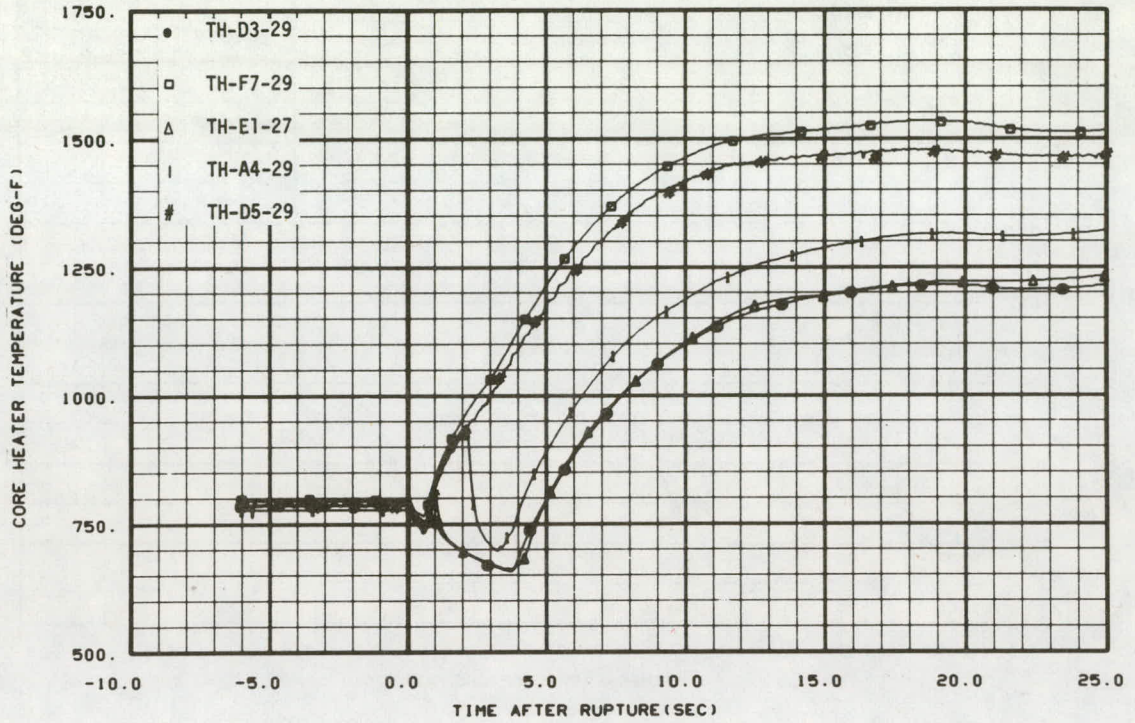

Fig. C-5 Cladding temperature response at 27- to 31-inch elevation – Test S-02-7.

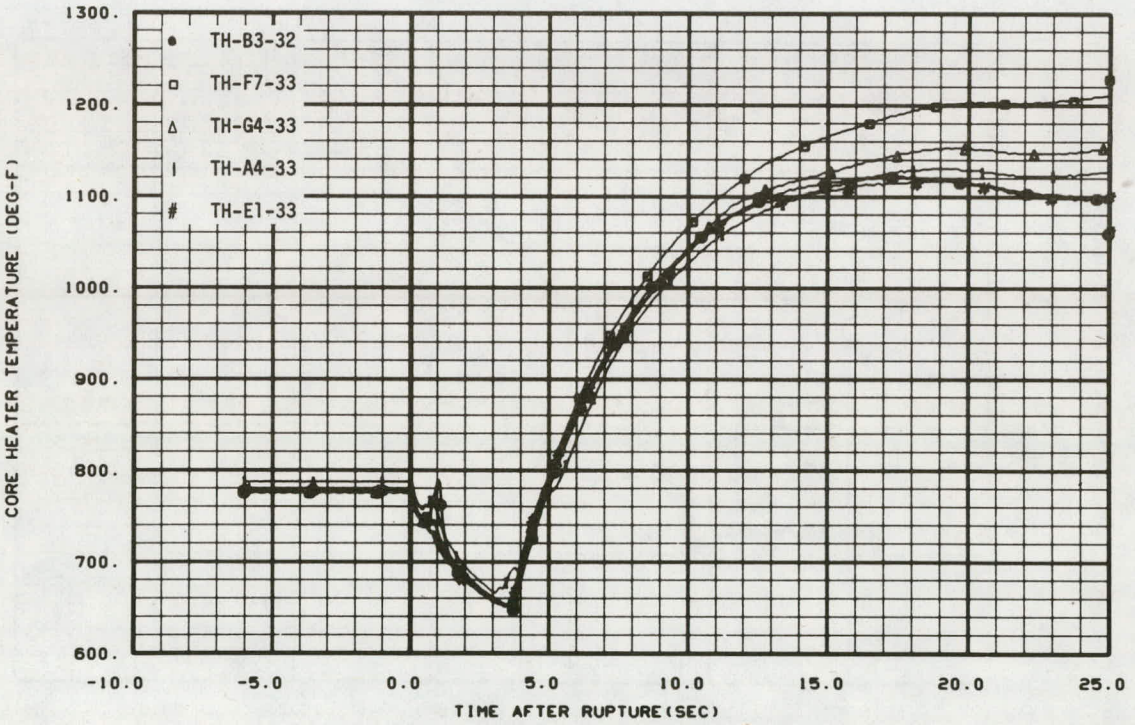

Fig. C-6 Cladding temperature response at 32- to 33-inch elevation – Test S-02-7.

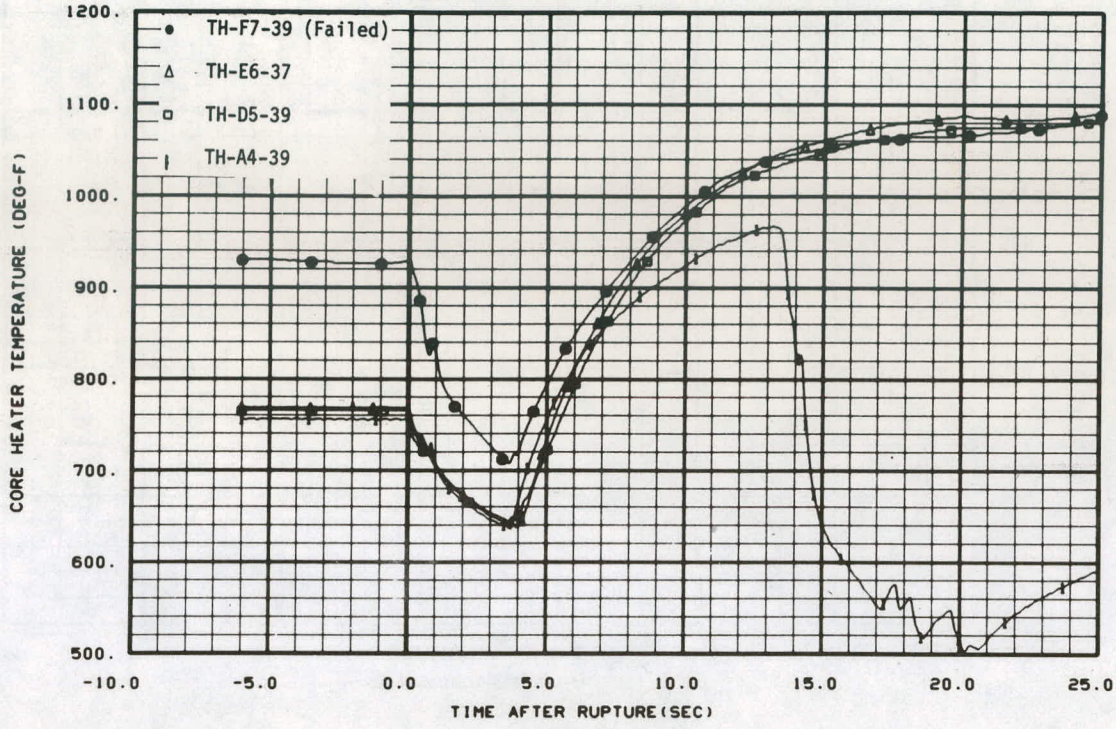

Fig. C-7 Cladding temperature response at 37- to 39-inch elevation – Test S-02-7.

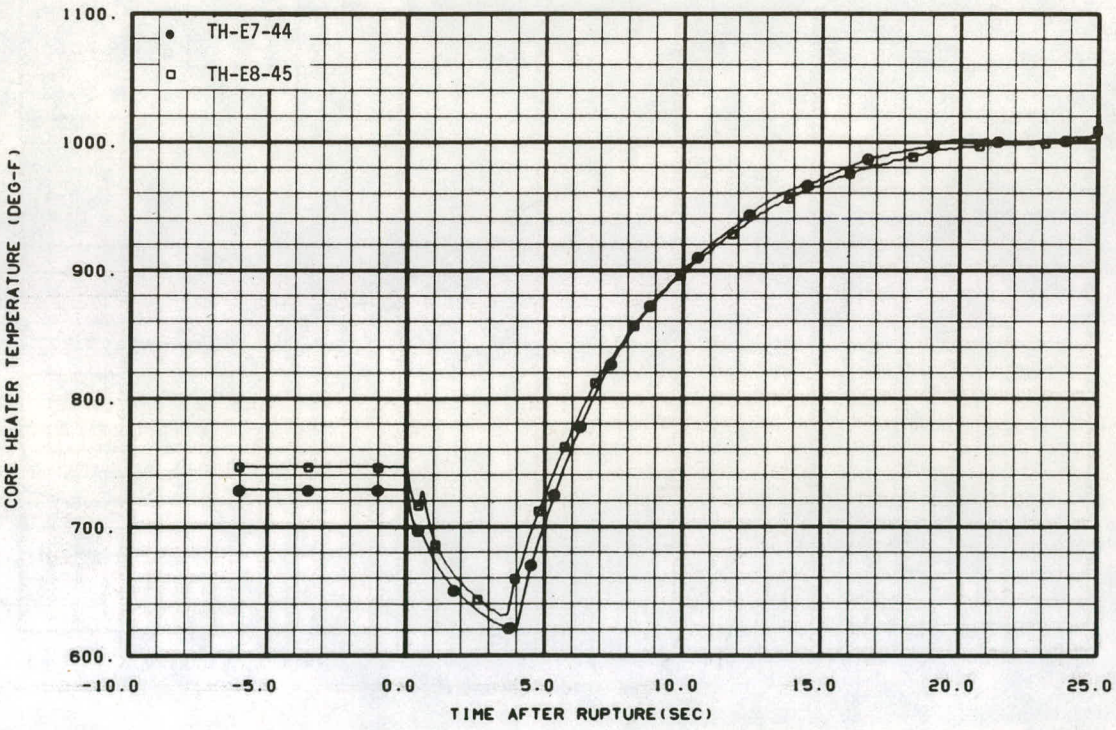

Fig. C-8 Cladding temperature response at 44- to 45-inch elevation – Test S-02-7.

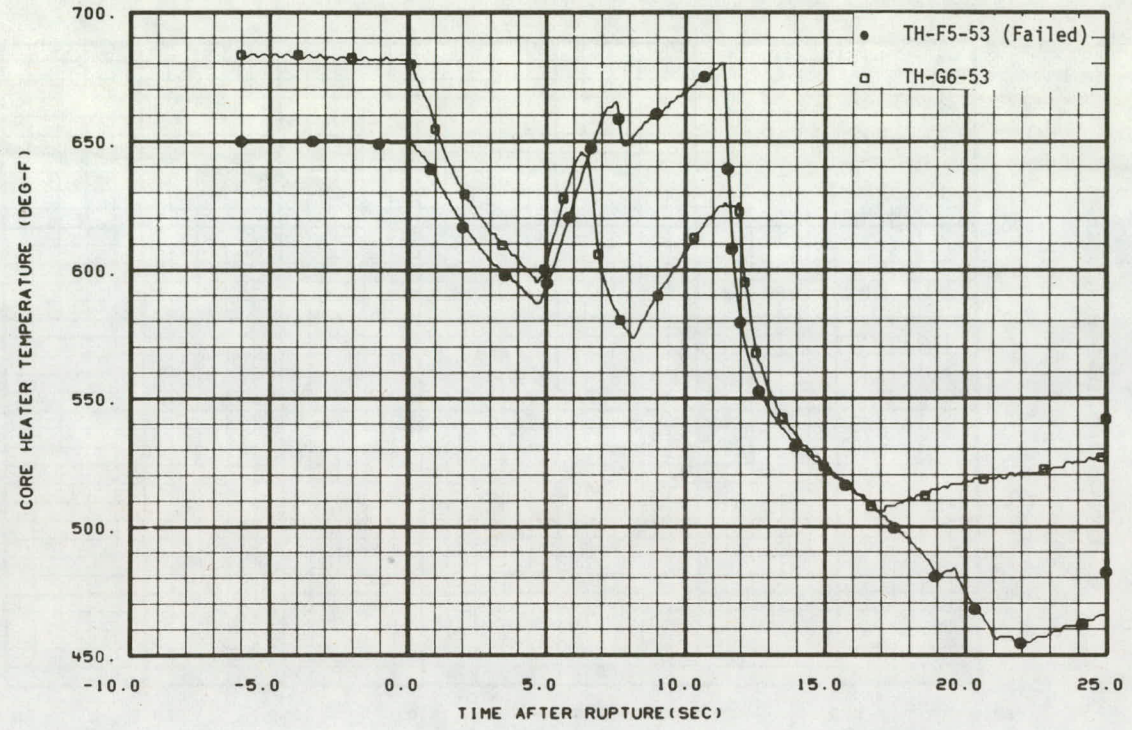

Fig. C-9 Cladding temperature response at 53-inch elevation – Test S-02-7.

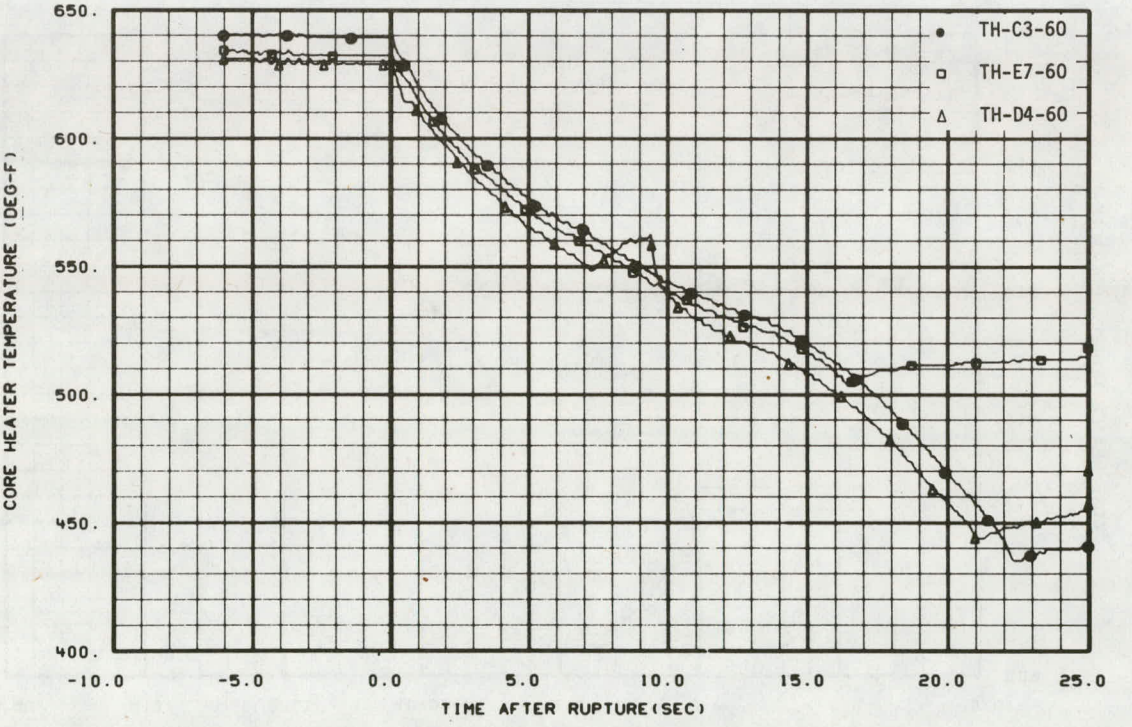

Fig. C-10 Cladding temperature response at 60-inch elevation – Test S-02-7.

TABLE C-I

SUMMARY OF HEATER ROD AXIAL REWET

DISTRIBUTION FOR TEST S-02-7

Core Elevation (in.)	Early DNB	Early DNB and Rewet	Delayed DNB	Delayed DNB and Rewet	No DNB
0-11	X				
11-16	X	X			
16-26	X				
27-31	X	X			
31-41		X	X		
41-48			X		
48-56				X	
56-66					X

from the axial pattern presented for Test S-02-7. These results indicate that for a certain range of rod operating power densities a relationship exists between the local power density (core elevation) and the core fluid conditions that control the DNB and rewet characteristics. Since Test S-02-2 and Test S-02-3 results did not fit the axial pattern that applied to the other blowdown heat transfer tests, the range of rod peak power densities for which the axial pattern holds can be limited to those power densities imposed on the rods during the 100% power tests. This range of peak power densities is probably about 11.5 to 14.25 kW/ft.

THIS PAGE

WAS INTENTIONALLY

LEFT BLANK

APPENDIX D

CORE THERMAL RESPONSE DATA REPEATABILITY

THIS PAGE

WAS INTENTIONALLY

LEFT BLANK

APPENDIX D

CORE THERMAL RESPONSE DATA REPEATABILITY

This appendix supplements the previous discussion concerned with data repeatability in the Semiscale system. The first part is concerned with specific differences in the rod rewet phenomena noted in comparing data from Tests S-02-4 and S-02-5. The second part explains the statistical analysis performed in connection with Test S-02-7, S-02-9A, and S-02-9.

1. CLADDING TEMPERATURE COMPARISON

Comparison of the cladding temperature behavior obtained from Tests S-02-4 and S-02-5 indicates that, with a few exceptions, the temperature responses were quite similar. Of the 73 cladding thermocouples common to both tests, only eight indicated responses that were not similar in both tests. Although the temperature profiles from the two tests were not exact overlays becuase the core power control was different in the two cases, the similarity existed to the extent that if in one test a thermocouple indicated DNB and then rewetted at a particular time, then it exhibited the same type of response (within a generally comparable time frame) in the other test. Of eight above mentioned thermocouples that exhibited different responses for the two tests, seven of these thermocouples were located on low power rod peak power zones. In six of these seven cases, the difference was that in Test S-02-5 the thermocouples indicated no rewet, whereas in Test S-02-4 rewet occurred. Figure D-1 illustrates this difference. This different response is probably related to the different power input to the core for the first few seconds of the transient because the rewets in Test S-02-4 generally occurred prior to three seconds after rupture. Only one of the low power rod hot spot thermocouples that indicated rewet in Test S-02-5 did not in Test S-02-4. This difference was probably due to local variation in the core hydraulics (quality, flow, etc.) between the two tests. Small local variations in core hydraulics are expected because the nature of two-phase flow is complicated and would be expected to be somewhat random in a blowdown situation.

2. STATISTICAL ANALYSIS

The results from Tests S-02-7, S-02-9A, and S-02-9 show that of the 31 thermocouples on the cladding at the rod hot spot common to all three tests only five experienced DNB rewet characteristics that were not essentially identical in all three tests. Assuming that whether or not a thermocouple will rewet during a test is random (the probability that a thermocouple will rewet is the same as the probability that it will not rewet), then the probability that a given thermocouple will respond in the same manner for three tests is given by the binomial theorem[D-1]:

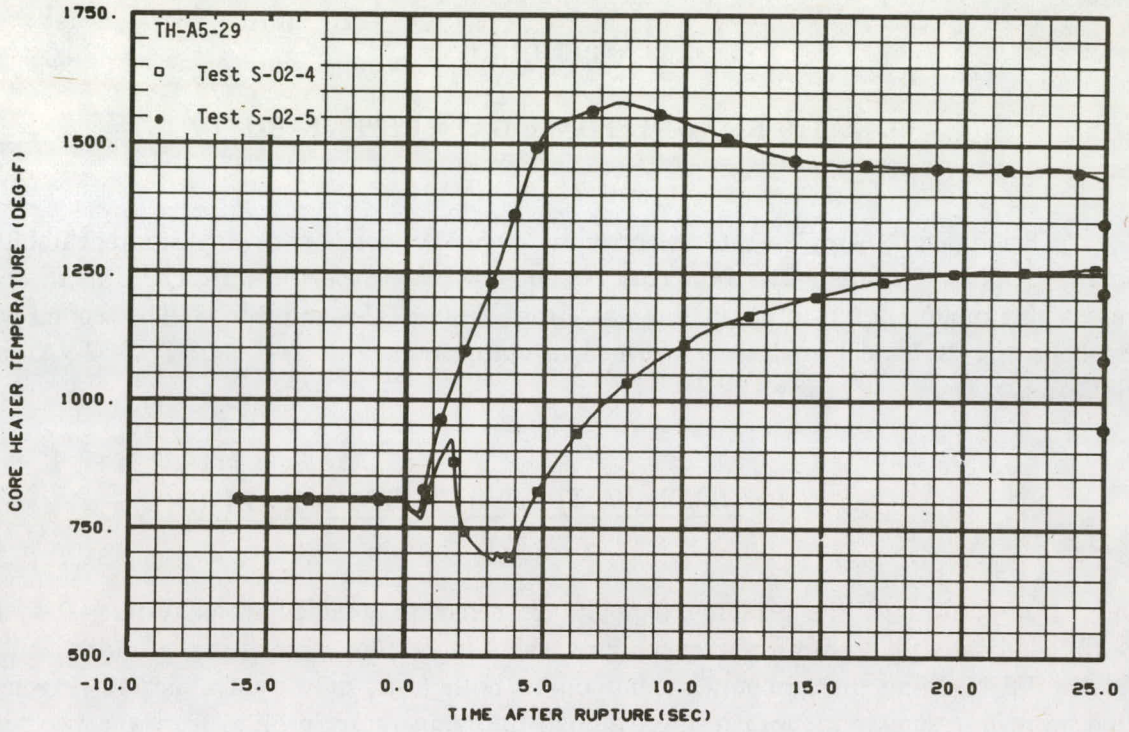

Fig. D-1 Response of Thermocouple TH-A5-29 – Tests S-02-4 and S-02-5.

$$b(x;\ n,\ p) = \frac{n!}{x!\ (n-x)!}\ (p)^{x}\ (1-P)^{n-x} \qquad \text{(D-1)}$$

where

x = number of successes

n = number of trials

p = probability on individual trial.

If Equation (D-1) is evaluated with x = 3, n = 3, and p = 0.5, the probability of consistent behavior of a given thermocouple in three similar tests is

b (3; 3, 0.5) = 0.1250.

To find the probability that 26 or more thermocouples will be consistent in their behavior for three tests, the cumulative probability[D-1] must be calculated. The cumulative probability is defined as

$$B\ (x;\ n,\ p) = \sum_{k=0}^{x}\ b\ (k;\ n,\ p) \text{ for } x = 0,1,2,\ \ldots.\ n.$$

The probability that at least 26 thermocouples will be consistent in three tests is then

$$P(x > 26) = 1 - B(26; 31, 0.125)$$

$$= 1 - 0.9841$$

$$= 0.0159.$$

This low value of probability indicates either that a rare event has been observed or that the original hypothesis (that the thermocouple response was random from test to test) was incorrect. Since the value is lower than 0.05 (the probability value commonly used in statistics to denote a rare event) the conclusion is reached that the thermocouple response is not random.

3. REFERENCE

D-1. I. Miller and J. E. Freund, *Probability and Statistics for Engineers,* New Jersey: Prentice-Hall, Inc., 1965.

THIS PAGE

WAS INTENTIONALLY

LEFT BLANK

APPENDIX E

RELAP4 CORE MODEL DESCRIPTION

THIS PAGE

WAS INTENTIONALLY

LEFT BLANK

APPENDIX E

RELAP4 CORE MODEL DESCRIPTION

The purpose of this appendix is to describe the model, nodalization scheme, and boundary conditions used in the component RELAP4 model of the Semiscale core.

1. DESCRIPTION OF MODEL

The model used for these analyses is shown in Figure E-1. It was constructed for the purpose of evaluating comparisons of hot spot cladding temperatures. The model had insufficient detail to provide good comparisons of cladding temperatures other than at the hot spot. It consisted of 15 volumes representing the core and upper and lower plenums. Volumes 3 through 6 represent the section of the core with average power levels, and Volumes 12 through 15 represent the hot region of the core comprised of roughly 10% of the total core volume and four heater rods which operated at a higher power level in Test S-02-5. The junctions between the volumes are placed at the location of the grid spacers in the core and upper plenum. Eight heat slabs in the hot channel model the ten steps in power present in the higher powered heater rods and provide good definition of the hot spots on these rods. The other heat slabs represent both active and inactive section of the other rods and the walls of the core and upper and lower plenums.

2. BOUNDARY CONDITIONS

The boundary conditions used for analysis were the mass flow rate and enthalpy at the bottom of the core and the pressure and quality in the upper plenum at the elevation of the hot leg inlet and outlet.

During the first four seconds of the computer run, mass flow rates based on the drag disc measurements were used to drive the model due to the inherent faster response characteristics of the drag disc relative to the turbine flowmeter. After four seconds, the turbine flowmeter data were used because of the better accuracy of the turbine flowmeter measurement during this period.

Volume 11 is the upper boundary volume in the model. The pressure versus time was based on the measured upper plenum pressure. The quality in the upper plenum was based on density data taken from the gamma densitometer located in the hot leg of the broken loop. This density is recognized as probably not being entirely typical of the fluid present in the part of the upper plenum represented by Volume 11, but it provided the best data which were available for use in this analysis.

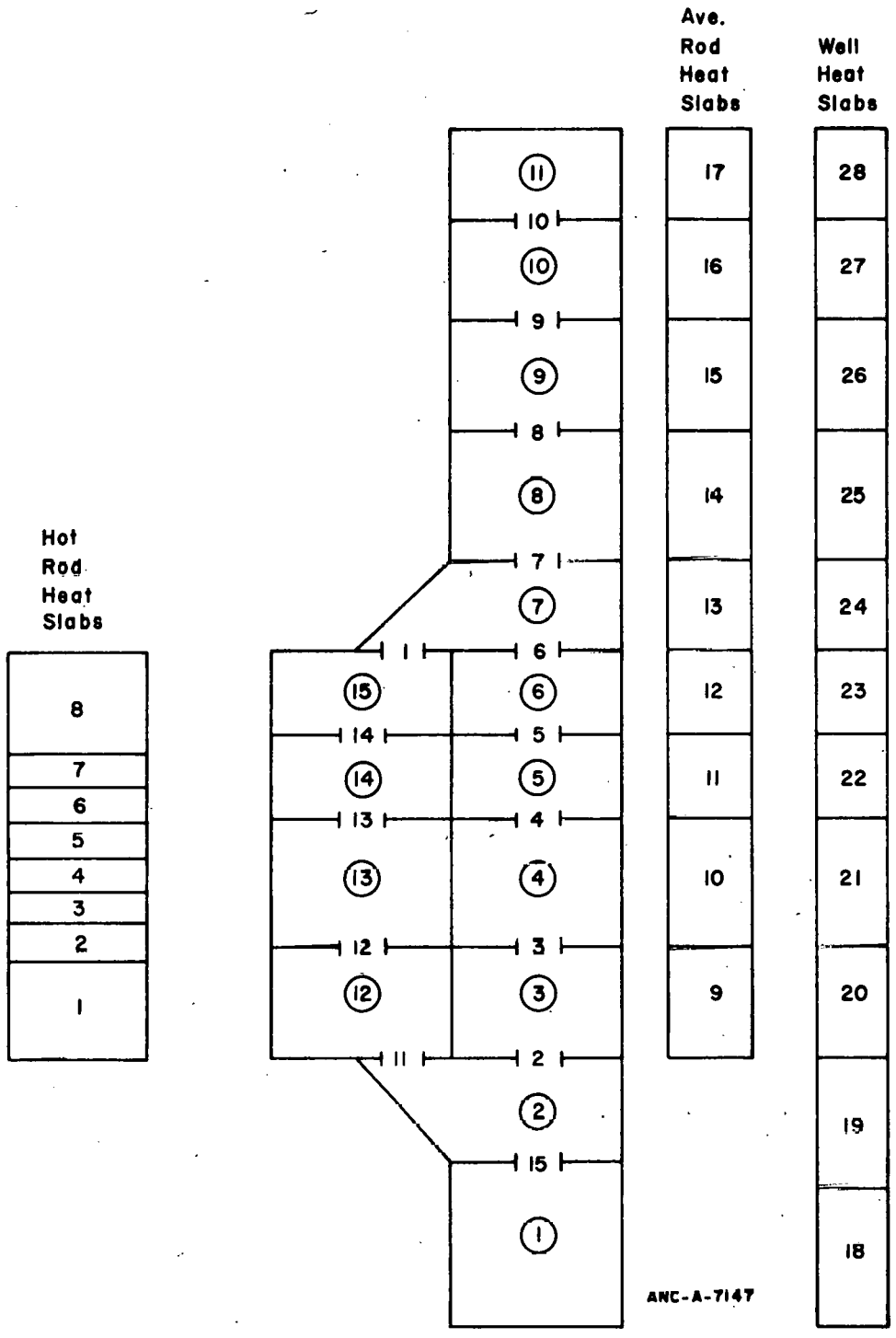

Fig. E-1 Semiscale Mod-1 core and plena node diagram.

3. INITIAL CONDITIONS

The initial conditions used in the RELAP4 model of the Semiscale core and plenums were determined as follows.

The initial measured mass flow at the bottom of the core was divided between the hot and cold channels of the core on the basis of the respective areas of those channels. The flow was assumed to be constant along the axial length of the core and upper plenum.

The initial fluid temperature distributions in the hot channel and average channels were set at the same value on the basis of the test data. The temperature of the fluid in any given volume was calculated on the basis of the initial mass flow rate and the energy added by the heat slabs representing the active heater rods. The pressure distribution in the core was adjusted to match the pretest determined flow resistances and the measured flow rate.

Report No. ANCR-NUREG-1285
Volume, Part, Revision Not Applicable
Distribution Category No. NRC-2

INTERNAL DISTRIBUTION

No. of Copies	Name of Recipient
1	Chicago Patent Group - ERDA 9800 South Cass Avenue Argonne, Illinois 60439
2 - 4	A. T. Morphew Classification and Technical Information Officer ERDA-ID Idaho Falls, Idaho 83401
5	R. J. Beers, ID
6	P. E. Litteneker, ID
7	R. E. Swanson, ID
8	V. A. Walker, ID
9	R. E. Wood, ID
10	H. P. Pearson, Supervisor Technical Information
11 - 20	INEL Technical Library
21 - 57	Special Internal Distribution
58 - 77	Author

EXTERNAL DISTRIBUTION

No. of Copies	Position Title, Organization of Recipient
78 - 79	H. J. C. Kouts, Director, Office of Nuclear Regulatory Research, NRC, Washington, D. C. 20555
80 - 383	Distribution under NRC-2